Electronic Supplementary Information (ESI)

On optical signaling in biofluids: nondenaturing photostable molecular probe for serum albumins

Gourab Dey, Pankaj Gaur, Rajanish Giri* and Subrata Ghosh*

School of Basic Sciences, Indian Institute of Technology Mandi, Mandi, Himachal Pradesh – 175001, India.

Reagents and Instruments

All solvents were purchased from Fischer Scientific and distilled before use. The biomolecules including proteins, enzymes and nucleic acids were purchased from Sigma Aldrich. Photophysical property studies were done in spectroscopic grade solvents. Doubly ionized water used in all experiments was from Milli-Q system. Phosphate buffer saline (pH = 7.4, 100 mM) was prepared using doubly ionized water. Proteins, enzymes and nucleic acid solutions were prepared in phosphate buffer saline (PBS). Stock solutions of 5 mM of each probe were prepared in DMSO and the aliquots of biomolecule stock solutions (5 μM) were incubated with 3 μL (5 μM) solution of each probe for absorption and emission titration experiments. ^{1}H and ^{13}C NMR were recorded on 500 MHz Jeol ECS-400 (or 125 MHz for ^{13}C) spectrometer in $CDCl_3$ and CD_3OD. Micro Mass ESI-TOF MS spectrometer was used for recording high resolution mass spectra of compounds. Shimadzu UV-2450 and Cary Eclipse spectrophotometers were used for recording the absorption and fluorescence spectra respectively. All spectral data were recorded at 25 °C. Fluorescence measurements were done using 3 cm quartz cell with 5 nm slit width for both excitation and emission experiments (except for undiluted urine experiment), and the excitation wavelength was 304 nm (λ_{ex}=304 nm). Experiments using pure urine samples were done in Horiba Fluorolog 3 using 3 nm slit and 5 nm width. Steady state anisotropy measurements were done using Horiba Fluorolog 3 spectrofluorimeter (Horiba Scientific, USA).

All time resolved fluorescence measurements were done on time correlated single photon counting (TCSPC) spectrometer (Horiba DeltaFlex, U.K.). Jasco – J1500 machine was used for Circular Dichroism spectra measurement. Stuart SMP 30 melting point apparatus was used to record melting point of the compounds. The melting point of all the compounds was recorded in open glass capillary and the values are reported directly.

Protein sensing studies

The amount of DMSO did not exceed 0.1 % in the case of protein sensing studies. In the case of protein quenching it did not exceed 1.2 % . This amount cannot create any type of structural change in biomolecules.

Photostabilty studies

Output (488 nm, 140 mW) of an optical parametric amplifier (TOPAS, Light Conversion) pumped by a Ti:sapphire ultrafast regenerative amplifier (Splitefire Ace, Spectra Physics) was used for analyzing photostabilty of probe molecule.

Calculation of quantum yield (Φ): 2-amino pyridine in 0.1 N H_2SO_4 was used as standard for determining the quantum yield.[1] The following equation was used for calculating the quantum yield, [2]

$$\Phi = \frac{A_s F_u n_u^2}{A_u F_s n_s^2} \times \Phi_s$$

A_s= the absorbance value of standard.

A_u= the absorbance value of unknown sample.

F_s = the fluorescence peak of standard.

F_u = the fluorescence peak of unknown sample.

n_s = the refractive index of the solvent used for standard.

N_u = the refractive index of the solvent used for standard.

Φ_s = the quantum yield of standard.

Φ_u = the quantum yield of unknown sample.

Calculation of lifetime and mean lifetime (τ_m): The curve which was generated due to intensity decay was fitted in the equation belwo to calculate the lifetime values.[1]

$$I(t) = \sum_i \alpha_i \exp\left(\frac{-t}{\tau_i}\right)$$

Here, the initial intensity of component *i* is α_i with lifetime τ. The equation which was used for determining the mean lifetime (τ_m) of compounds in different experimental conditions is,[3]

$$\tau_m = \frac{\sum_i \alpha_i \tau_i}{\sum_i \alpha_i}$$

Steady state anisotropy(r) calculation:

$$r = \frac{I_{VV} - GI_{VH}}{I_{VV} + 2GI_{VH}}$$

I_{VV} = the intensity obtained when the excitation polarizer orientated vertically and emission polarizer orientated vertically.

I_{VH} = the intensity obtained when the excitation polarizer orientated vertically and emission polarizer orientated horizontally.

The *G* factor is defined as, [1]

$$G = \frac{I_{HV}}{I_{HH}}$$

Non-radiative decay rate constant calculation (k_{nr}): The following equation was used to calculate the non-radiative decay rate constant (k_{nr}).[4]

$$k_{nr} = k_r \left[\frac{1}{\Phi} - 1 \right]$$

Here k_r represents the radiative decay constant and Φ represents the quantum yield of the compound. k_r can be determined through the following equation,

$$K_r = \frac{\Phi_f}{\tau_f}$$

Here τ_f is the lifetime of compounds and Φ_f is the quantum yield of the compounds.

Calculation of change in free energy (ΔG): The complexation between the probes and the proteins associated with the change in free energy which was calculated by using the following equation, [5]

$$\Delta G = -2.303RT \log K_a$$

Scheme S1: Synthetic routes for the probes

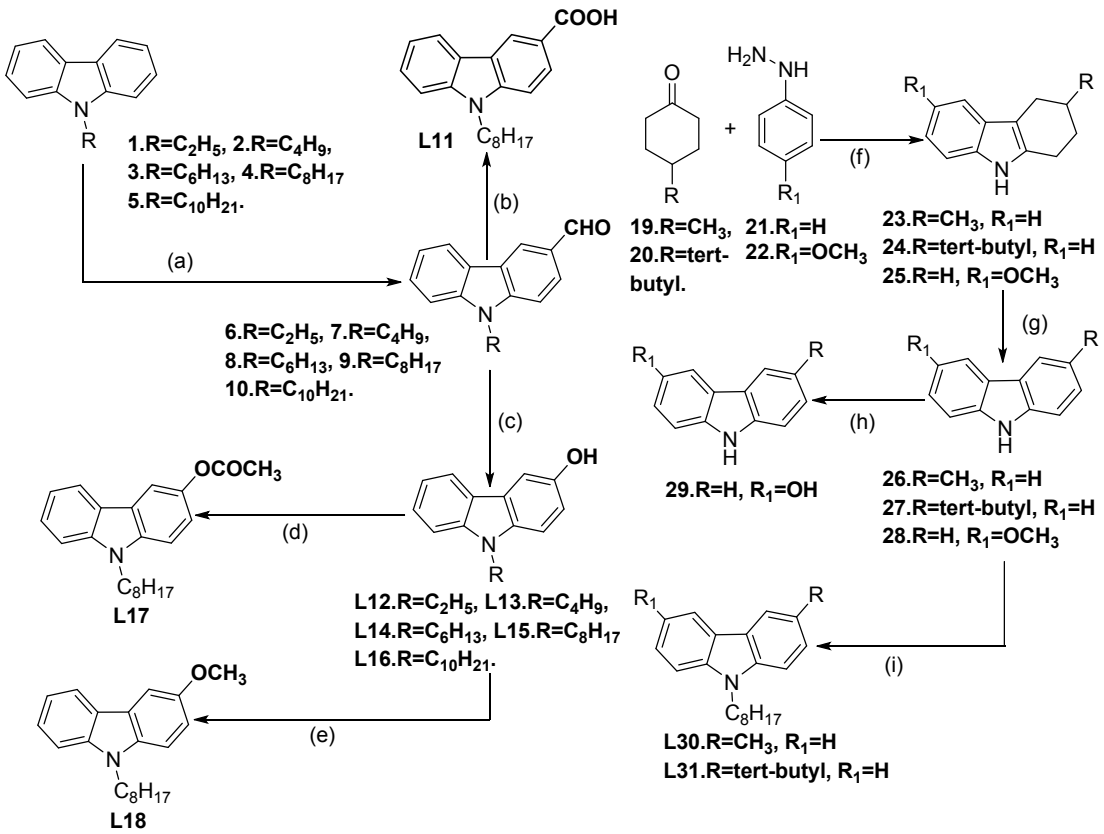

a) $POCl_3$, DMF, 0 ˚C to 105 ˚C , 30 mins in MW, (b) $KMnO_4$, acetone, 80 ˚C, 5h, c) H_2O_2, MeOH, H_2SO_4, 2 h, rt, d) Acetic anhydride, dry DCM, triethyl amine, 12 h, rt, e) Methyl iodide, NaOH, 80 ˚C, 8 h, f) Glacial acetic acid, reflux, 3h, g) Palladium charcoal (10 %), 290 ˚C, 45 min, h) HBr, glacial acetic acid, reflux, 3 h, i) KOH, 1 Bromooctane, rt, 12 h.

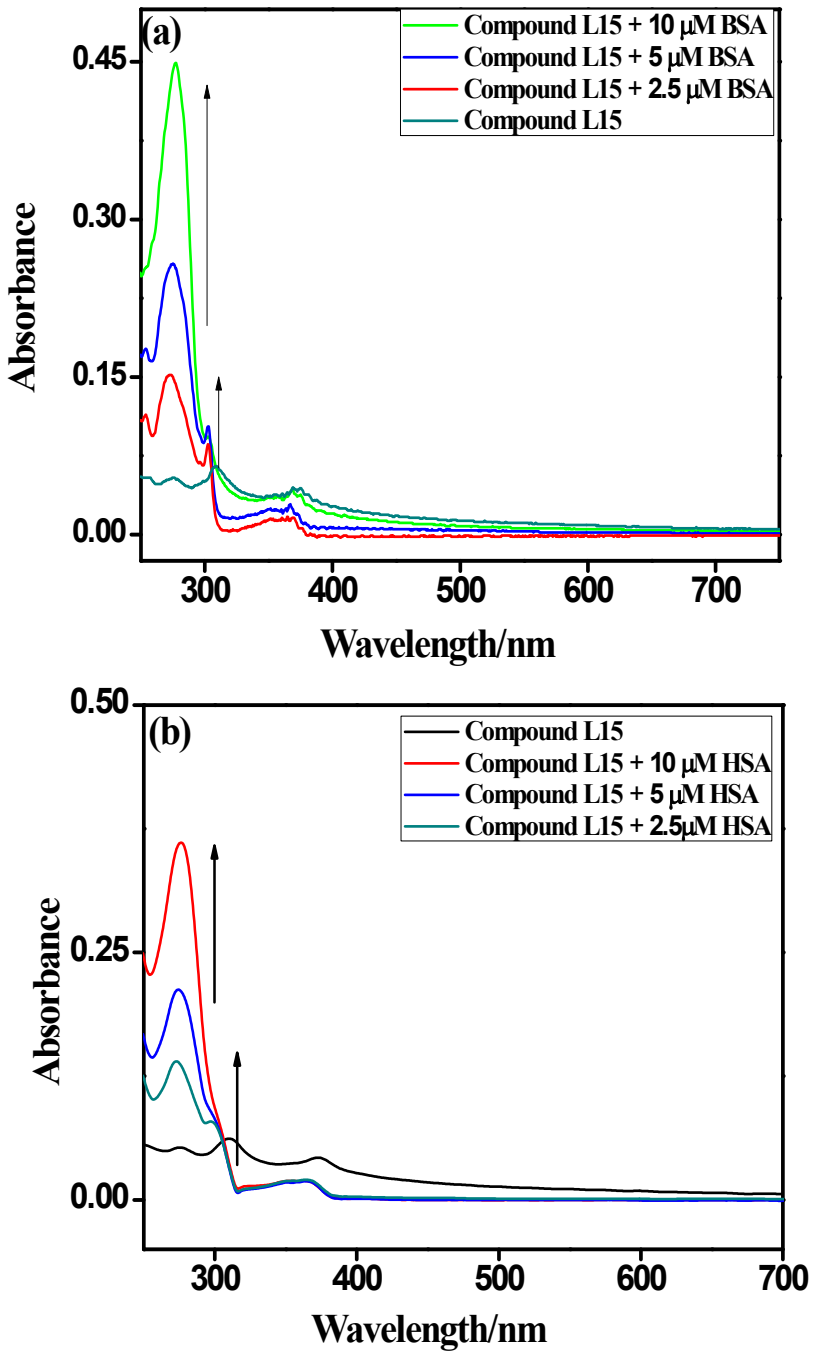

Fig. S1 UV-vis spectra of **L15** (5 μM) in the presence of increasing amount of a) BSA, b) HSA (0 to 5 μM) in PBS buffer (pH = 7.4).

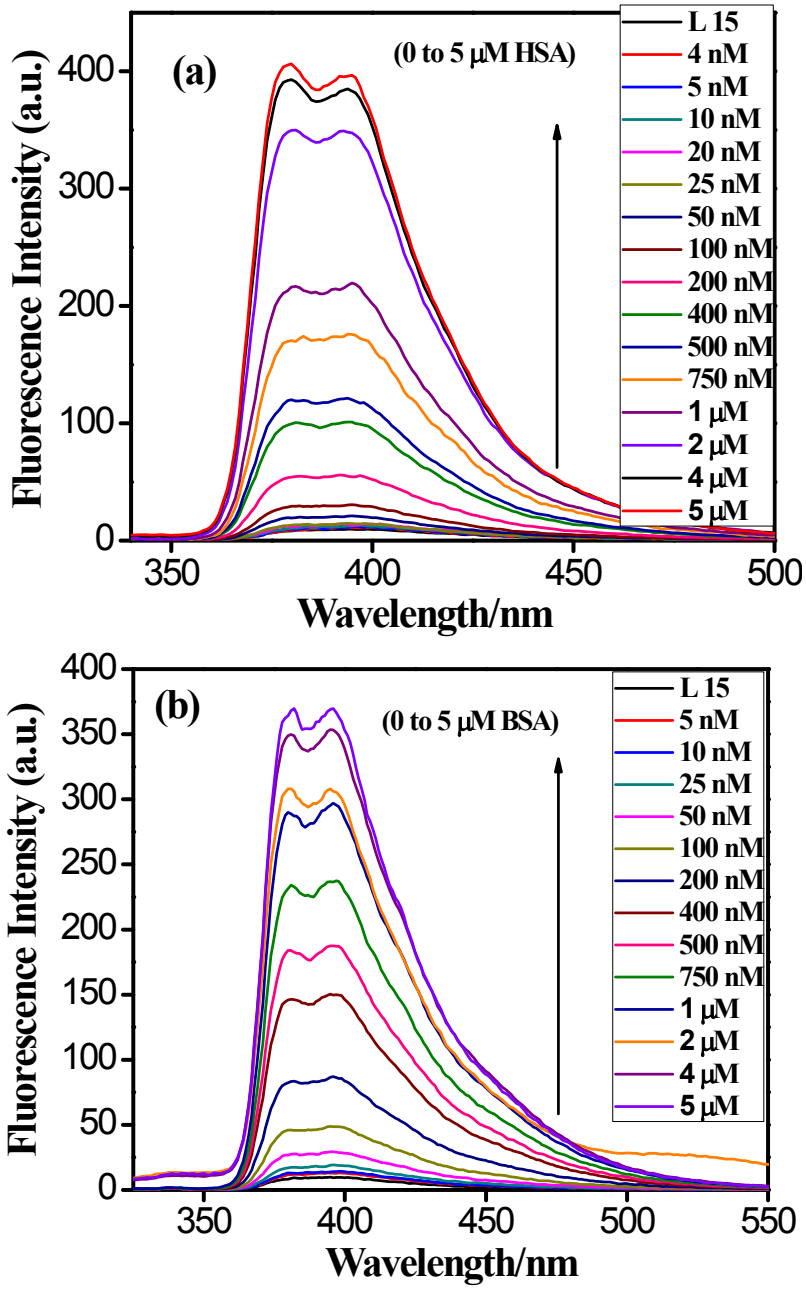

Fig. S2 Fluorescence response of **L15** (5 μM) in the presence of increasing amount of a) HSA (0 to 5 μM), b) BSA (0 to 5 μM).

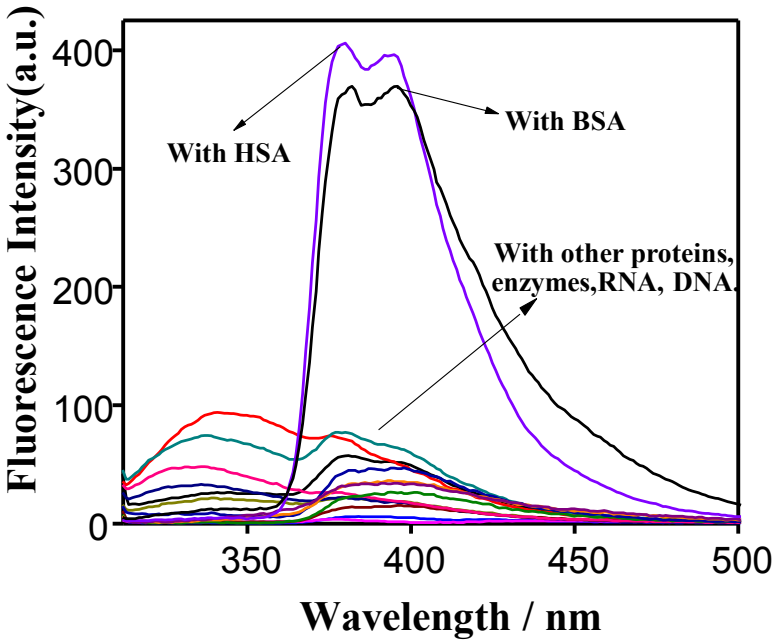

Fig. S3 Fluorescence response of **L15** (5 μM) in the presence of different types of proteins (5 μM), enzymes (5 μM), nucleic acids (3 mg/mL) in PBS buffer (pH = 7.4).

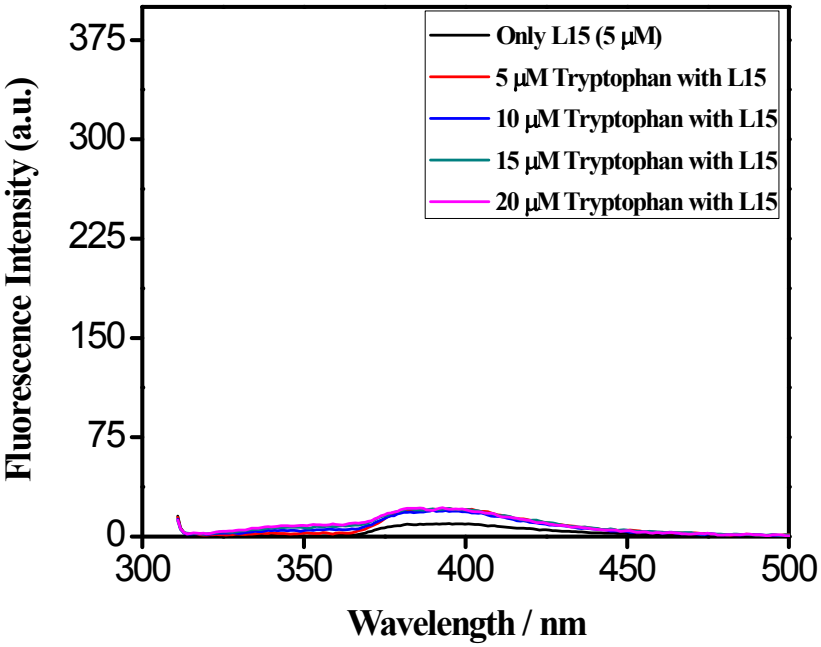

Fig. S4 Fluorescence response of **L15** (5 μM) in the presence of tryptophan amino acid (0 to 20 μM) in PBS buffer (pH = 7.4).

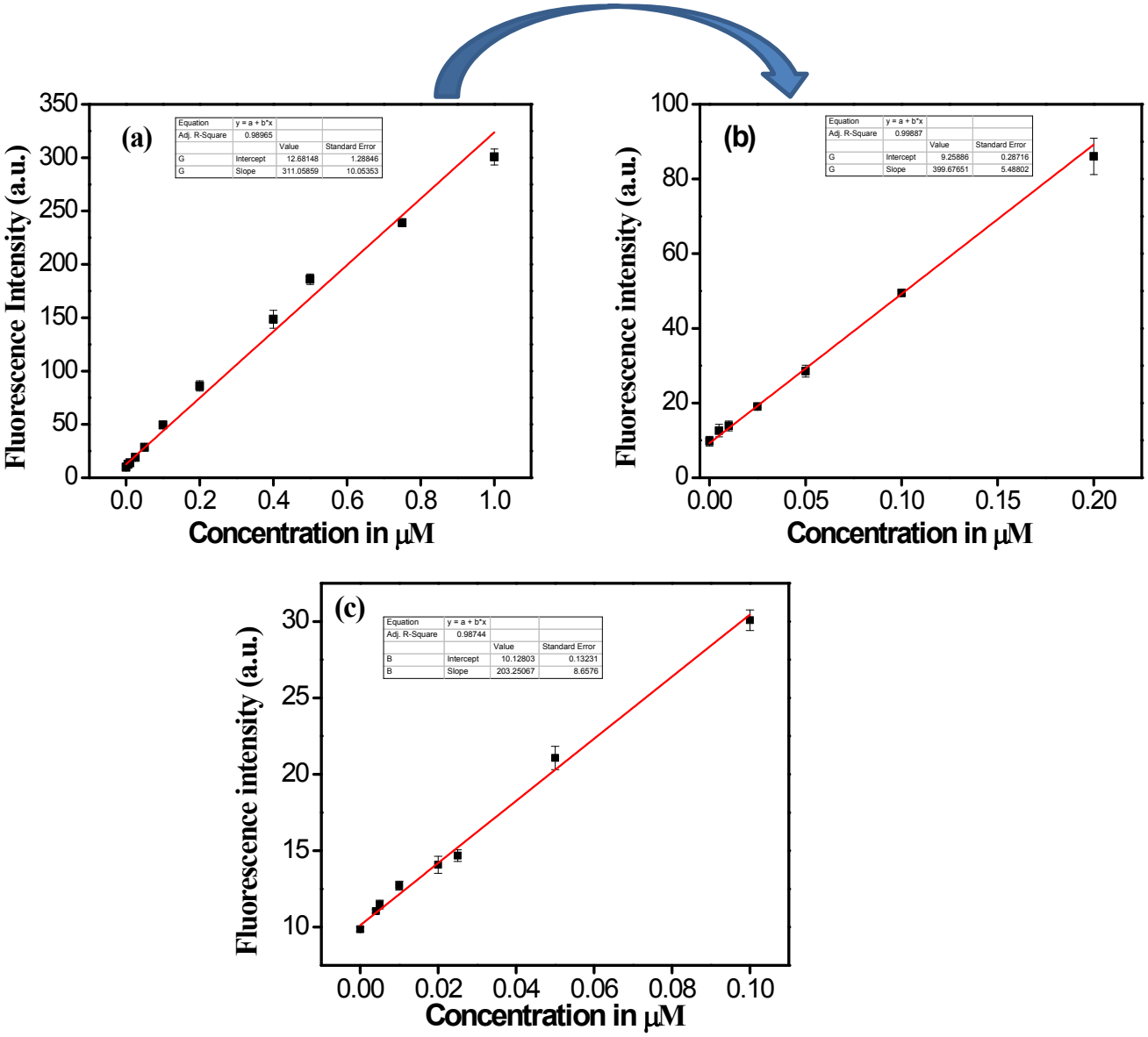

Fig. S5 a) Fluorescence intensity of **L15** (5μM) increased linearly with the BSA concentration (0–1 μM), b) fluorescence response of **L15** (5μM) in lower concentration of BSA (0-0.02 μM). c) fluorescence response of **L15** (5μM) in lower concentration of HSA (0-0.01 μM).

Table S1 Analytical parameters obtained for BSA/HSA using **L15**

Compound	Protein	Linear Range	Correlation Coefficient
L15	BSA	0.00 – 1 μM	0.989
L15	HSA	0.00 – 1 μM	0 .99

Table S2 Detection limit calculation of **L15** for HSA and BSA

Entry	Probe	Protein	Concentration	% Fluorescence intensity change	S/N	Detection limit (M)
1	**L15**	BSA	5×10^{-9} M	30.26	3	**5×10^{-9}**
2	**L15**	HSA	4×10^{-9} M	14.87	3	**4×10^{-9}**

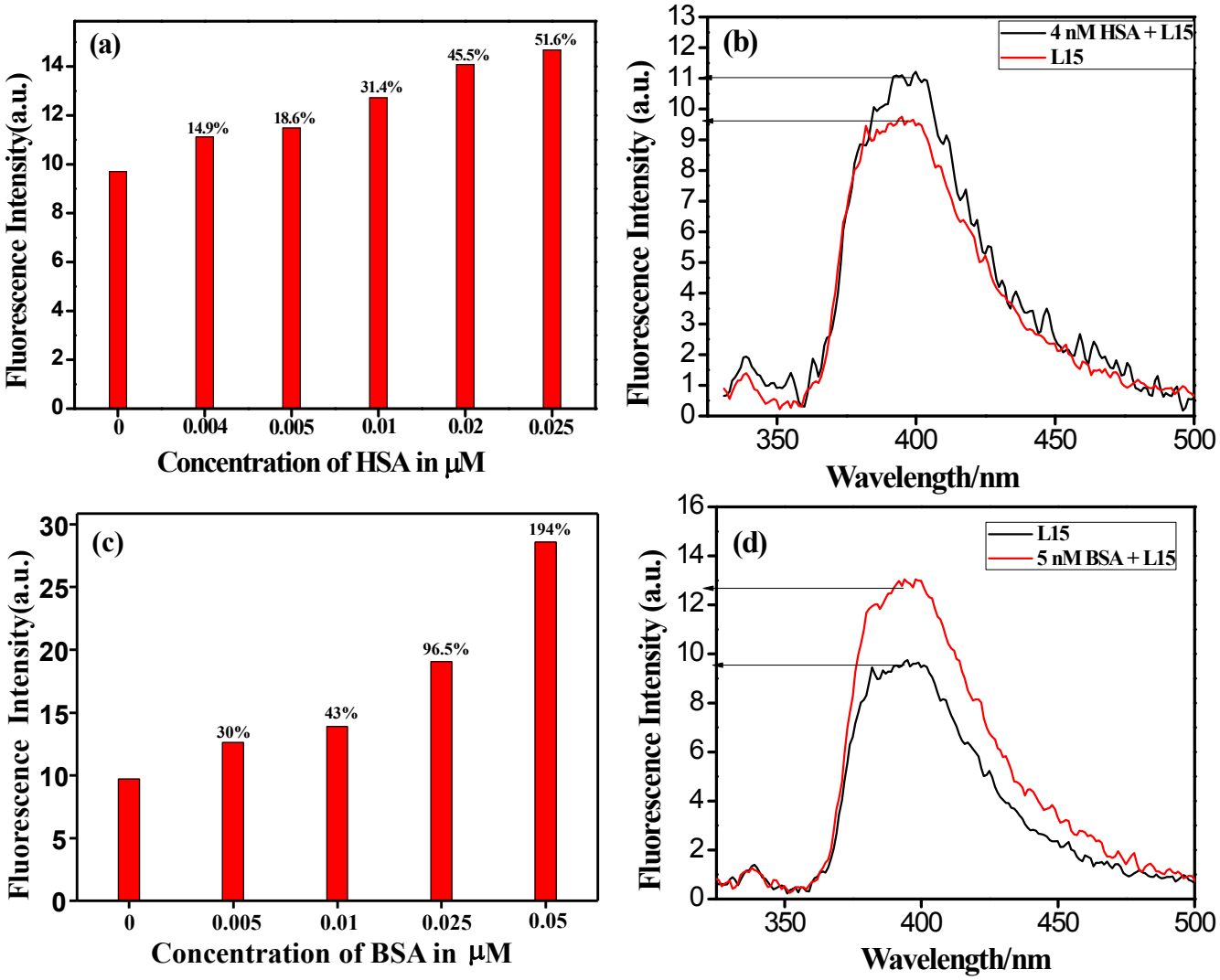

Fig. S6 a) Bar graph of percentage increment of fluorescent signal of **L15** (5μM) in the presence of different amount of HSA, b) fluorescence intensity of **L15** (5μM) in the presence of 4 nM HSA, c) bar graph of percentage increment of fluorescent signal of **L15** (5μM) in the presence of different amount of BSA, d) fluorescence intensity of **L15** (5μM) in the presence of 5 nM BSA.

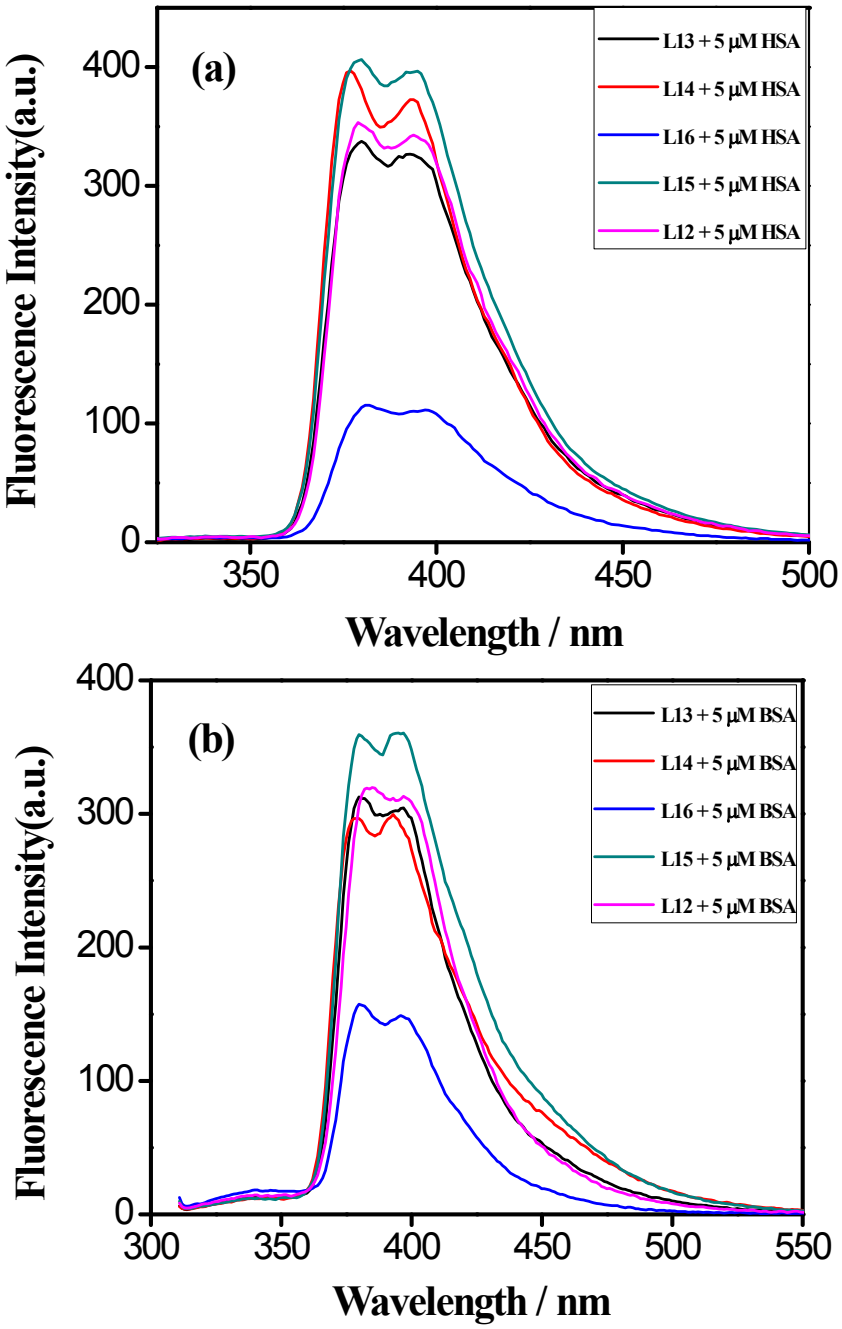

Fig. S7 Fluorescence response of **L12-16** (5μM) in the presence of 5 μM a) HSA, b) BSA in PBS buffer (pH = 7.4), λ_{exc} = 304nm.

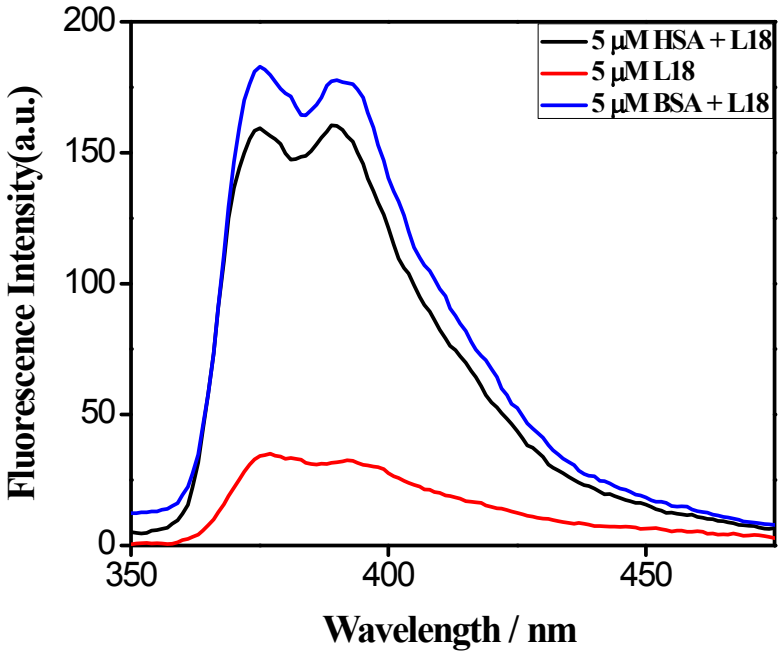

Fig. S8 Fluorescence response of **L18** (5μM) in the presence of 5 μM HSA, BSA in PBS buffer (pH = 7.4), λ_{exc} = 304nm.

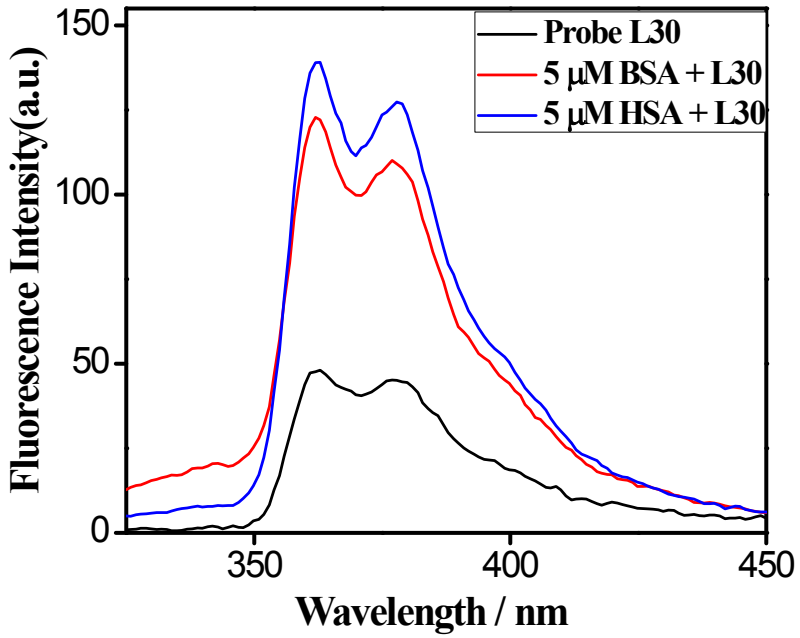

Fig. S9 Fluorescence response of probe **L30** (5μM) in the presence of 5 μM HSA, BSA in PBS buffer (pH = 7.4), λ_{exc} = 304nm.

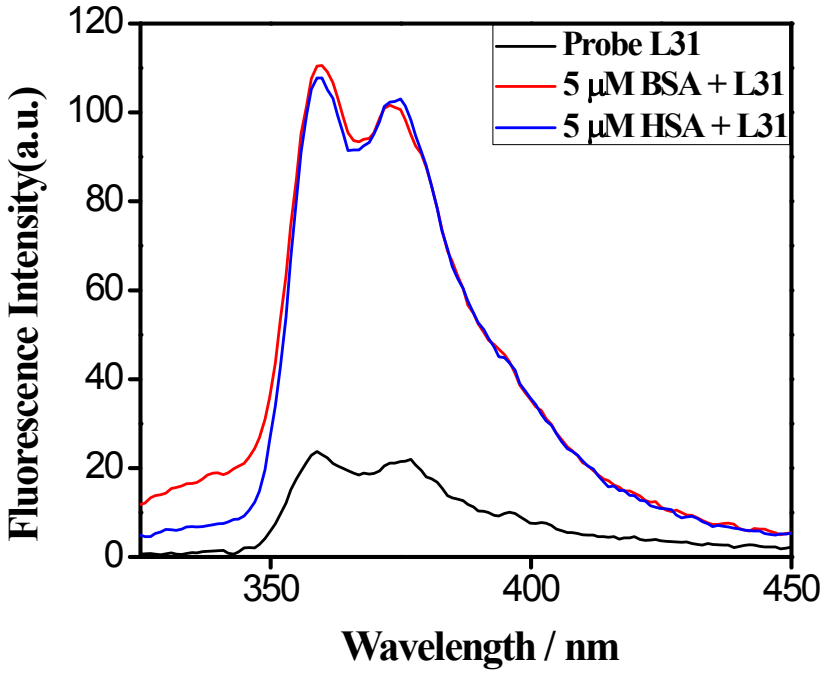

Fig. S10 Fluorescence response of **L31** (5μM) in the presence of 5 μM HSA, BSA in PBS buffer (pH = 7.4), λ_{exc} = 304nm.

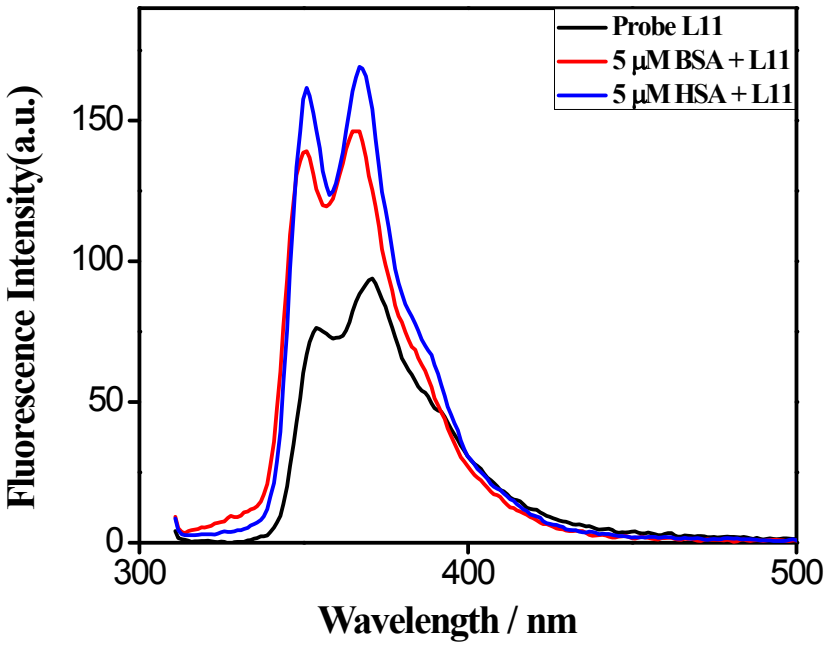

Fig. S11 Fluorescence response of **L11** (5μM) in the presence of 5 μM HSA, BSA in PBS buffer (pH = 7.4), λ_{exc} = 304nm.

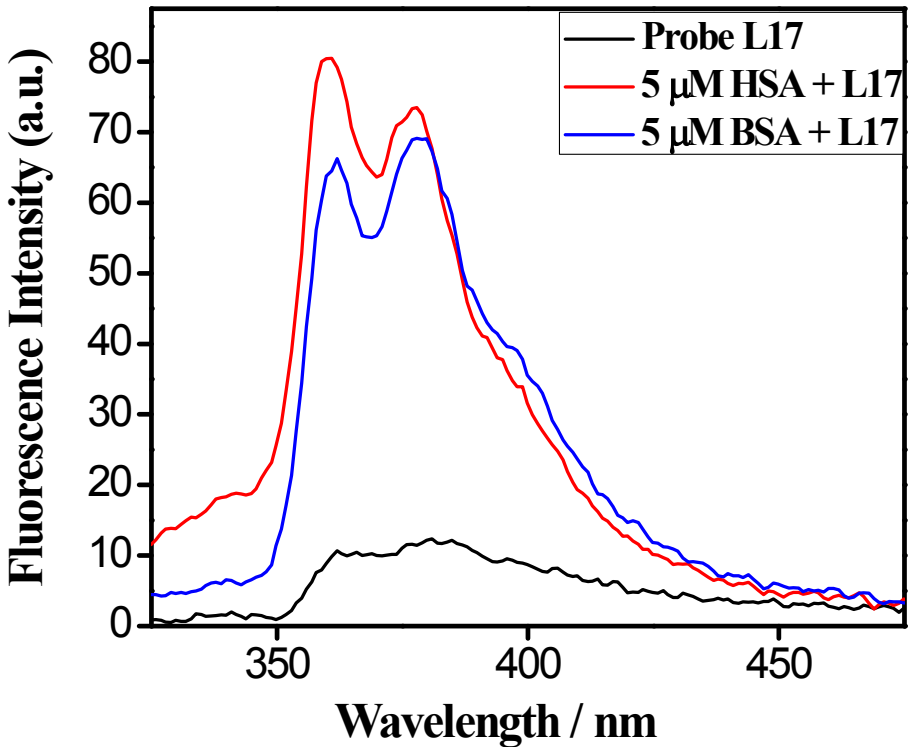

Fig. S12 Fluorescence response of **L17** (5μM) in the presence of 5 μM HSA, BSA in PBS buffer (pH = 7.4), λ_{exc} = 304nm.

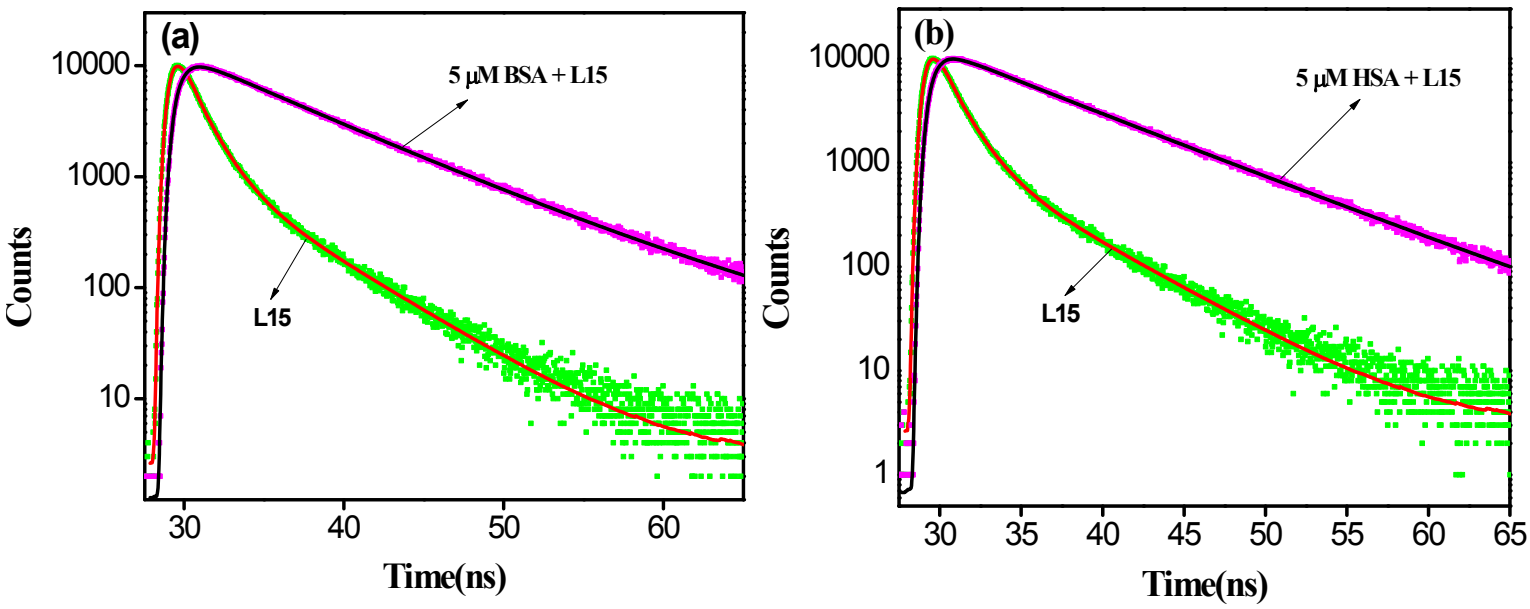

Fig. S13 Time resolved fluorescence spectra of **L15** with a) BSA and b) HSA (5 μM) respectively.

Table S3 Lifetime data of **L15** in the presence of HSA and BSA

Serial No	**Sample**	λ_{max}	τ_1	τ_2	τ_3	α_1	α_2	α_3	τ_m	χ^2
1	**L15**	395	1.3175	.3885	4.9282	.0179	.0498	.00287	.8097	1.07
2	**L15** with BSA	395	6.61	13.446	-	.02432	.00197	-	7.122	1.11
3	**L15** with HSA	395	6.436	8.636	-	.01944	.007145	-	7.03	0.99

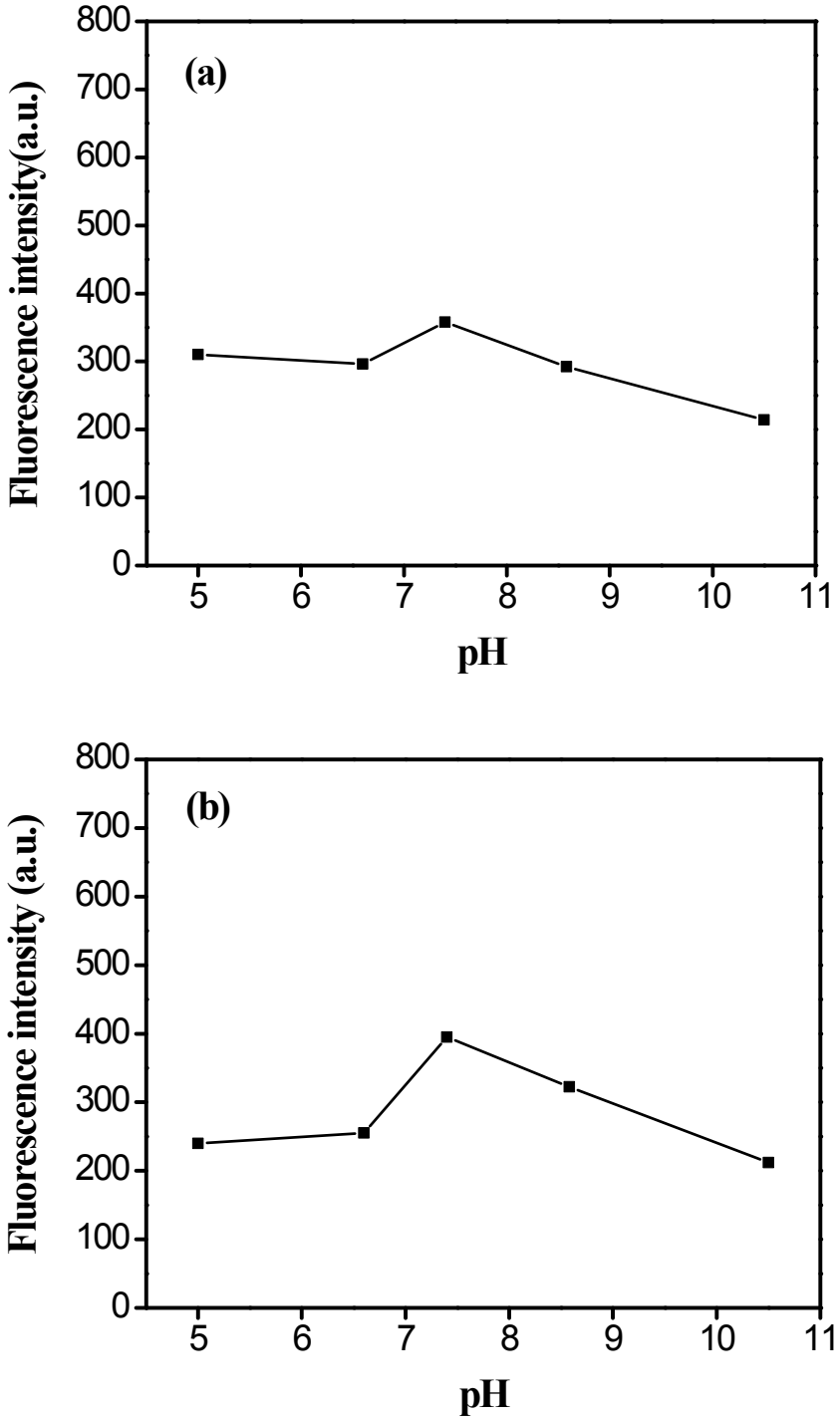

Fig. S14 The effect of pH on the interaction of **L15** with (a) BSA, (b) HSA. Here the concentration of serum albumins and **L15** are 5 μM.

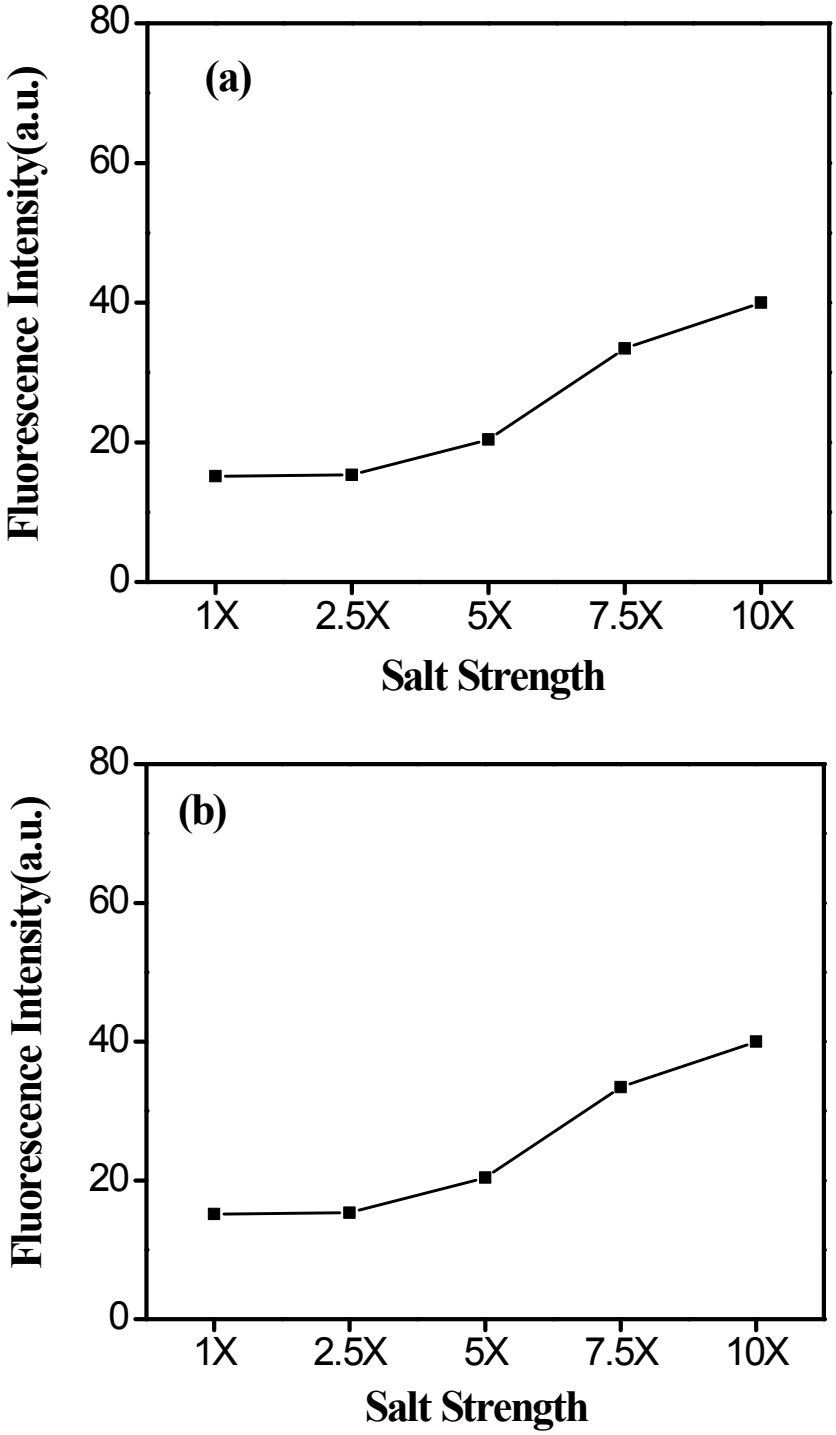

Fig. S15 The effect of salt strength on the interaction of **L15** with (a) BSA, (b) HSA. Here the concentrations of serum albumins and **L15** are 5 μM.

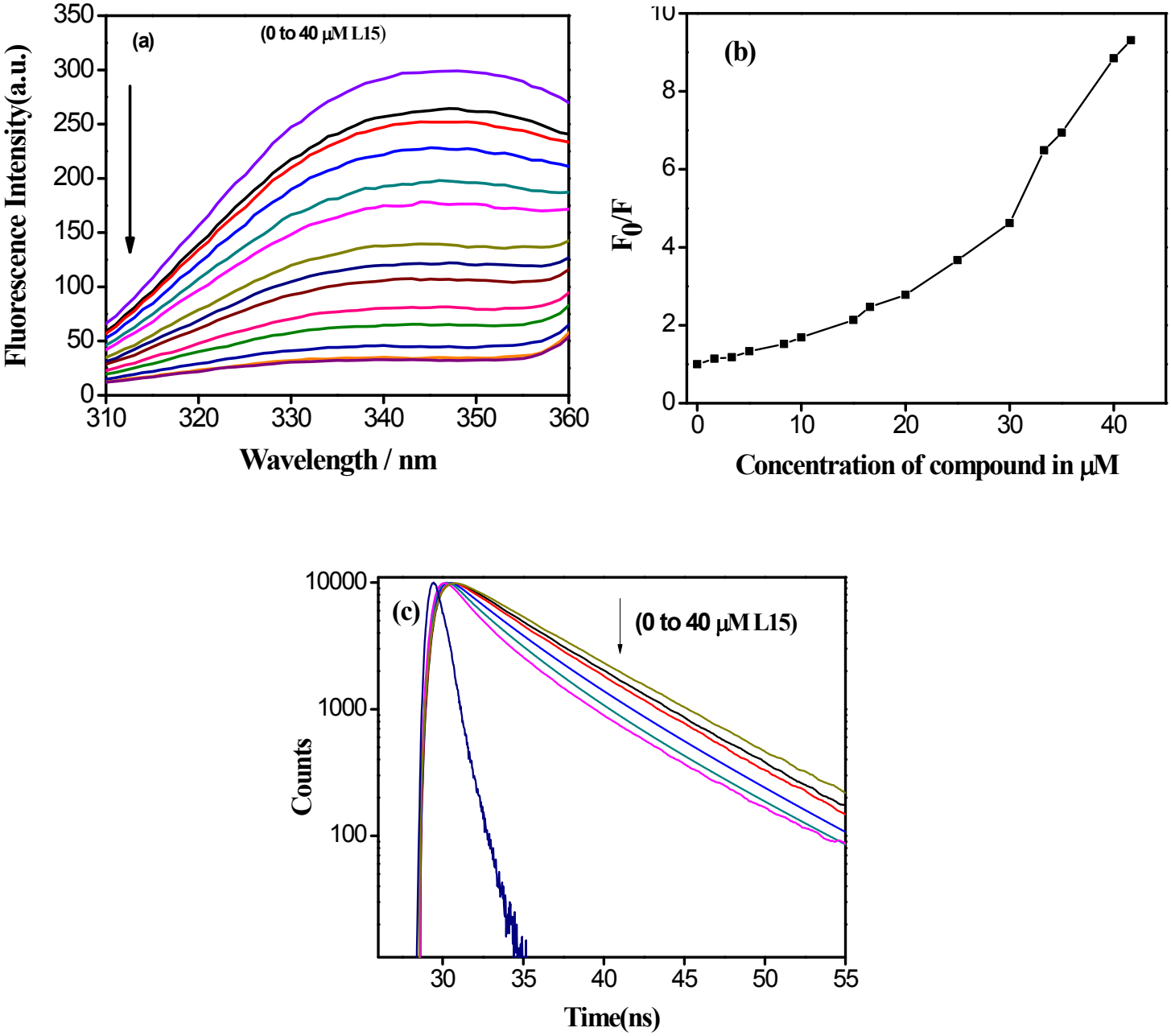

Fig. S16 a) Florescence quenching of BSA (10 μM) by **L15** (0 to 40 μM), b) Stern – Volmer plot of probe – protein composites. c) Time resolved fluorescence quenching decays of BSA (10 μM) in the presence of **L15** (0 to 40 μM).

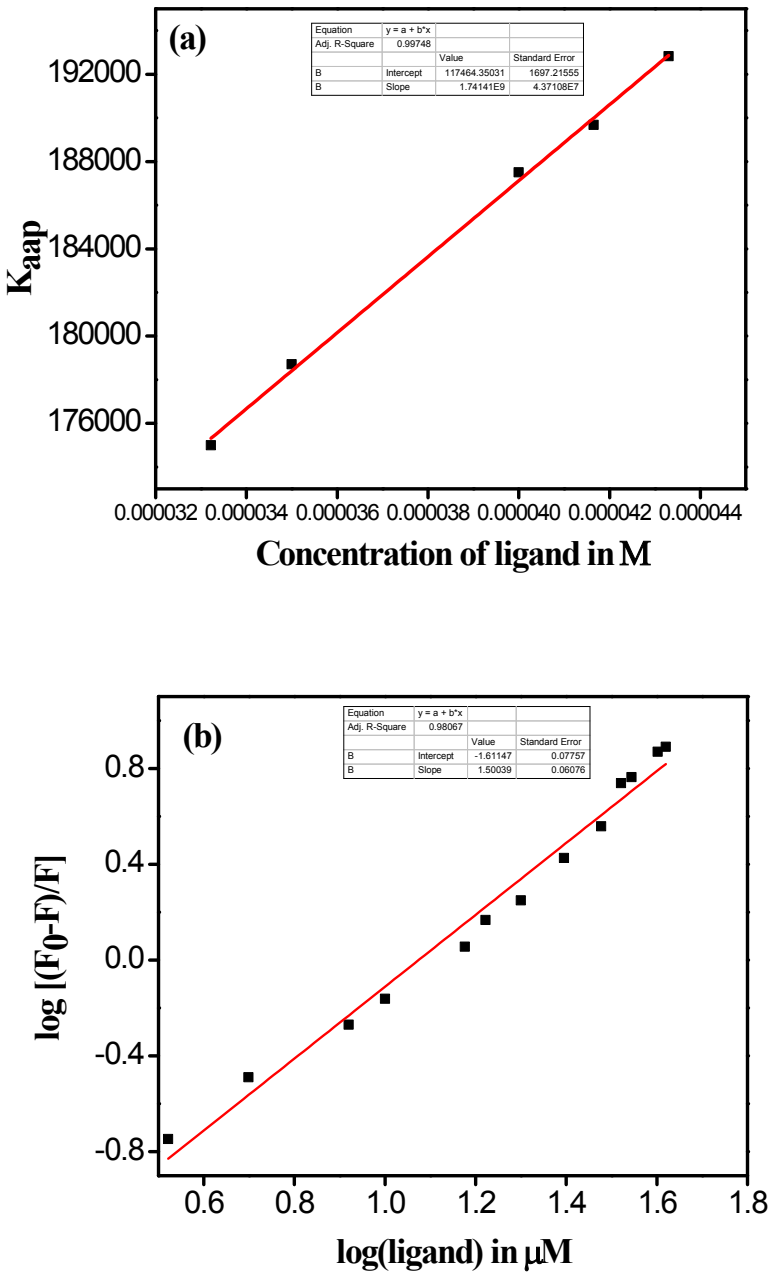

Fig. S17 a) Plot of K_{app} *Vs* the concentration of probe, b) Plot of log [$(F_0$-F)/F] *Vs* log [probe] for probe – protein (BSA) composites in PBS at pH = 7.4.

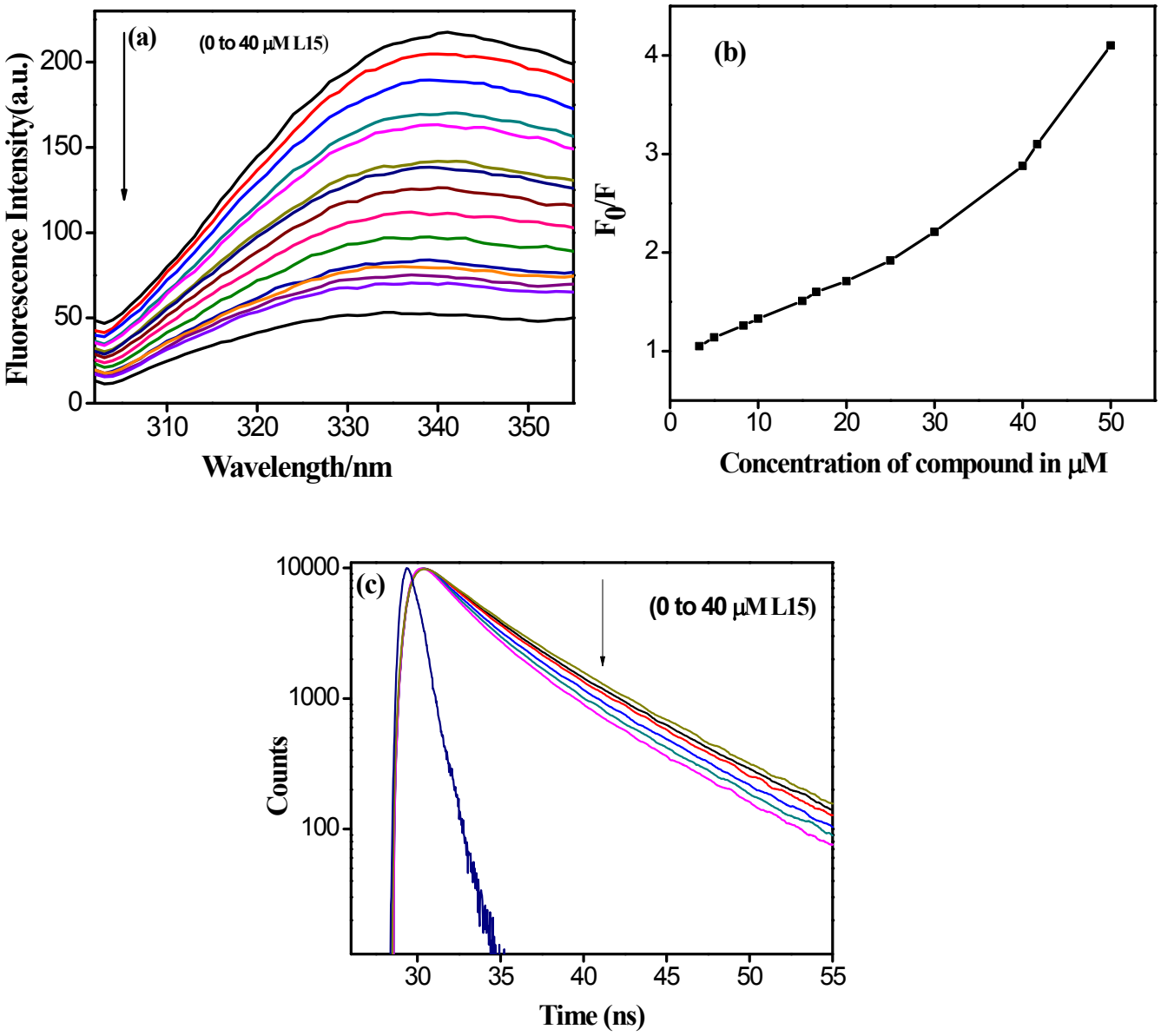

Fig. S18 a) Florescence quenching of HSA (30 μM) by **L15** (0 to 40 μM), b) Stern – Volmer plot of probe – protein composites. c) Time resolved fluorescence quenching decays of HSA (30 μM) in the presence of **L15** (0 to 40 μM).

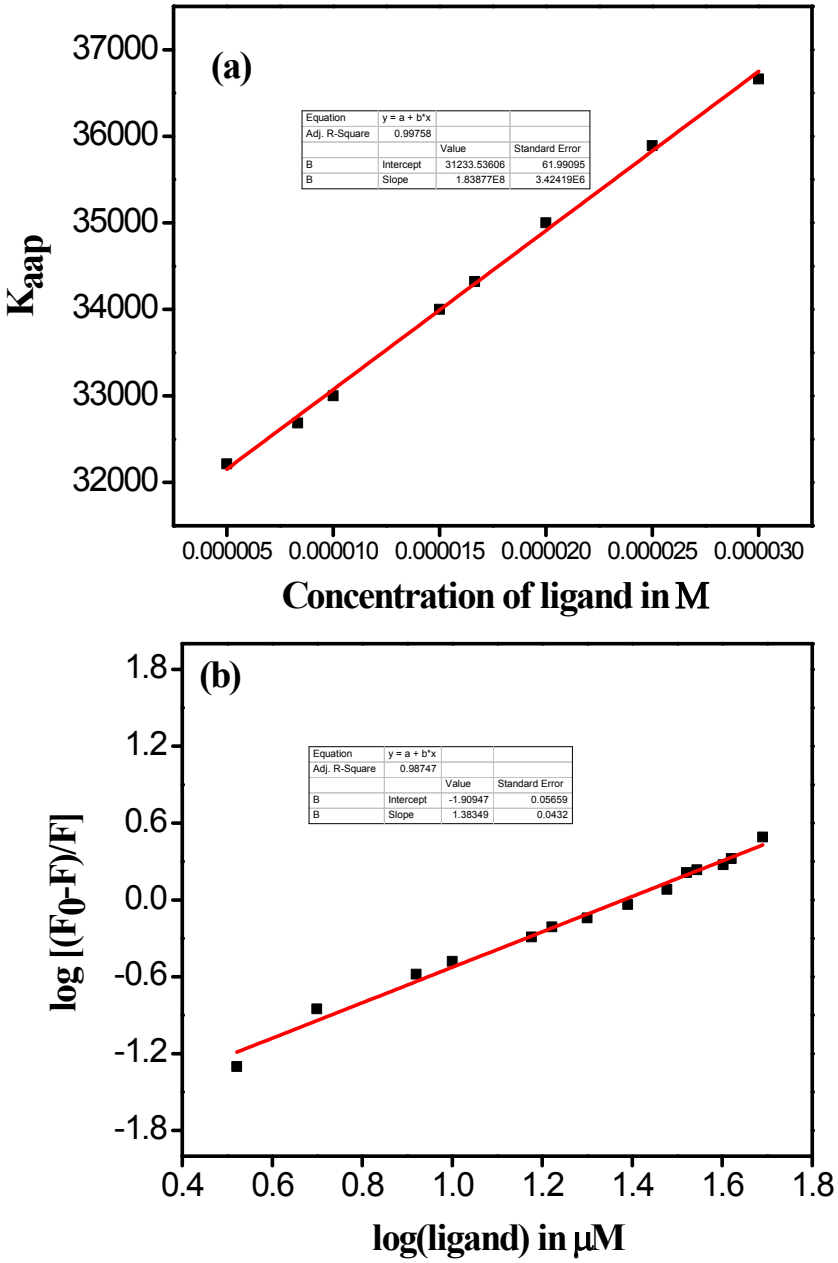

Fig. S19 a) Plot of K_{app} *Vs* the concentration of probe, b) Plot of log [(F_0-F)/F] *Vs* log [probe] for probe – protein (HSA) composites in PBS at pH = 7.4.

Table S4 Quenching parameter of **L15** in the presence of HSA and BSA

	K_S (M^{-1})	K_D (M^{-1})
L15 with BSA	7.8×10^3	2.34×10^4
L15 with HSA	1.73×10^4	10×10^4

Table S5 Time resolved fluorescence quenching decay parameters of HSA and BSA in the presence of **L15**

Serial No	Sample	λ_{max}	τ_1	τ_2	τ_3	α_1	α_2	α_3	τ_m	χ^2
1	Native BSA	345	5.33	7.865	-	.02098	.00654	-	5.93	1.12
2	BSA + 5 μM dye	395	3.309	6.32	-	.009855	.01858	-	5.27	1.06
3	BSA + 10 μM dye	395	1.053	4.227	6.758	.00466	.0149	.011	4.65	1.05
4	BSA + 20 μM dye	395	3.182	.593	6.259	.0144	.0118	.012	3.59	1.13
5	BSA + 30 μM dye	395	3.046	.537	6.550	.0157	.0209	.0078	2.48	1.11
6	BSA + 40 μM dye	395	2.959	.4915	7.196	.0166	.0312	.0054	1.93	1.07
7	Native HSA	345	1.014	3.78	7.482	.00767	.0160	.0088	4.13	1.08
8	HSA + 5 μM dye	395	.818	3.318	7.189	.0088	.01647	.0093	3.72	1.09
9	HSA + 10 μM dye	395	.830	3.355	7.252	.0101	.0171	.0081	3.53	1.09
10	HSA + 20 μM dye	395	1.033	3.466	7.35	.0134	.0163	.0063	3.24	1.08
11	HSA + 30 μM dye	395	.801	2.975	6.98	.0145	.01768	.006	2.85	1.16
12	HSA + 40 μM dye	395	.793	2.91	6.95	.017	.0176	.0057	2.60	1.11

Table S6 Association constant of **L15** with proteins

Probe with protein	**Association Constant (M^{-1})**
L15 + HSA	1.23×10^4
L15 + BSA	2.44×10^4

Docking result

The molecular modeling of the probe with HSA was analyzed using Autodock 4.2. The close view of the molecular simulation analysis clearly (<1 Å) showed that the most stable conformations (according to the energy) of **L15**-HSA complex were resulted from the binding of **L15** to the binding site–I of HSA near TRP-214 amino acid. The encapsulation of **L15** in the hydrophobic environment, created by the amino acid residues, along with the presence of π-π stacking interaction with TRP-214 led to stabilization of **L15** in the site-I binding pocket of HSA (Fig. S21a, S21c). The molecular simulation analysis demonstrated the existence of two stable conformations of **L15**-HSA complex with negligible energy difference of 0.03 K.cal.mole^{-1}. In the second conformation, the hydrophobic interaction of **L15** with nonpolar amino acids residues and the hydrogen bonding between the –OH group of **L15** and the carboxylic acid group of glutamine with a distance of 2.014 Å further enhanced the binding interaction of **L15** at site-I of HSA (Fig. S20a, S20c). Moreover, the cluster distribution showed that **L15** has almost equal distribution in two binding sites (one arises from π-π stacking and another one from H-bonding) with 7 Å (in the case of π-π stacking) and 24.04 Å (in the case of H-bonding) intermolecular distances from TRP-214 of HSA (Fig. S20b, Fig. S20d, Fig. S21b). Interestingly, experimental findings from FRET process revealed a 25.46 Å intermolecular distance between **L15** and tryptophan residue of HSA which was in close agreement with the molecular simulation results (24 Å) for the second conformation. However, for the first conformation, the computational distance was bit different from the FRET calculated one (Fig. S21b). As reported in the literature[6], this could be possibly due to the difference in the X-ray structure of the protein from crystals and from the aqueous system (the experimental medium). As a result, there are many factors including difference in the microenvironment are not considered during docking studies.

a)

b)

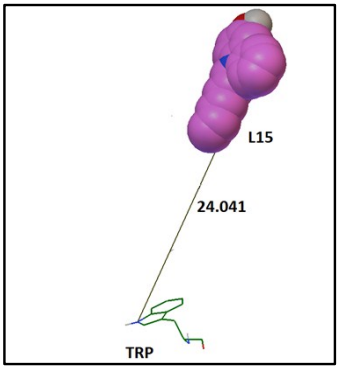

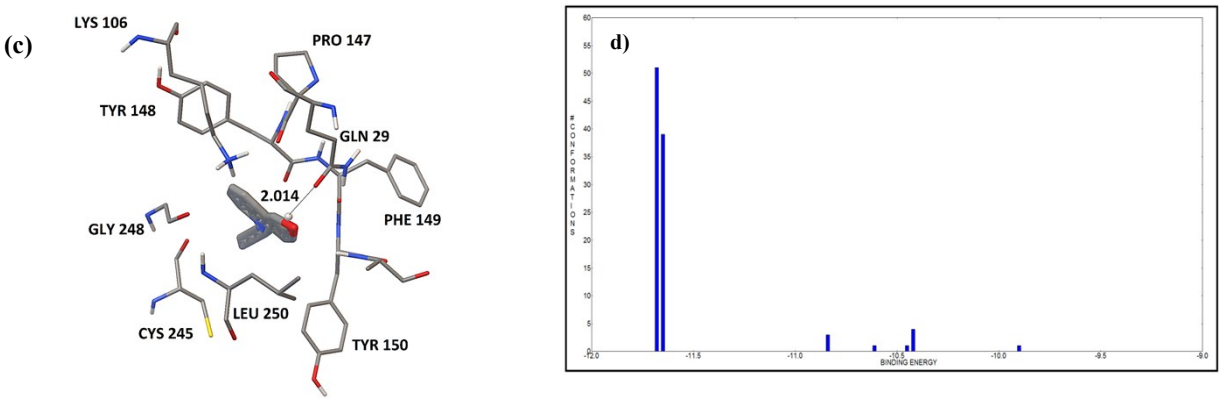

Fig. S20 a) Protein- **L15** complex in 2nd conformation, b) distance between TRP 214 and **L15** in 2nd conformation, c) contact amino acid residues in protein-**L15**complex in 2nd conformation, d) cluster distribution picture of **L15-**protein complex conformations.

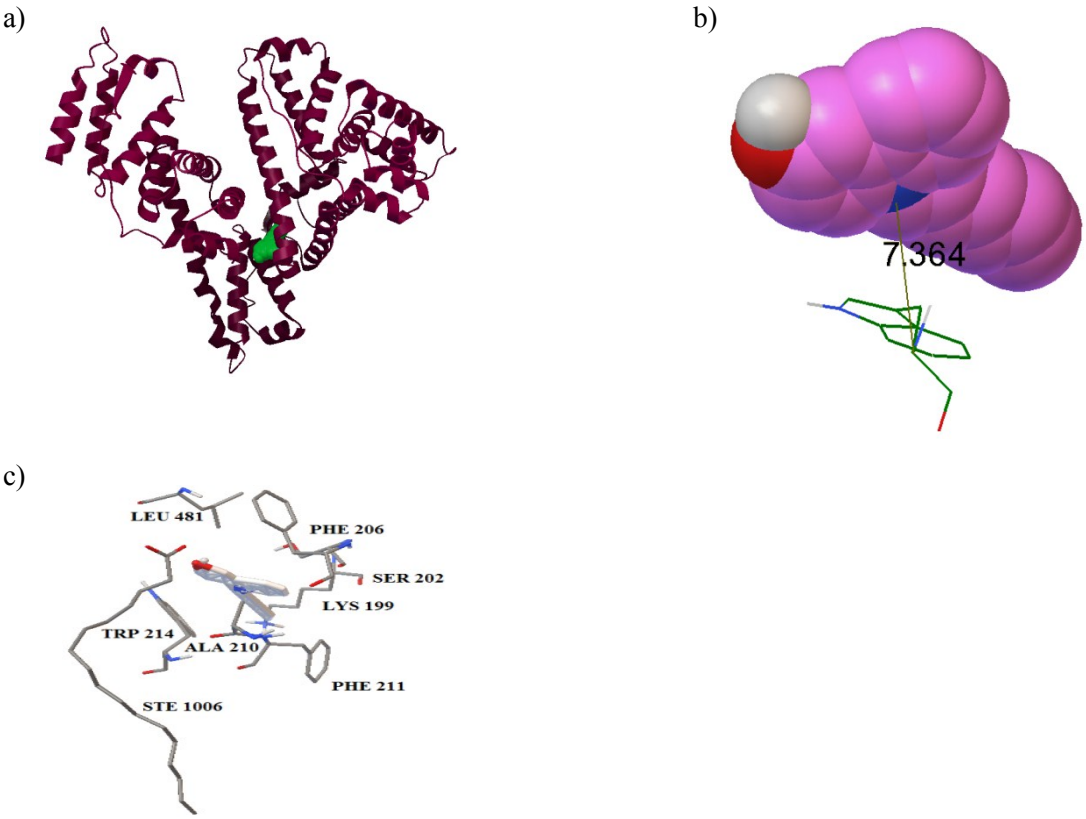

Fig. S21 a) Protein- **L15** complex in 1st conformation, b) distance between TRP 214 and **L15** in 1st conformation, c) contact amino acid residues in protein-**L15**complex in 1st conformation.

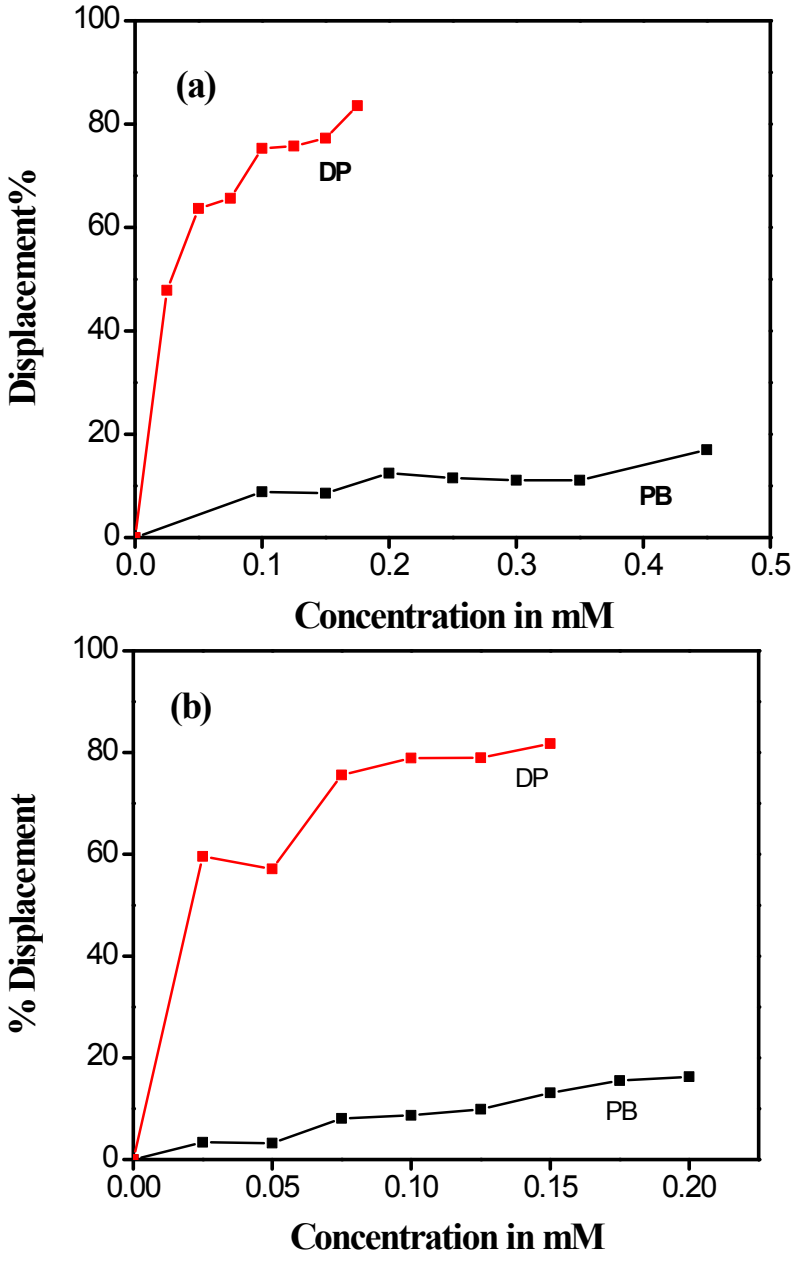

Fig. S22 (a) Displacement of **L15** (%) from BSA-**L15** complex upon the addition of PB and DP and (b) Displacement of probe **L15** (%) from the HSA-**L15** complex upon the addition of PB and DP.

Table S7 Photophysical parameters of **L15** in the presence of protein

Compound	Protein	Anisotropy	ϕ	$K_{n.r \times 10^8}$ (S^{-1})	ΔG(kj mol^{-1})
L15	-	.002	.003	12.2	-
L15	BSA	.041	.213	1.1	-28
L15	HSA	.03	.215	1.11	- 23.33

"**FRET Processes:** We observed that the absorption spectra of **L15** overlaps with the emission spectra of BSA/HSA. As these events lead to efficient energy transfer from probe to protein resulting in fluorescence signaling through FRET process, we became curious to use FRET technique in order to know the distance between the tryptophan unit of protein and the **L15** in protein–**L15** complex. While BSA/HSA showed strong absorption at 295 nm with emission range 300-380 nm (when excited at 295 nm),[7] the probe **L15** alone showed very poor absorption at 295 nm with negligible emission when excited at 295 nm (Fig. S23). The probe **L15** showed strong absorption at 304 nm with a strong emission at 395 nm when excited at 304 nm. Detailed overlap integral picture is shown in Fig. S24. All these results indicated that when HSA/BSA were excited at 295 nm in the presence of **L15** the protein emission was absorbed by **L15** (FRET process) resulting in strong emission at 395 nm from **L15** (Fig. 2a, Fig. S25). The energy transfer efficiency (E) is related to the distance between tryptophan and probe (R), and was calculated using the following equation,

$$\boldsymbol{E = R_0^6/ (R_0^6 + r^6) = 1 - F_0/F}$$

Here **F** is the fluorescence intensity of BSA/HSA in the presence of **L15**, $\mathbf{F_0}$ is the fluorescence intensity of BSA/HSA alone, **r** is the distance between the acceptor (**L15**) and donor (protein) molecule, $\mathbf{R_0}$ is the distance between donor and acceptor when energy transfer efficiency is 50%. R_0 was calculated using the following equation,

$$\boldsymbol{R_0 = 0.211[k^2 n^{-4} \Phi_D J(\lambda)]^{1/6}}$$

The R_0 value for BSA and HSA were calculated to be 25.22 Å and 25.46 Å respectively which were in good agreement with the FRET process. Here k^2 is the orientation factor, n is the refractive index of the medium, Φ_D is the quantum yield of the donor, *J* is the spectral integral of

the donor emission spectra and acceptor's absorption spectra. *J* is calculated from the following equation,

$$J = \frac{\int_0^{\infty} F_D(\lambda)\varepsilon(\lambda)\lambda^4 d\lambda}{\int_0^{\infty} F_D(\lambda) d\lambda}$$

Here F_D represents fluorescent intensity of donor at wavelength λ and ε is molar extinction coefficient of acceptor at wavelength λ. In the present case, the values of k, n and Φ_D are 2/3, 1.336, 0.118 respectively. *J* is obtained by integrating the overlapped portion of donor′s emission and acceptor's absorption spectra shown in Fig. S24. The values of J for BSA and HSA were in the order of 10^{14}, and r values are 17.73 Å and 21.05 Å for BSA and HSA respectively. These r values suggested that the tryptophan unit is close to probe molecule in protein-probe complex, and therefore the quenching of tryptophan emission is due to efficient energy transfer from tryptophan to probe (Fig. S26).

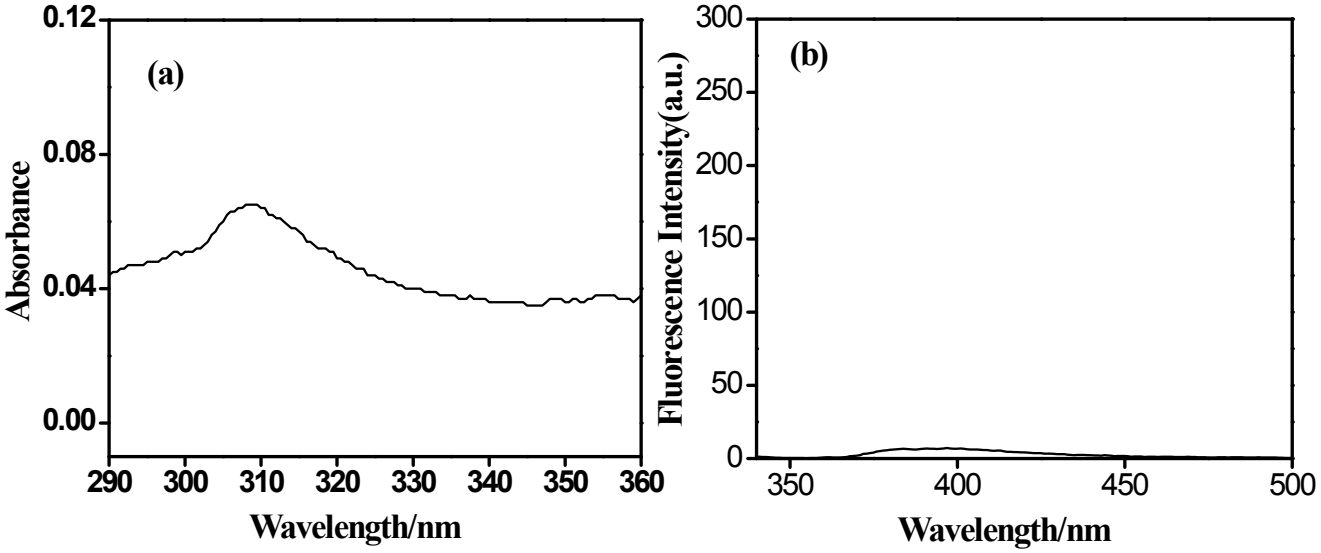

Fig. S23 a) UV-vis spectra of L15, b) fluorescence emission spectra of L15 while excitation at 295 nm of wavelength.

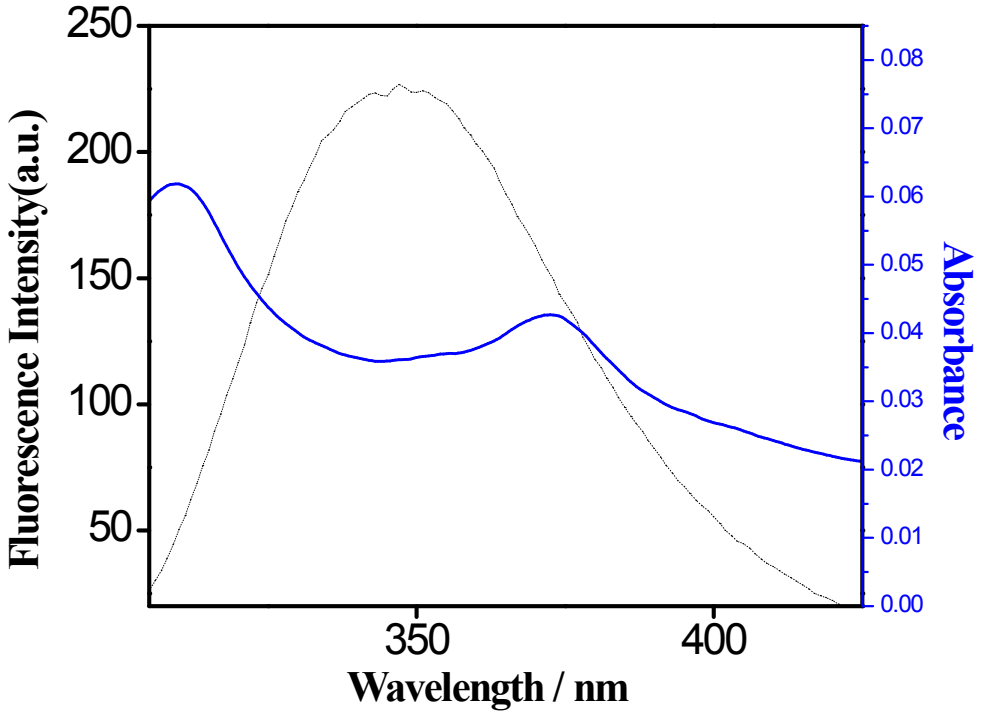

Fig. S24 The overlap of the fluorescence spectra of HSA (dotted line) and the absorption spectra of **L15** (solid line).

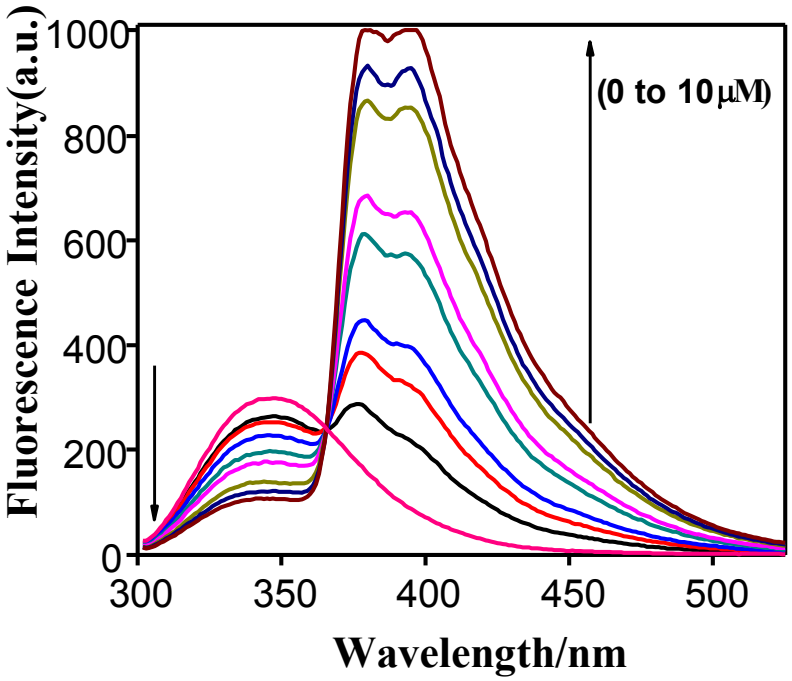

Fig. S25 Fluorescence emission spectra of **BSA** (10μM) with increasing concentration of **L15** (0-10 μM).

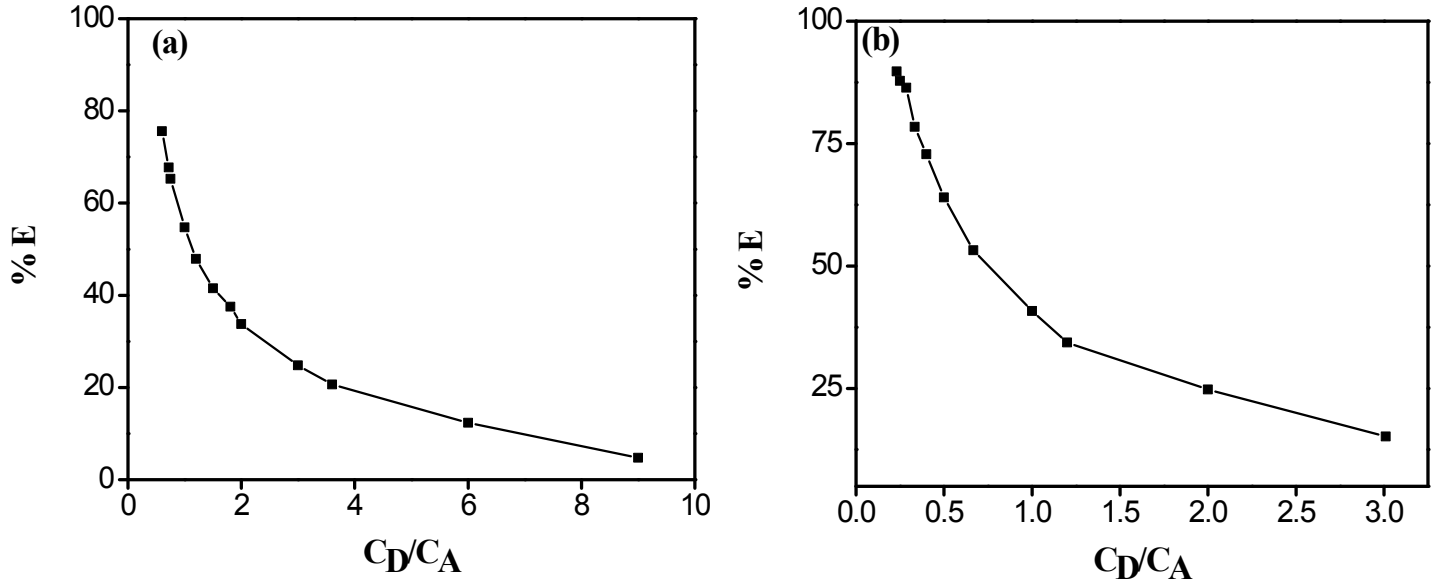

Fig. S26 Energy transfer efficiency (in percentage) from a) HSA to **L15**, b) BSA to **L15.**

Table S8 Energy transfer parameter for different protein probe composites

	Molar extinction coefficient	**J ($M^{-1}cm^{-1}nm^4$)**	**R_0 (Å)**	**r (Å)**	**E**
L15 + HSA	1.303×10^3	1.1943×10^{14}	25.46	21.05	0.7561
L15 + BSA	1.303×10^3	1.20×10^{14}	25.223	17.738	0.89735

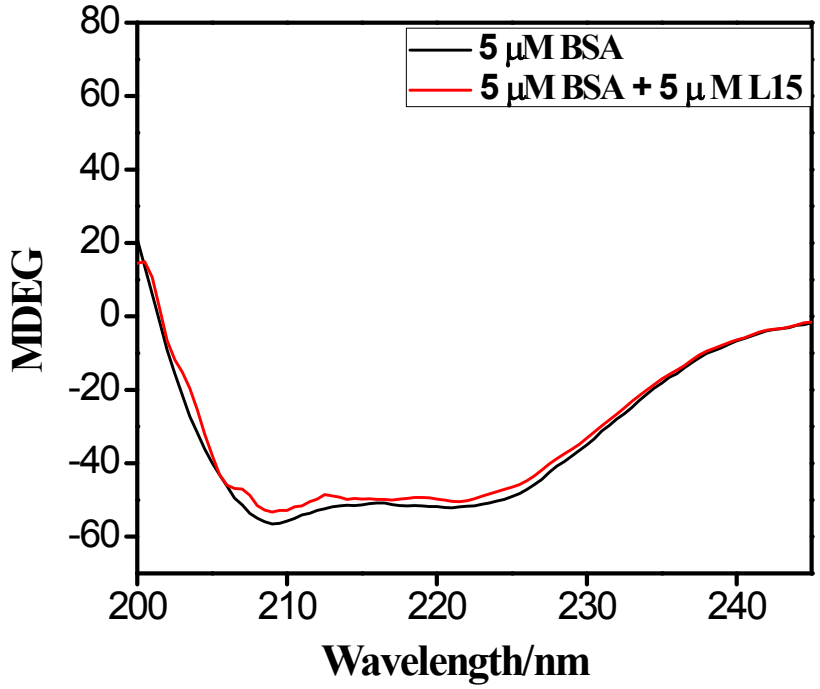

Fig. S27 Circular dichroism spectra of BSA in the presence of **L15** in PBS (10X).

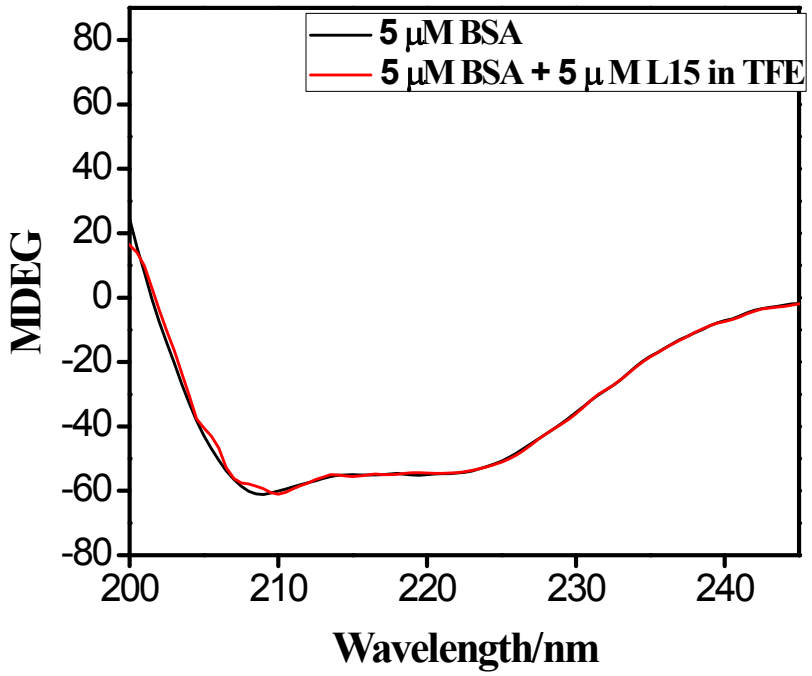

Fig. S28 Circular dichroism spectra of BSA in the presence of **L15** in 10 % TFE and 90 % PBS (10X).

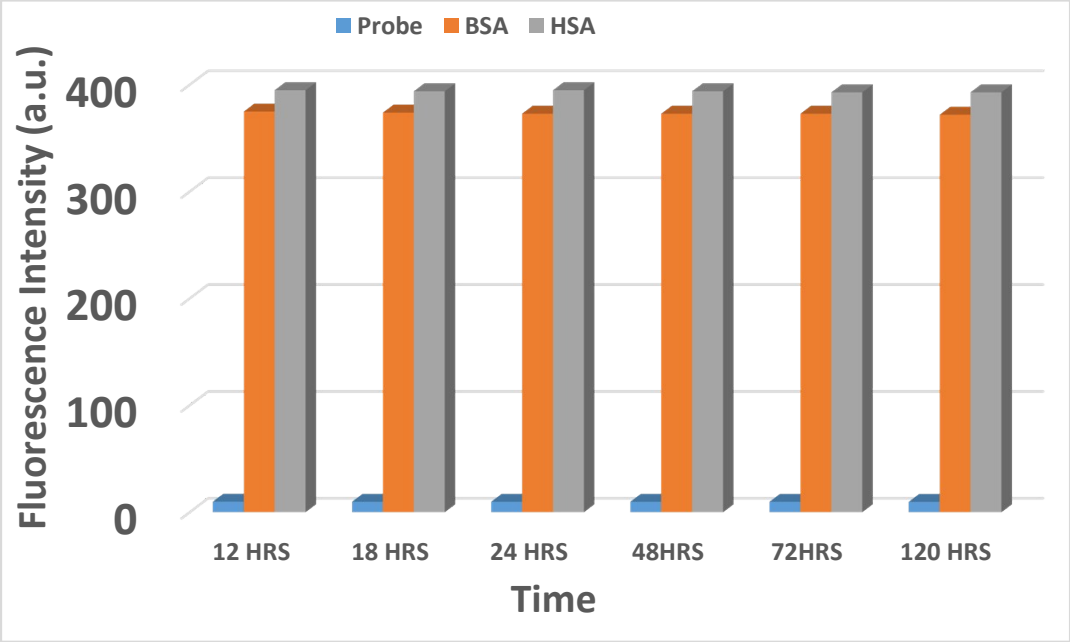

Fig. S29 Photostability of **L15** in laboratory condition.

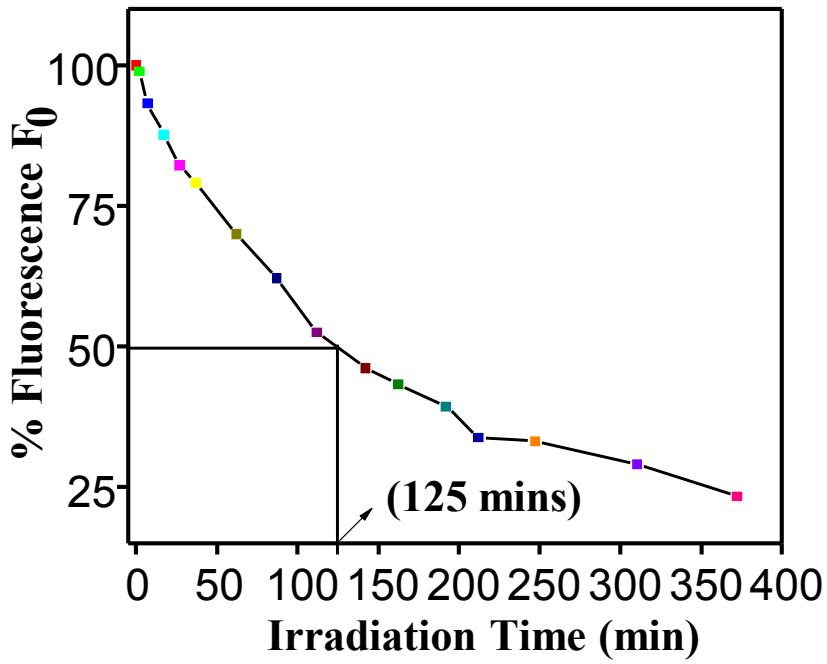

Fig. S30 Photostability of **L15** in the presence of 5 μM HSA and illuminated by laser - light (488 nm, 145mW)

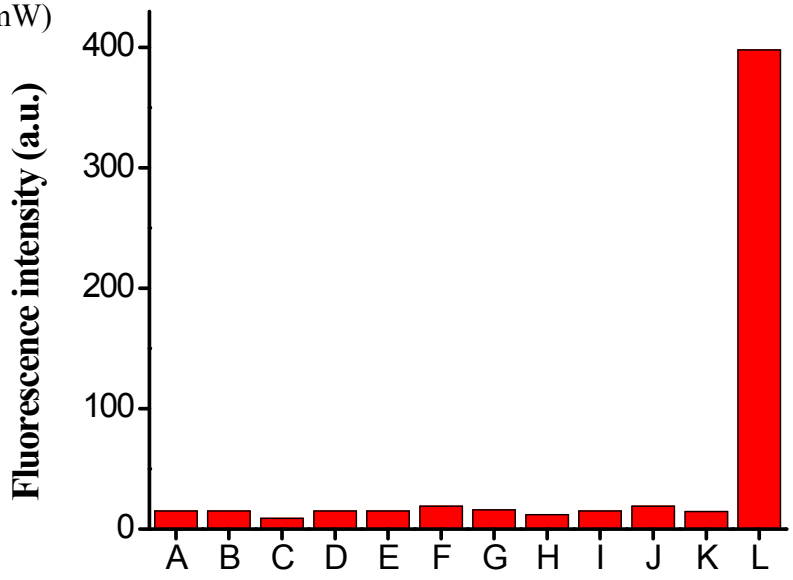

Fig. S31 Fluorescence response of **L15** (5 μM) in the presence of different cations. [A = Na^{+}, B = Zn^{2+}, C = Ni^{+}, D = K^{+}, E = Al^{3+}, F = Fe^{2+}, G = Cd^{2+}, H = Cu^{2+}, I =Hg^{2+}, J = Ca^{2+}, K = Cu^{+}, L = HSA.] Here the concentrations of all cations are 20 μM.

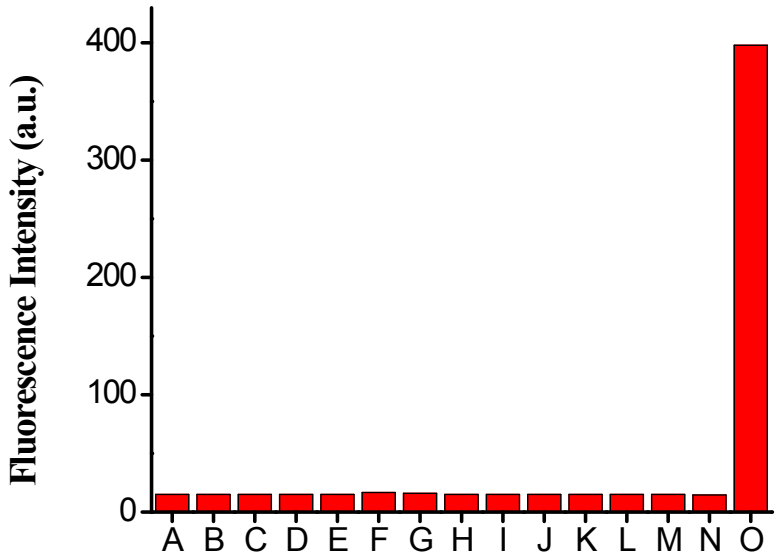

Fig. S32 Fluorescence response of **L15** (5 μM) in the presence of different anions. [A = I^-, B = Br^-, C = F^-, D = OAc^-, E = Cl^-, F = CO_3^{2-}, G = SO_4^{2-}, H = SO_3^{2-}, I = HS^-, J = ClO_3^-, K = $S_2O_3^{2-}$, L = NO_3^-, M = NO_2^-, N=$C_2O_4^{2-}$, O = HSA.] Here the concentrations of all anions are 20 μM.

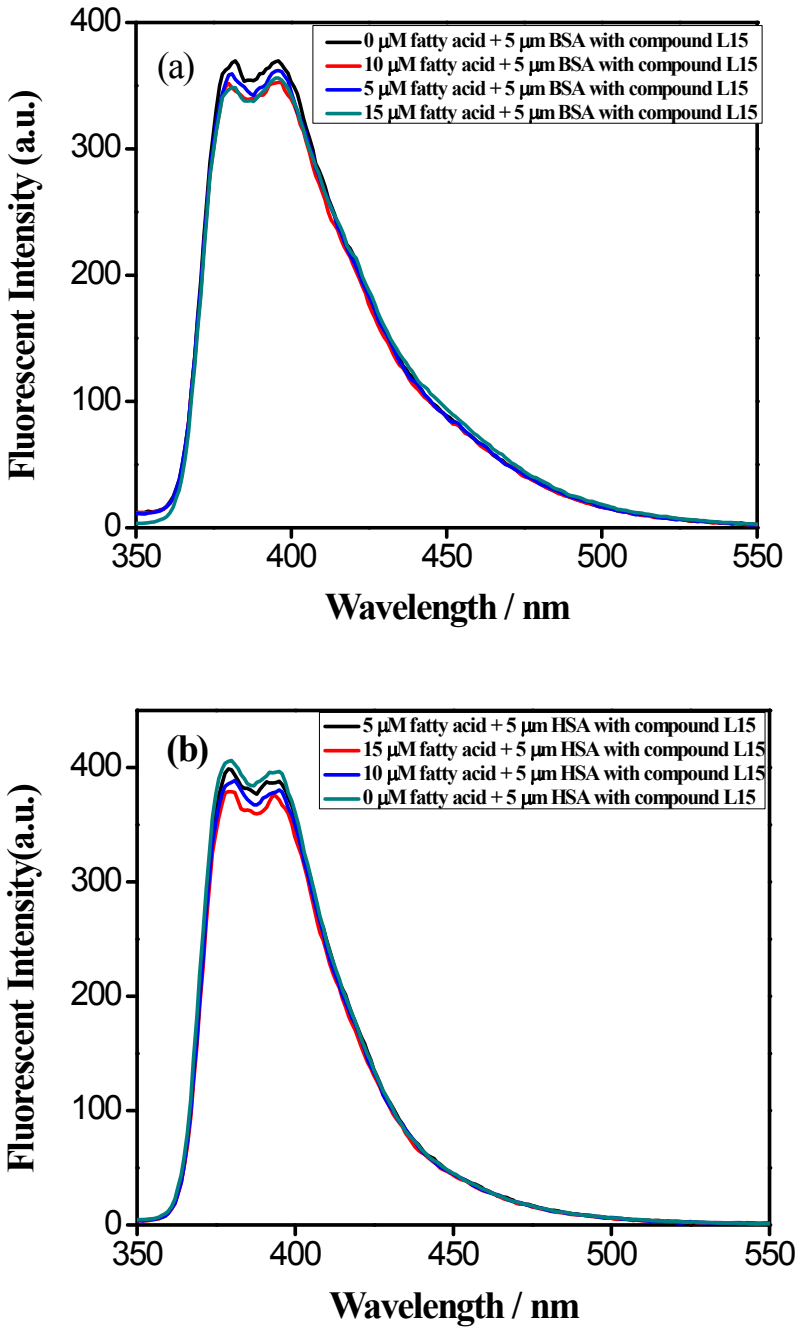

Figure S33. The effect of fatty acid (isovaleric acid) (5 μM) on fluorescence emission spectra of (a) **L15** in the presence of BSA (5 μM); (b) **L15** in the presence of HSA (5 μM).

Table S9 Interaction of **L15** with blood serum - analytical parameters

Compound	**Protein**	**Linear Range**	**Regression Equation**	**Co-efficient**
L15	HSA in blood serum	0.001 - .4 μM	I_f= 548.11C + 30.72	0.9863

Table S10 Interaction of **L15** with HSA in 10 % urine - analytical parameters

Compound	**Protein**	**Linear Range**	**Regression Equation**	**Co-efficient**
L15	HSA in Urine (10%)	0.02 - .75 μM	I_f= 119.91 C + 45.16	0.99

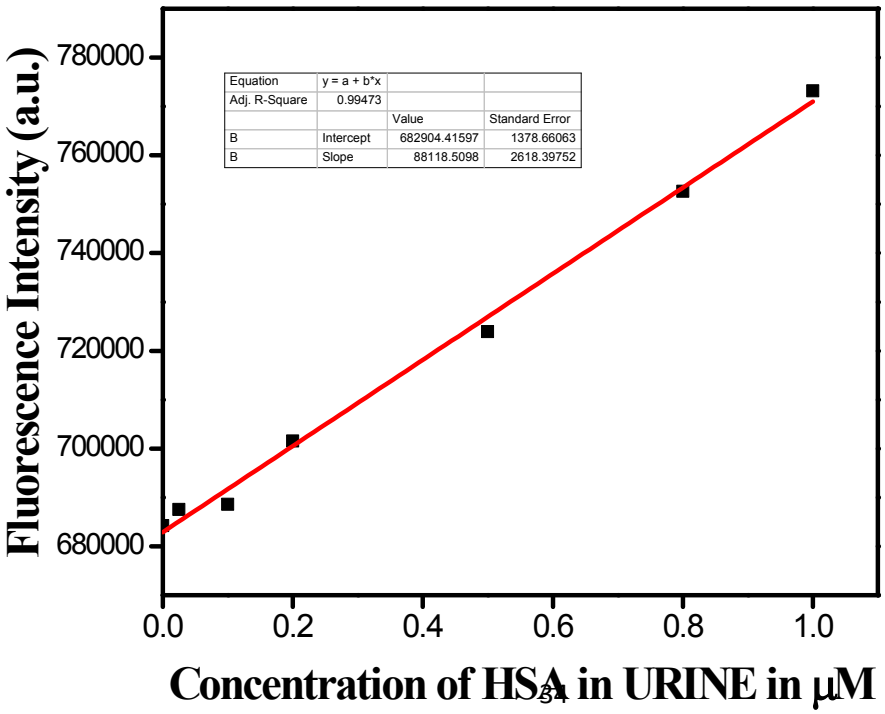

Fig. S34 Fluorescence response of **L15** (10 μM) toward HSA in undiluted urine.

Table S11 Interaction of **L15** with HSA in urine - analytical parameters

Compound	**Protein**	**Linear Range**	**Regression Equation**	**Co-efficient**
L15	HSA in Urine	0.025 - 1 μM	I_f = 88118.5 C + 682904	0.99

General procedure for the synthesis of 6 – 10:

Alkylation of carbazole was done following literature procedure.[8] Alkylated product (1 equiv) was dissolved in dry DMF at 0 °C. After that, phosphorus oxychloride (1.5 equiv) was added in the solution with vigorous stirring at 0 °C under nitrogen atmosphere. Then the reaction mixture was allowed to come to room temperature and left stirring for 20 min followed by microwave heating (P = 10, T = 105 C) for 30 minutes. The resulting mixture was then was cooled to room temperature and extracted with ethyl acetate and water. The organic layer was collected and dried over anhydrous sodium sulfate. The volatiles were removed under vacuum, the crude product was purified using column chromatography.

[9-ethyl-9H-carbazole-3-carbaldehyde] (6)

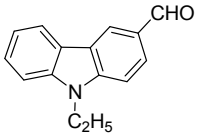

^{1}H-NMR (500 MHz, $CDCl_3$): δ 10.07(s, 1H), 8.58(s, 1H), 8.14(d, *J* = 8.25 Hz, 1H), δ 8.0(d, *J* = 8.95 Hz, 1H), δ 7.54 – 7.51(m, 1H), 7.45(d, *J* = 8.95 Hz, 2H), 7.33(t, *J* = 7.55 Hz, 1H), 4.39 – 4.35(m, 2H), 1.46(t, *J* = 7.55 Hz, 3H).

^{13}C-NMR (125 MHz, $CDCl_3$): δ 191.8, 143.5, 140.6, 128.4, 127.1, 126.7, 123.9, 123.1, 122.9, 120.7, 120.2, 109.1, 108.6, 37.9, 13.8.

HRMS (ESI): Calc. for $C_{15}H_{13}NO$ $[M]^+$: 223.0097; Found: 224.1081.

IR ν_{max} : 3054, 2980, 2827, 2746, 2356, 1668, 1577, 1329, 1223 cm^{-1}.

Physical Properties: Yellow solid (960 mg, 84% yield, 4.29 mmol, m.p. 85 ˚C).

[9-butyl-9H-carbazole-3-carbaldehyde] (7)

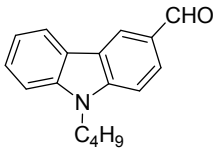

^{1}H-NMR (500 MHz, $CDCl_3$): δ 9.97(s, 1H), 8.48(s,1H), 8.04(d, *J* = 7.55 Hz, 1H), 7.9(dd, *J* = 8.9, 1.37 Hz, 1H), 7.44 – 7.41(m, 1H), 7.35(d, *J* = 8.95 Hz, 2H), 7.23(t, *J* = 7.55 Hz, 1H), 4.21(t, *J* = 7.22 Hz, 2H), 1.78 – 1.72(m, 2H), 1.33 – 1.16(m, 2H), 0.86(t, *J* = 7.6 Hz, 3H).

^{13}C-NMR (125 MHz, $CDCl_3$): δ 191.5, 143.7, 140.8, 128.1, 126.8, 126.4, 123.6, 122.7, 122.6, 120.4, 119.9, 109.1, 108.6, 42.8, 330.7, 20.2, 13.6.

HRMS (ESI): Calc. for $C_{17}H_{18}NO$ $[M+H]^+$: 252.1388; Found: 252.1383.

IR ν_{max} : 2954, 2872, 2727, 2356, 1685, 1594, 1468, 1332 cm^{-1}.

Physical Properties: Yellow viscous liquid (980 mg, 87.1% yield, 4.38 mmol).

[9-hexyl-9H-carbazole-3-carbaldehyde] (8)

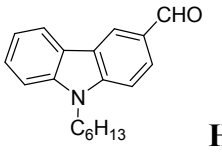

H-NMR (500 MHz, $CDCl_3$): δ 10.09(s,1H), 8.6(s, 1H), 8.16(d, *J* = 8.2 Hz, 1H), 8.01 – 7.99(m, 1.7 Hz, 1H), 7.55 – 7.52(m, 1H), 7.47 – 7.44(m, 2H), 7.33 – 7.3(m, 1H), 4.33(t, *J* = 7.55 Hz, 2H), 1.9 – 1.84(m, 2H), 1.4 – 1.22(m, 6H), 0.88(t, *J* = 6.85 Hz, 3H).

^{13}C-NMR (125 MHz, $CDCl_3$): δ 191.8, 144.1, 141.1, 128.4, 127.1, 126.7, 122.9, 120.7, 120.2, 109.4, 108.9, 43.4, 31.5, 28.9, 26.9, 22.5, 13.7.

HRMS (ESI): Calc. for $C_{19}H_{21}NO$ $[M+H]^+$: 280.1701; Found: 280.1696.

IR ν_{max} : 2918, 2854, 2718, 2365, 1688, 1586, 1468, 1332 cm^{-1}.

Physical Properties: Yellow solid (1 gm., 90 % yield, 3.57 mmol, m.p. 54 ˚C).

[9-octyl-9H-carbazole-3-carbaldehyde] (9)

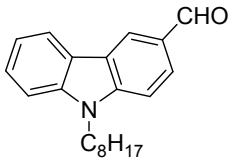

^{1}H-NMR (500 MHz, $CDCl_3$): δ 10.08(s,1H), 8.59(s, 1H), 8.14(d, *J* = 7.55 Hz, 1H), 8.005(dd, *J* = 8.25, 1.37 Hz, 1H), 7.54 – 7.51(m, 1H), 7.45 – 7.43(m, 2H), 7.33(t, *J* = 7.55 Hz, 1H), 4.31(t, *J* = 7.225 Hz, 2H), 1.88 – 1.85(m, 2H), 1.38 – 1.20(m, 10H), 0.86(t, *J* = 6.85 Hz, 3H).

^{13}C-NMR (125 MHz, $CDCl_3$): δ 191.8, 144.0, 141.1, 128.4, 127.1, 126.7, 123.9, 122.96, 122.9, 120.7, 120.2, 109.3, 108.9, 43.4, 31.7, 29.3, 29.1, 28.9, 27.2, 22.6, 14.0.

HRMS (ESI): Calc. for $C_{19}H_{21}NO$ $[M+H]^+$: 308.2014; Found: 308.2013.

IR ν_{max} : 2918, 2854.71, 2709, 2364.9, 1685.69, 1585.5, 1468.3, 1332.1 cm^{-1}.

Physical Properties: Yellow solid (1 gm., 84% yield, 3.24 mmol, m.p. 53 ˚C).

[9-decyl-9H-carbazole-3-carbaldehyde] (10)

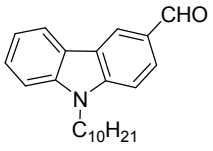

^{1}H-NMR (500 MHz, $CDCl_3$): δ 9.98(s, 1H), 8.49(s, 1H), 8.05(d, *J* = 7.55 Hz, 1H), 7.91(d, *J* = 6.85 Hz, 1H), 7.45 – 7.41(m, 1H), 7.36 – 7.34(m, 2H), 7.24 – 7.21(m, 1H), 4.22(t, *J* = 7.2 Hz, 2H), 1.79 – 1.76(m, 2H), 1.29 – 1.1(m, 14H), 0.79(t, *J* = 7.22 Hz, 3H).

^{13}C-NMR (125 MHz, $CDCl_3$): δ 191.7, 143.9, 141.1, 128.4, 126.6, 122.9, 122.9, 120.7, 120.2, 109.3, 108.9, 43.3, 31.8, 29.4, 29.4, 29.3, 19.2, 27.2, 22.6, 14.1.

HRMS (ESI): Calc. for $C_{23}H_{29}NO$ $[M+H]^+$: 336.2327; Found: 336.2380.

IR ν_{max} : 2927, 2855, 2710, 2365, 1683, 1585, 1468, 1332 cm^{-1}.

Physical Properties: Yellow solid (920 mg, 84.4% yield, 2.82 mmol, m.p. 64 ˚C).

Procedure for the synthesis of L11:

Compound **L9** (1 equiv) was first dissolved in acetone (10 mL) followed by addition of otassium permanganate (4 equivs) under nitrogen atmosphere, and the reaction mixture was refluxed for 5 h at 75 °C. After that the reaction mixture was cooled to room temperature and filtered through sintered funnel. The filtrate was extracted with water and the organic layer was collected. The organic layer was dried over anhydrous sodium sulfate and the volatiles were removed under vacuum. The crude product was purified through column chromatography.

[9-octyl-9H-carbazole-3-carboxylic acid] (L11)

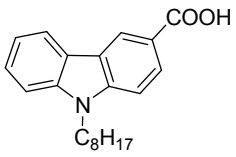

^{1}H-NMR (500 MHz, $CDCl_3$): δ 8.83(s, 1H), 8.17(d, *J* = 7.55 Hz, 1H), 8.08(d, *J* = 7.55 Hz, 1H), 7.44 – 7.41(m, 1H), 7.34 – 7.3(m, 2H), 7.23 – 7.2(m, 1H), 4.21(t, *J* = 8.075 Hz, 2H), 1.8 – 1.76(m, 2H), 1.75 – 1.12(m, 10H), 0.78 – 0.76(t, *J* = 6.85 Hz, 3H).

^{13}C-NMR (125 MHz, $CDCl_3$): δ 173.2, 143.6, 140.9, 127.8, 126.4, 123.7, 122.9, 122.6, 120.7, 119.9, 119.6, 109.3, 108.2, 43.3, 31.7, 29.3, 29.1, 28.9, 27.2, 22.6, 14.0.

HRMS (ESI): Calc. for $C_{21}H_{25}NO_2$ $[M+H]^+$: 324.1964; Found: 324.2077.

IR ν_{max} : 2926, 2855, 2645, 2519, 2365, 1667, 1595, 1169 cm^{-1}.

Physical Properties: Yellow solid (165 mg, 39.28 % yield, 0.051 mmol, m.p. 146 ˚C).

General procedure for the synthesis of L12 – L16

The carbaldehyde derivatives **L6-10** (1 equiv) were taken in a round bottomed flask and dry methanol was added in nitrogen atmosphere. After that hydrogen peroxide (30 % , 1 equiv) ,

concentrated sulphuric acid (0.1 equiv) was added in the reaction mixture in 0 °C in nitrogen atmosphere and the reaction mixture was allowed to stir at room temperature for 2 h. After completion of reaction, as judged by TLC, methanol was removed under vacuum, and the crude was extracted with ethyl acetate and water. The organic layer was collected and dried over anhydrous sodium sulfate, and the volatiles were removed under vacuum. The crude product was purified through column chromatography.

[9-ethyl-9H-carbazol-3-ol] (L12)

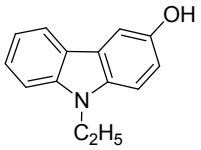

^{1}H-NMR (500 MHz, $CDCl_3$): δ 7.98(d, *J* = 7.6 Hz, 1H), 7.5(d, *J* = 2.75 Hz, 1H),), 7.45 – 7.41(m,1H), 7.35(d, *J* = 8.25 Hz, 1H), 7.24(d, *J* = 8.9 Hz, 1H), 7.17 – 7.14(m, 1H), 7.02 – 7(m, 1H), 4.31 – 4.27(m, 2H), 1.39(t, *J* = 7.22 Hz,3H).

^{13}C-NMR (125 MHz, $CDCl_3$): δ 148.7, 140.5, 135, 125.7, 123.5, 122.4, 120.5, 118.2, 114.5, 108.9, 108.5, 105.9, 37.5, 13.8.

HRMS (ESI): Calc. for $C_{14}H_{13}NO$ $[M]^+$: 211.0997; Found: 212.1069.

IR ν_{max} : 3280, 3051, 2972, 2347, 1677, 1459, 1350, 1178 cm^{-1}.

Physical Properties: White solid (380 mg, 40.16% yield, 1.8 mmol, m.p. 112 ˚C).

[9-butyl-9H-carbazol-3-ol] (L13)

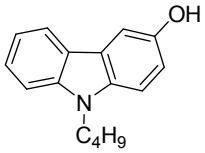

^{1}H-NMR (500 MHz, $CDCl_3$): δ 7.99(d, *J* = 7.6 Hz, 1H), 7.51(s, 1H), 7.45 – 7.42(m, 1H), 7.36(d, *J* = 8.25 Hz, 1H), 7.26(d, *J* = 8.95 Hz, 1H), 7.18 – 7.15(m, 1H), 7.03(dd, *J* = 8.6, 2.4 Hz, 1H), 4.96(s, broad, 1H), 4.25(t, *J* = 7.2 Hz, 2H), 1.84 – 1.78(m, 2H), 1.39 – 1.35(m, 2H), 0.94(t, *J* = 7.22 Hz, 3H).

^{13}C-NMR (125 MHz, $CDCl_3$): δ 148.7, 141.0, 135.5, 125.6, 123.3, 122.2, 120.4, 118.1, 114.5, 109.2, 108.7, 105.9, 42.9, 31.1, 20.5, 13.9.

HRMS (ESI): Calc. for $C_{16}H_{17}NO$ $[M+H]^+$: 240.1388; Found: 240.1383.

IR ν_{max} : 3272, 2945, 2873, 2365, 1622, 1468, 1350, 1178 cm^{-1}.

Physical Properties: White solid (410 mg, 43 % yield, 1.71 mmol, m.p. 75 ˚C).

[9-hexyl-9H-carbazol-3-ol] (L14)

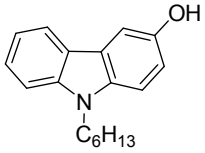

^{1}H-NMR (500 MHz, $CDCl_3$): δ 7.93(d, *J* = 7.55 Hz, 1H), 7.44(s,1H), 7.38 – 7.34(m, 1H), 7.29(d, *J* = 8.25 Hz,1H), 7.19(d, *J* = 8.25 Hz,1H), 7.11 – 7.08(m, *J* = 1H), 6.95 – 6.93(m, 1H), 4.67(s, broad, 1H), 4.18(t, *J* = 7.2 Hz, 2H), 1.79 – 1.73(m, 2H), 1.32 - .82(m, 6H), 0.79(t, *J* = 6.85 Hz, 3H).

^{13}C-NMR (125 MHz, $CDCl_3$): δ 148.8, 141.0, 135.6, 125.7, 123.4, 122.2, 120.4, 118.2, 114.5, 109.2, 108.7, 105.9, 43.2, 31.6, 28.9, 26.9, 22.5, 13.9.

HRMS (ESI): Calc. for $C_{18}H_{21}NO$ $[M+H]^+$: 268.1701; Found: 268.1696.

IR ν_{max} : 3307, 2918, 2861, 2365, 1604, 1460, 1232, 1178 cm^{-1}.

Physical Properties: White solid (380 mg, 39.7 % yield, 1.42 mmol, m.p. 79 ˚C).

[9-octyl-9H-carbazol-3-ol] (L15)

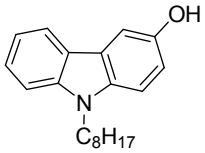

^{1}H-NMR (500 MHz, $CDCl_3$): δ 7.99(d, *J* = 8.2 Hz, 1H), 7.51(d, *J* = 2.75 Hz, 1H), 7.45 – 7.42(m, 1H), 7.36(d, *J* = 8.25 Hz, 1H), 7.26 – 7.24(m, 1H), 7.18 – 7.15(m, 1H), 7.03(dd, *J* = 8.95, 2.75 Hz, 1H), 4.24(t, *J* = 7.22 Hz, 2H), 1.84 – 1.79(m, 2H), 1.37 – 1.21(m, 10H), 0 .87(t, *J* = 6.85 Hz, 3H).

^{13}C-NMR (125 MHz, $CDCl_3$): δ 148.7, 141.0, 135.6, 125.7, 123.3, 122.2, 120.4, 118.2, 114.5, 109.2, 108.7, 105.8, 41.39, 31.8, 29.3, 29.2, 28.9, 27.3, 22.6, 14.1.

HRMS (ESI): Calc. for $C_{20}H_{26}NO$ $[M+H]^+$: 296.2014; Found: 296.2009.

IR ν_{max} : 3335, 2918, 2845, 2356, 1468, 1350, 1169 cm^{-1}.

Physical Properties: White solid (395 mg, 41.14 % yield, 1.33 mmol, m.p. 77 ˚C).

[9-decyl-9H-carbazol-3-ol] (L16)

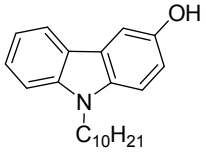

^{1}H-NMR (500 MHz, $CDCl_3$): δ 7.91(d, *J* = 7.55 Hz, 1H), 7.43(s, 1H), 7.37 – 7.33(m, 1H), 7.28(d, *J* = 8.25 Hz, 1H), 7.17 – 7.16(m, 1H), 7.1(t, *J* = 7.55 Hz, 1H), 6.94 – 6.92(m, 1H), 4.62(s, Broad, 1H), 4.16(t, *J* = 7.2 Hz, 2H), 1.77 – 1.71(m, 2H), 1.3 – 1.14(m, 15H), 0.8(t, *J* = 6.87 Hz, 3H).

^{13}C-NMR (125 MHz, $CDCl_3$): δ 148.7, 141.1, 135.6, 125.7, 123.4, 122.3, 120.4, 118.2, 114.5, 109.2, 108.7, 105.9, 43.2, 31.8, 29.5, 29.5, 29.4, 29.3, 27.3, 22.6, 14.1.

HRMS (ESI): Calc. for $C_{22}H_{30}NO$ $[M+H]^+$: 324.2327; Found: 324.2372.

IR ν_{max} : 3334, 2927, 2855, 2362, 1612, 1468, 1350, 1169 cm^{-1}.

Physical Properties: White solid (280 mg, 29 % yield, .86 mmol, m.p. 76 ˚C).

[9-octyl-9H-carbazol-6-yl acetate] (L17)

Procedure:

The phenol derivative (**L15**) (1 equiv) was dissolved in dry DCM under nitrogen atmosphere followed by addition of 1.5 equiv of trimethylamine and 5 equivs of acetic anhydride. The reaction mixture was left stirring for 12 h at room temperature. After completion of reaction as

judged by the TLC organic layer was washed with water and collected. Then the organic layer was removed under vacuum and the residue was purified by column chromatography.

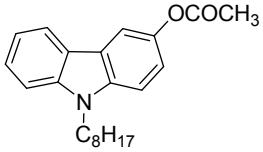

^{1}H-NMR (500 MHz, $CDCl_3$): δ 7.92(d, *J* = 7.55 Hz, 1H), 7.69(s, 1H), 7.35(t, *J* = 7.55 Hz, 1H), 7.26 – 7.21(m, 2H), 7.1 – 7.04(m, 2H), 4.11(t, *J* = 7.22 Hz, 2H), 2.23(s, 3H), 1.73 – 1.67(m, 2H), 1.29 – 1.12(m, 10H), .77(t, *J* = 6.9 Hz, 3H).

^{13}C-NMR (125 MHz, $CDCl_3$): δ 170.4, 143.4, 140.9, 138.1, 125.9, 122.9, 122.4, 120.5, 119.1, 118.7, 112.8, 108.8, 108.8, 40.1, 31.7, 29.6, 29.3, 28.9, 27.2, 22.5, 21.1, 14.0.

HRMS (ESI): Calc. for $C_{22}H_{27}NO_2$ $[M+H]^+$: 338.2120; Found: 338.2080.

IR ν_{max} : 2927, 2863, 2356, 1767, 1477, 1214, 1160 cm^{-1}.

Physical Properties: Yellow viscous liquid (450 mg, 51.4 % yield, 1.33 mmol).

[3-methoxy-9-octyl-9H-carbazole] (L18)

Compound **L15** (1 equiv) was dissolved in propanol followed by addition of methyl iodide (1.2 equiv) and crushed sodium hydroxide (1 equiv) at 0 °C. Then the reaction mixture was refluxed at 85 °C for 8 h. With the completion of reaction, as judged by the TLC, DCM was added to the reaction mixture and the organic layer was extracted with water. The organic layer was dried over anhydrous sodium sulfate and removed under reduced pressure. The crude product was purified using column chromatography.

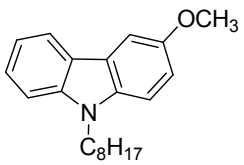

^{1}H-NMR (500 MHz, $CDCl_3$): δ 7.94(d, *J* = 8.25 Hz, 1H), 7.47(s, 1H), 7.33(t, *J* = 7.55 Hz, 1H), 7.24(d, *J* = 8.25 Hz, 1H), 7.16(d, *J* = 8.95 Hz, 1H), 7.08 – 7.05(m, 1H), 7.0 –

6.98(m, 1H), 4.1(t, *J* = 7.22 Hz, 2H), 3.8(s, 3H), 1.72 – 1.66(m, 2H), 1.32 – 1.11(m, 10H), 0.76(t, *J* = 6.85 Hz, 3H).

^{13}C-NMR (125 MHz, $CDCl_3$): δ 153.4, 140.8, 135.4, 125.5, 122.9, 122.5, 120.2, 118.1, 114.7, 109.3, 108.7, 103.2, 56.0, 43.0, 31.8, 29.3, 29.1, 28.9, 27.2, 22.6, 14.0.

HRMS (ESI): Calc. for $C_{21}H_{27}NO$ $[M]^+$: 309.2093; Found: 309.2132.

IR ν_{max} : 2921, 2844, 2365, 1463, 1196 cm^{-1}.

Physical Properties: Colorless viscous liquid (300 mg, 31.42 % yield, 0.96 mmol).

Procedure for the synthesis of 23:

Phenylhydrazine (1 equiv) was added portion wise for 30 minutes to a boiling solution of 4-methylcyclohexonone (1 equiv) in glacial acetic acid, and resulting mixture was refluxed for 3 h. Then the reaction mixture was cooled to 0 °C using ice bath which resulted in the formation of white solid as precipitate. The solid was washed with cold water several times and dissolved in DCM. The DCM solution was dried over anhydrous sodium sulphate, and the volatiles were removed under vacuum. The crude was purified using column chromatography.

[2,3,4,9-tetrahydro-3-methyl-1H-carbazole] (23)

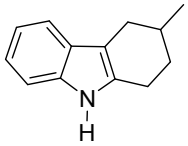

^{1}H-NMR (500 MHz, $CDCl_3$): δ 7.42(s, 1H), 7.37(d, *J* = 7.55 Hz, 1H), 7.12 – 7.1(m, 1H), 7.03 – 6.97(m, 2H), 2.76 – 2.72(m, 1H), 2.2 – 2.15(m, 1H), 1.873 – 1.81(m, 2H), 1.5 – 1.42(m, 1H), 1.05(d, *J* = 6.2 Hz, 3H).

^{13}C-NMR (125 MHz, $CDCl_3$): δ 135.8, 133.8, 127.6, 120.8, 118.9, 117.6, 110.3, 109.9, 31.3, 29.6, 29.3, 22.8, 21.7.

HRMS (ESI): Calc. for $C_{13}H_{15}N$ $[M+H]^+$: 186.1283; Found: 186.1278.

IR ν_{max} : 3388, 2935, 2864, 2362, 1603, 1460 cm^{-1}.

Physical Properties: White solid (1.4 gm., 84.8 % yield, 7.55 mmol, m.p. 98 ˚C).

Procedure for the synthesis of 26:

Compound **L23** (4.3 mmol) was heated at 290 °C with 10 % Pd/C (100 mg) for 45 min under nitrogen atmosphere. Then the reaction mixture was cooled to room temperature and extracted with boiling ethanol/water mixture (95:5). The resulting crude mixture was filtered through sintered funnel and the filtrate was dried in rotavapor. The crude was purified using column chromatography.

[3-methyl-9H-carbazole] (26)

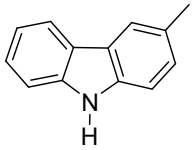

^{1}H-NMR (500 MHz, CD_3OD): δ 11.09(s, 1H), 8.05(d, *J* = 7.55 Hz, 1H), 7.88(s, 1H), 7.45(d, *J* = 7.55 Hz, 1H), 7.37 – 7.33(m, 2H), 7.2(dd, *J* = 8.25, 1.35 Hz, 1H), 7.12 – 7.09(m, 1H), 2.45(s, 3H).

^{13}C-NMR (125 MHz, CD_3OD): δ 140.0, 138.0, 127.2, 126.9, 125.4, 122.6, 122.3, 120.1, 119.9, 118.3, 110.9, 110.7, 21.2.

HRMS (ESI): Calc. for $C_{13}H_{11}N$ $[M+H]^+$: 182.097; Found: 182.1011.

IR ν_{max} : 3406, 3044, 2918, 2347, 1603, 1460, 1341 cm^{-1}.

Physical Properties: White solid (630 mg, 80.66 % yield, 3.47 mmol, m.p. 206 ˚C).

[3-methyl-9-octyl-9H-carbazole] (30)

Compound **L26** (1 equiv) was added slowly to a solution of KOH (3.77 equiv) in acetone at 0 °C and the mixture was left stirring for 30 minutes at room temperature. 1-Bromooctane (1.5 equiv) in acetone was then added drop wise and stirred for 12 hours at room temperature. The progress of the reaction was monitored by TLC. After completion of reaction, the organic solvent was

removed under vacuum and the crude mixture was extracted with DCM. The organic layer was dried over magnesium sulfate and the volatiles were removed under vacuum. The crude product was collected and purified using column chromatography.

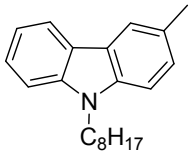

^{1}H-NMR (500 MHz, $CDCl_3$): δ 7.95(d, *J* = 7.55 Hz, 1H), 7.78(s, 1H), 7.33 – 7.29(m, 1H), 7.24(d, *J* = 8.25 Hz, 1H), 7.15(s, 2H), 7.09(t, *J* = 6.87 Hz, 1H), 4.11(t, *J* = 7.22 Hz, 2H), 2.42(s, 3H), 1.71 – 1.67(m, 2H), 1.24 – 1.11(m, 10H), 0.77(t, *J* = 6.85 Hz, 3H).

^{13}C-NMR (125 MHz, $CDCl_3$): δ 140.6, 138.7, 127.9, 126.8, 125.3, 122.9, 122.6, 120.24, 120.2, 183.3, 108.5, 108.3, 42.9, 31.8, 29.4, 29.2, 28.9, 27.3, 22.6, 21.4, 14.1.

HRMS (ESI): Calc. for $C_{21}H_{28}N$ $[M+H]^+$: 294.2222; Found: 294.2246.

IR ν_{max} : 2918, 2885, 2356, 1520, 1465, 1350 cm^{-1}.

Physical Properties: Colorless viscous liquid (1.06 gm., 66.1% yield, 3.61 mmol).

Procedure for the synthesis of 24 :

Compound **24** was synthesized following the same procedure as that of **23**.

[3-tert-butyl-2, 3, 4, 9-tetrahydro-9-octyl-1H-carbazole] (24)

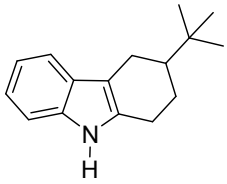

^{1}H-NMR (500 MHz, $CDCl_3$): δ 7.45(s, Broad, 1H), 7.39(d, *J* = 7.55 Hz, 1H), 7.14 – 7.12(m, 1H), 7.03 – 6.97(m, 2H), 2.75 – 2.72(m, 1H), 2.63 – 2.6(m, 2H), 2.33 – 2.28(m,1H), 2.01 – 1.98(m, 1H), 1.48 – 1.39(m, 2H), 0.91(s, 9H).

^{13}C-NMR (125 MHz, $CDCl_3$): δ 136.0, 134.1, 127.9, 120.9, 119, 117.6, 110.5, 110.4, 45.4, 32.6, 27.5, 24.7, 24.1, 22.2.

HRMS (ESI): Calc. for $C_{16}H_{21}N$ $[M+H]^+$: 228.1752; Found: 228.1932.

IR ν_{max} : 3407, 2963, 2909, 2365, 1450, 1321 cm^{-1}.

Physical Properties: White solid (1.21 gm., 81.24 % yield, 5.27 mmol, m.p. 130 ˚C).

Procedure for the synthesis of 27:

Compound **24** was synthesized following the same procedure as that of **23**.

[3-tert-butyl-9H-carbazole] (27)

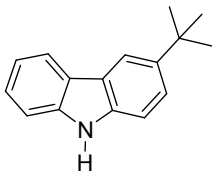

^{1}H-NMR (500 MHz, $CDCl_3$): δ 8.13 – 8.12(d, 2H), 7.83(s, 1H), 7.53(dd, *J* = 8.25, 2.05 Hz, 1H), 7.43 – 7.4(m, 1H), 7.36 – 7.31(m, 1H), 7.27 – 7.24(m, 1H), 1.48(s, 9H).

^{13}C-NMR (125 MHz, $CDCl_3$): δ 142.4, 139.8, 137.5, 125.5, 123.8, 123.5, 122.9, 120.1, 119.1, 116.3, 110.5, 110.1, 34.6, 31.9.

HRMS (ESI): Calc. for $C_{16}H_{17}N[M+H]^+$: 224.1439; Found: 224.1517.

IR ν_{max} : 3416, 2963, 2872, 2365, 1603, 1460, 1241 cm^{-1}.

Physical Properties: White solid (580 mg, 78.88 % yield, 2.59 mmol, m.p. 152 ˚C).

[3-tert-butyl-9-octyl-9H-carbazole] (31)

L31 was synthesized following the same procedure as that of **L30**.

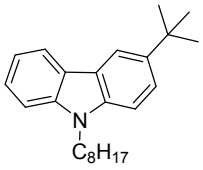

^{1}H-NMR (500 MHz, $CDCl_3$): δ 8.01 – 7.99(m, 2H), 7.48 – 7.41(m, 1H), 7.33 – 7.3(m, 1H), 7.25 – 7.19(m, 2H), 7.1 – 7.08(m, 1H), 4.13(t, *J* = 7.2 Hz, 2H), 1.73 – 1.7(m, 2H),1.35(s, 9H), 1.17 – 1.13(m, 10H), .77(t, *J* = 6.85 Hz, 3H).

^{13}C-NMR (125 MHz, $CDCl_3$): δ 141.6, 140.7, 138.6, 125.2, 123.5, 122.9, 122.4, 120.1, 118.4, 116.4, 108.5, 108.1, 43.0, 34.6, 32.0, 31.8, 29.4, 29.2, 29, 27.3, 22.6, 14.1.

HRMS (ESI): Calc. for $C_{24}H_{33}N$ $[M+H]^+$: 336.2691; Found:336.2721.

IR ν_{max} : 2927, 2844, 2356, 1486, 1359, 1269 cm^{-1}.

Physical Properties: Colorless viscous liquid (960 mg, 64 % yield, 2.86 mmol).

Procedure for the synthesis of 25:

L25 was synthesized following the same procedure as that of **L24**, and using 4-methoxyphenylhydrazine instead of phenylhydrazine.

[6,7,8,9-tetrahydro-3-methoxy-5H-carbazole] (25)

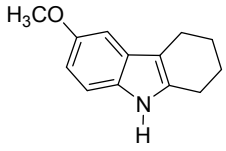

^{1}H-NMR (500 MHz, $CDCl_3$): δ 7.45(s, Broad, 1H), 7.05(d, *J* = 8.95 Hz, 1H), 6.84(s, 1H), 6.69 – 6.67(m, 1H), 3.7723(s, 3H), 2.61 – 2.57(m, 4H), 1.82 – 1.54(m, 4H).

^{13}C-NMR (125 MHz, $CDCl_3$): δ 153.8, 135.1, 130.6, 128.1, 110.9, 110.4, 109.9, 100.2, 55.9, 23.3, 23.1, 20.9.

HRMS (ESI): Calc. for $C_{13}H_{15}NO$ $[M+H]^+$: 202.1232; Found: 202.1254.

IR ν_{max} : 3302, 2915, 2844, 2353, 1586, 1434, 1483, 1212 cm^{-1}.

Physical Properties: White solid (1.2 gm., 58.5 % yield, 5.96 mmol, m.p. 96 ˚C).

Procedure for the synthesis of 28:

28 was synthesized following the same procedure as that of **27**.

[3-methoxy-9H-carbazole] (28)

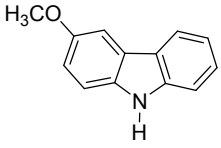

^{1}H-NMR (500 MHz, $CDCl_3$): δ 8.08 – 8.02(m, 1H), 7.9(s, Broad, 1H), 7.55(d, *J* = 2.1 Hz, 1H), 7.42 – 7.38(m, 2H), 7.32(d, *J* = 8.9 Hz, 1H), 7.24 – 7.19(m, 1H), 7.07 – 7.05(m 1H), 3.92(s, 3H).

^{13}C-NMR (125 MHz, $CDCl_3$): δ 153.8, 140.2, 134.3, 125.8, 123.7, 123.3, 120.2, 119.0, 115.0, 111.3, 110.7, 103.1, 56.0.

HRMS (ESI): Calc. for $C_{13}H_{11}NO$ $[M+H]^+$: 198.0919; Found: 198.1035.

IR ν_{max} : 3396, 3051, 2370, 2998, 2848, 1583, 1452, 1177 cm^{-1}.

Physical Properties: White solid (440 mg, 56.1 % yield, 2.23 mmol, m.p. 144 ˚C).

[9H-carbazol-3-ol] (L29)

Procedure:

Compound **L28** (2 mmol) was dissolved in HBr (4 mL) and glacial acetic acid (10 mL) under inert atmosphere, and the resulting mixture was refluxed for 5 h. After the completion of reaction, as judged by the TLC, a solid product precipitated out. The solid product was collected and washed with water. The crude solid was dissolved in DCM and dried over sodium sulfate. The organic layer was removed under vacuum and the residue was purified using column chromatography.

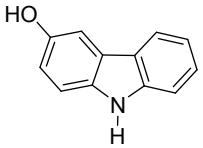

^{1}H-NMR (500 MHz, $CDCl_3$): 7.92(d, *J* = 5.05 Hz, 1H), 7.43(d, *J* = 2.05 Hz, 1H), 7.36(d, *J* = 8.2 Hz, 1H), 7.31 – 7.24(m, 2H), 7.07 – 7.04(m, 1H), 6.92 – 6.9(m, 1H).

^{13}C-NMR (125 MHz, $CDCl_3$): δ 151.3, 142.3, 135.9, 126.5, 125, 124.2, 120.9, 119.1, 115.8, 112.2, 111.7, 105.9.

HRMS (ESI): Calc. for $C_{12}H_9NO$ $[M+H]^+$: 184.0762; Found: 184.0758.

IR ν_{max} : 3395, 3063, 1587, 1450, 1178 cm^{-1}.

Physical Properties: White solid (135 mg, 36.38 % yield, .73 mmol, m.p. 263 ˚C).

NMR Spectra of Compounds:

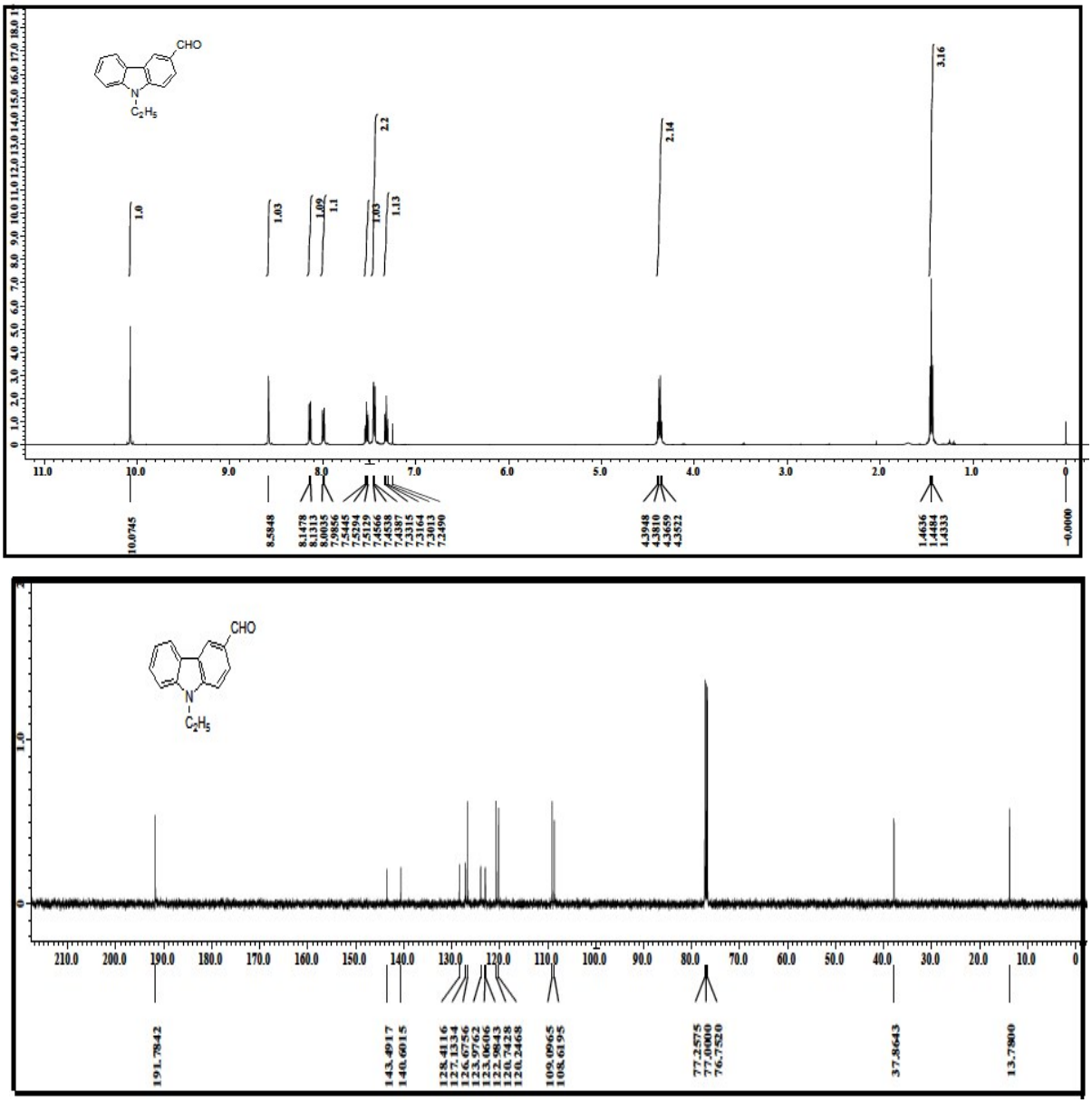

Fig. S35 ^{1}H and ^{13}C spectra of **6**.

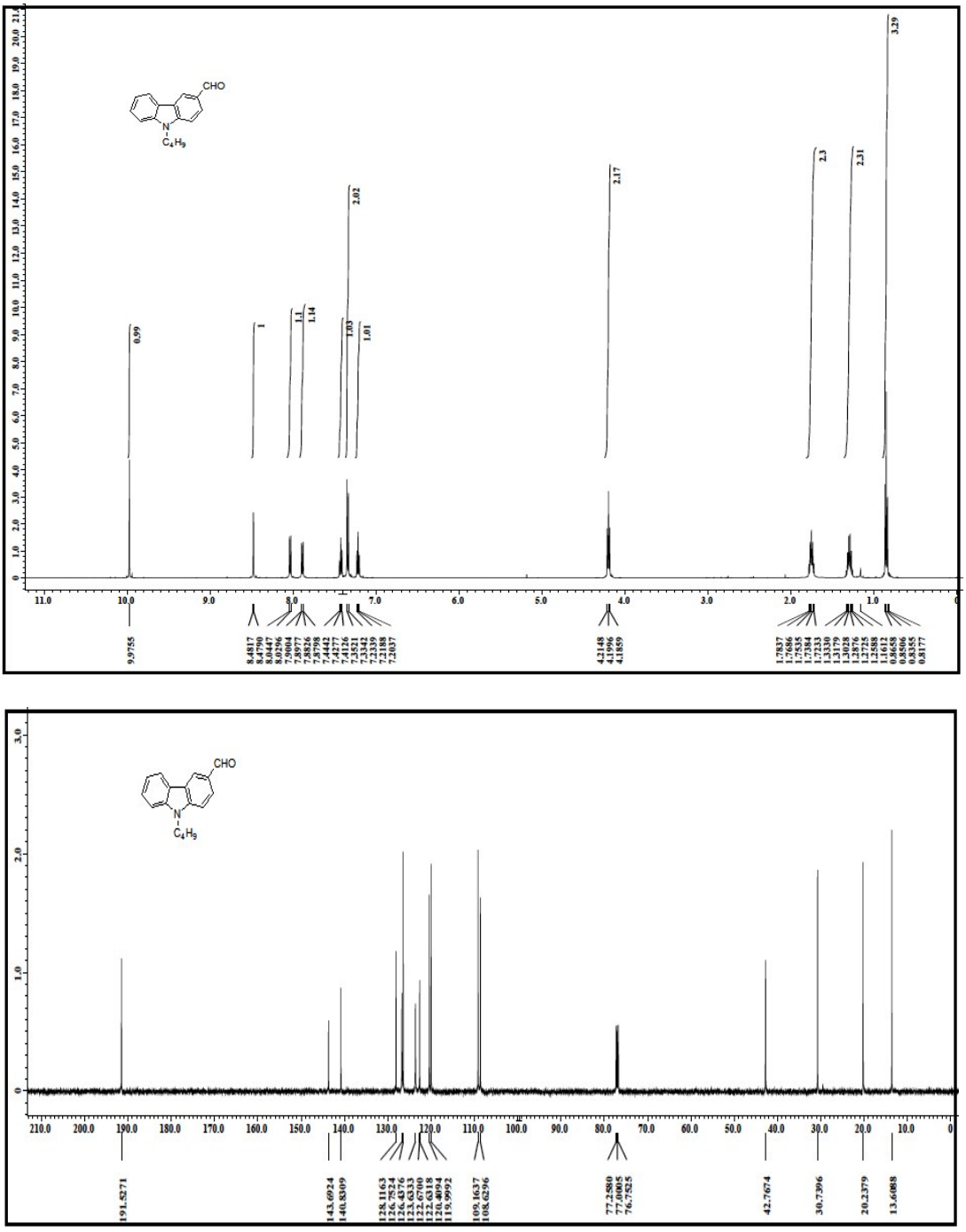

Fig. S36 ^{1}H and ^{13}C spectra of **7**.

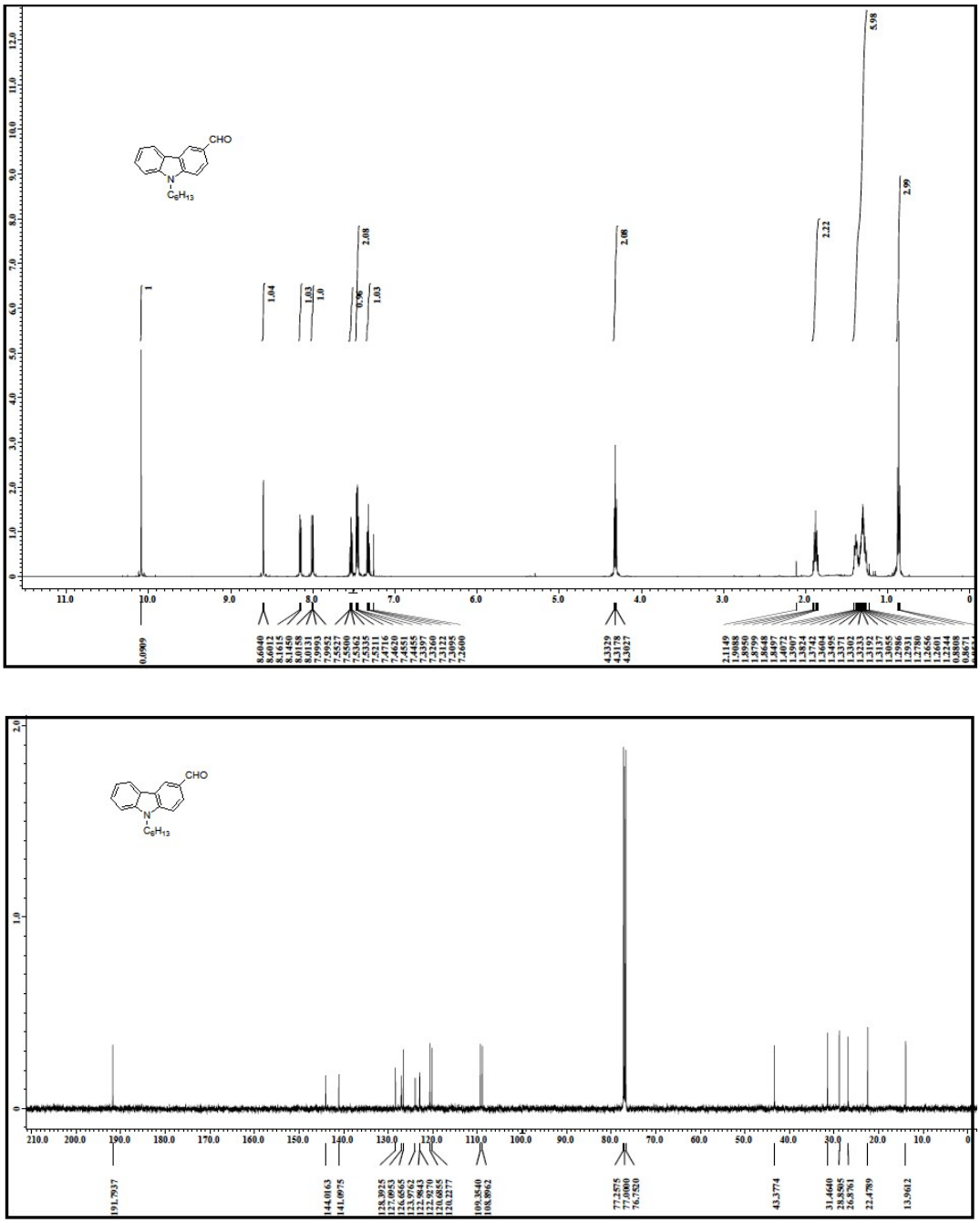

Fig. S37 ^{1}H and ^{13}C spectra of **8**.

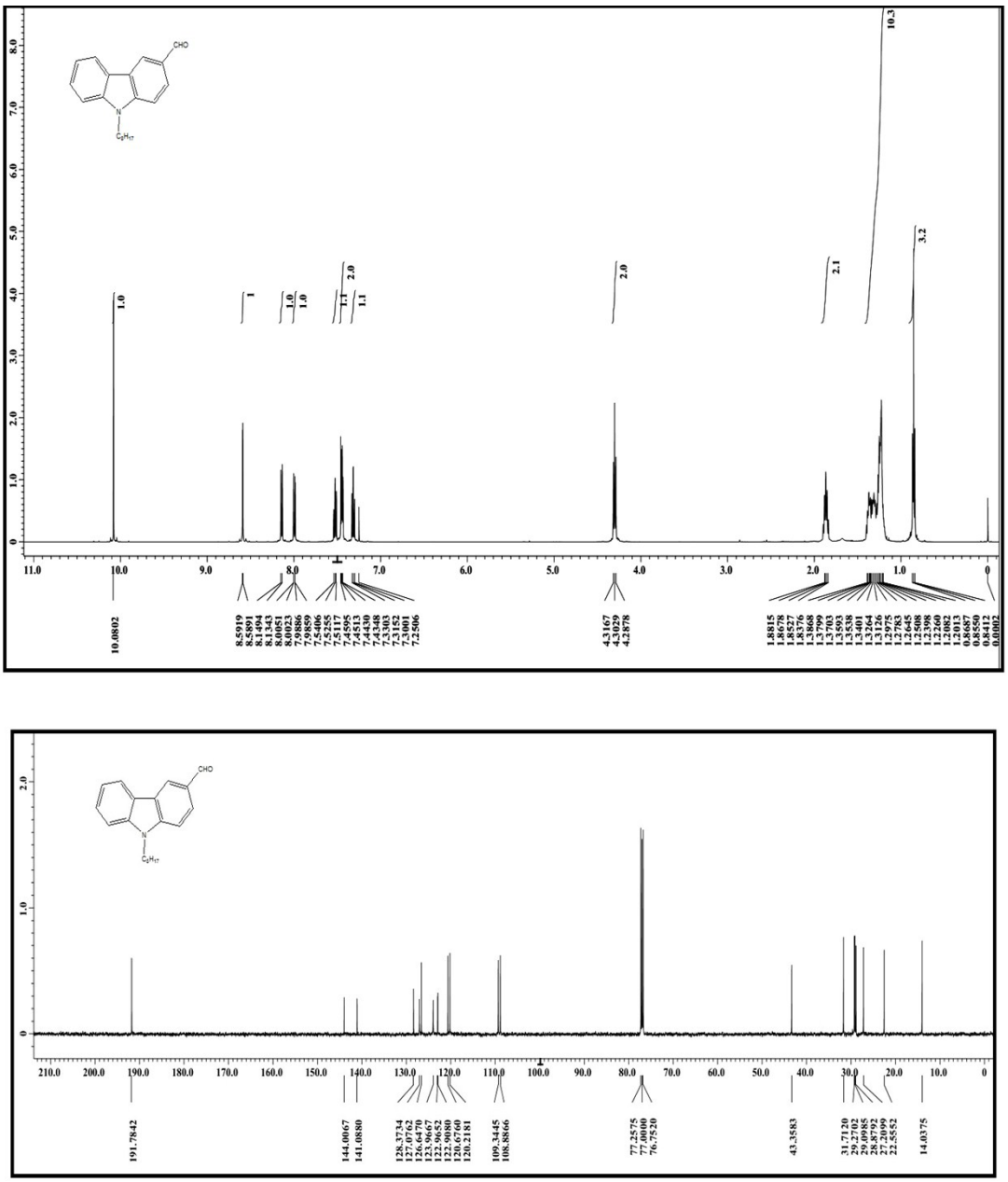

Fig. S38 ^{1}H and ^{13}C spectra of **9**.

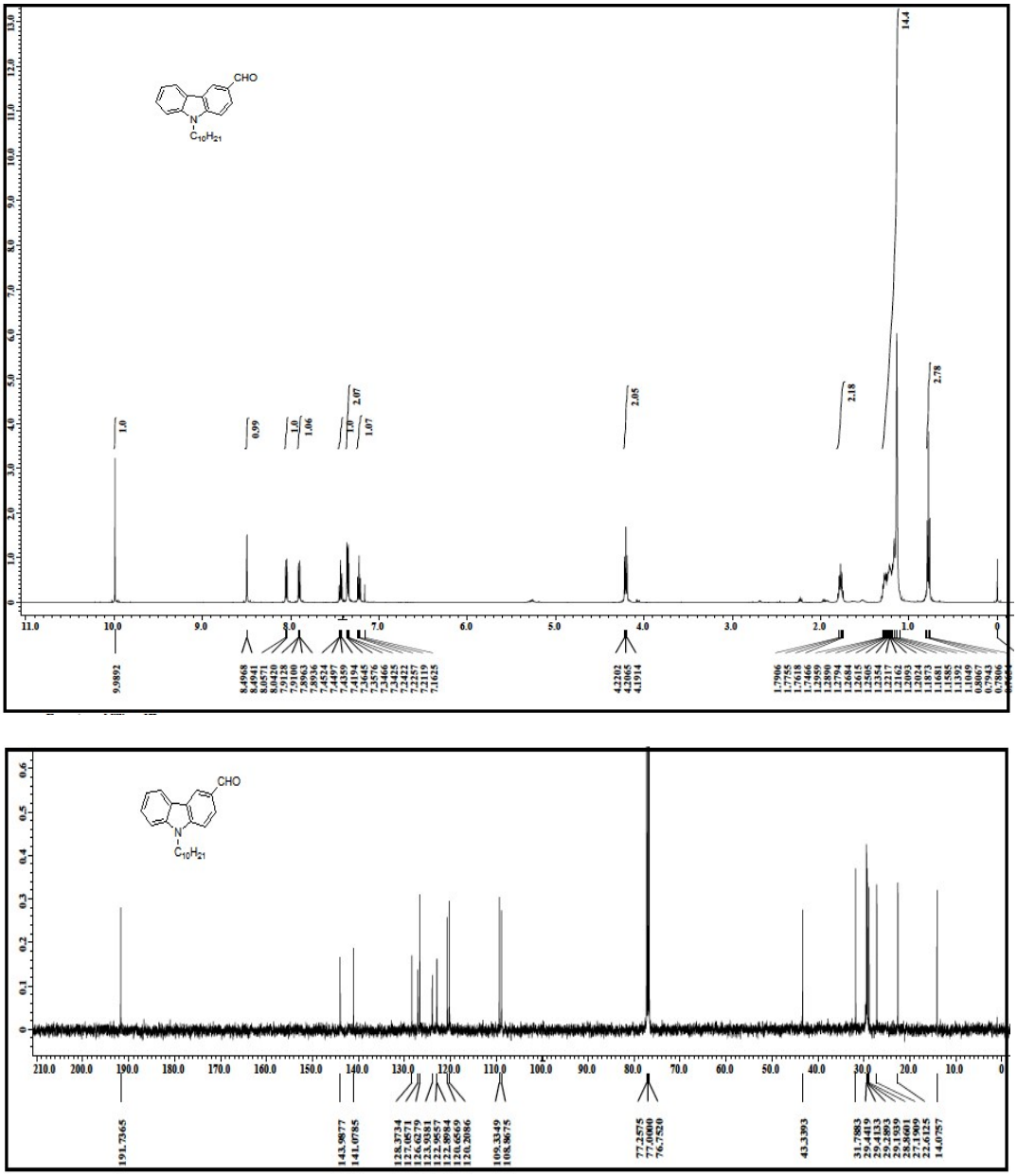

Fig. S39 ^{1}H and ^{13}C spectra of **10**.

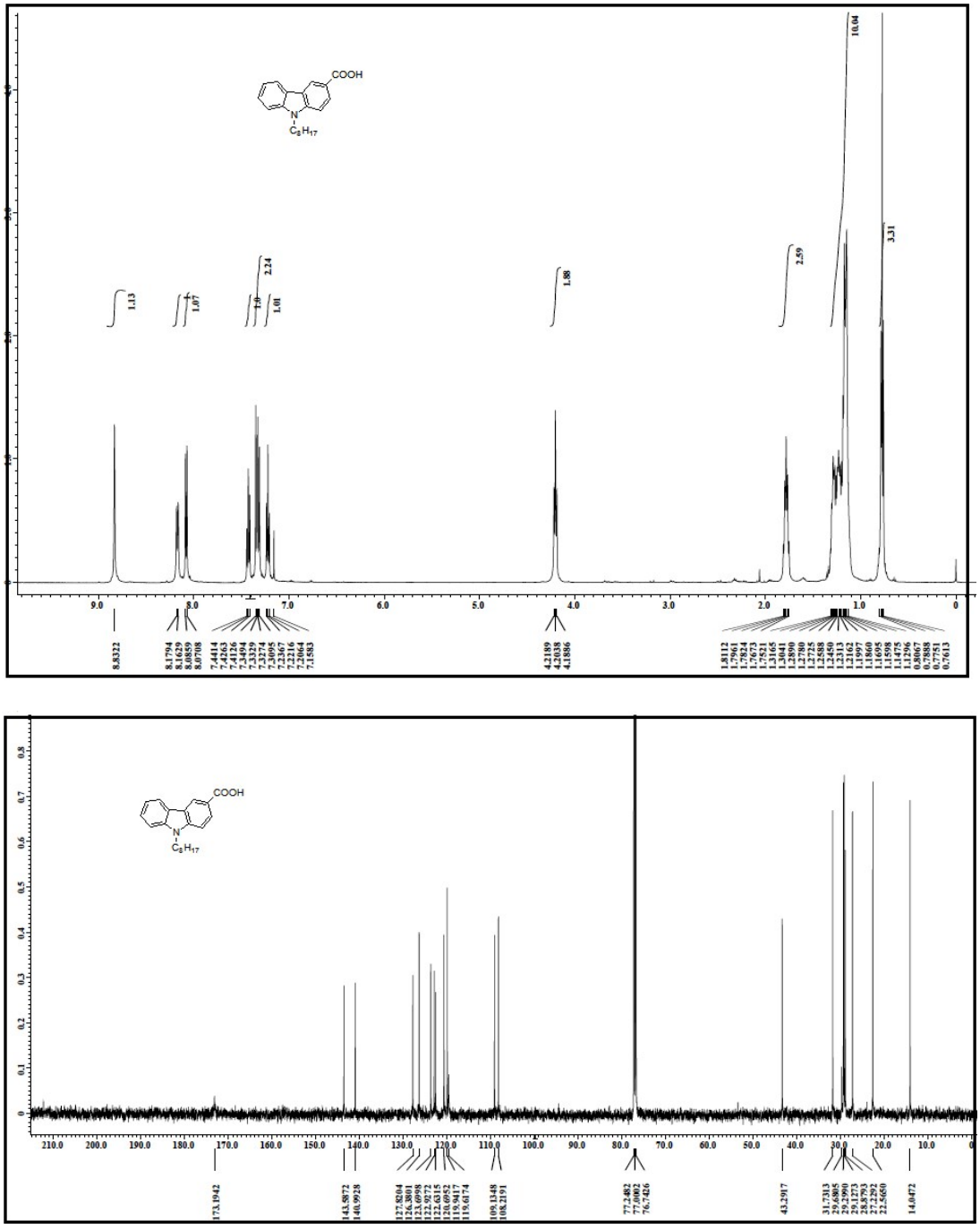

Fig. S40 ^{1}H and ^{13}C spectra of **L11**.

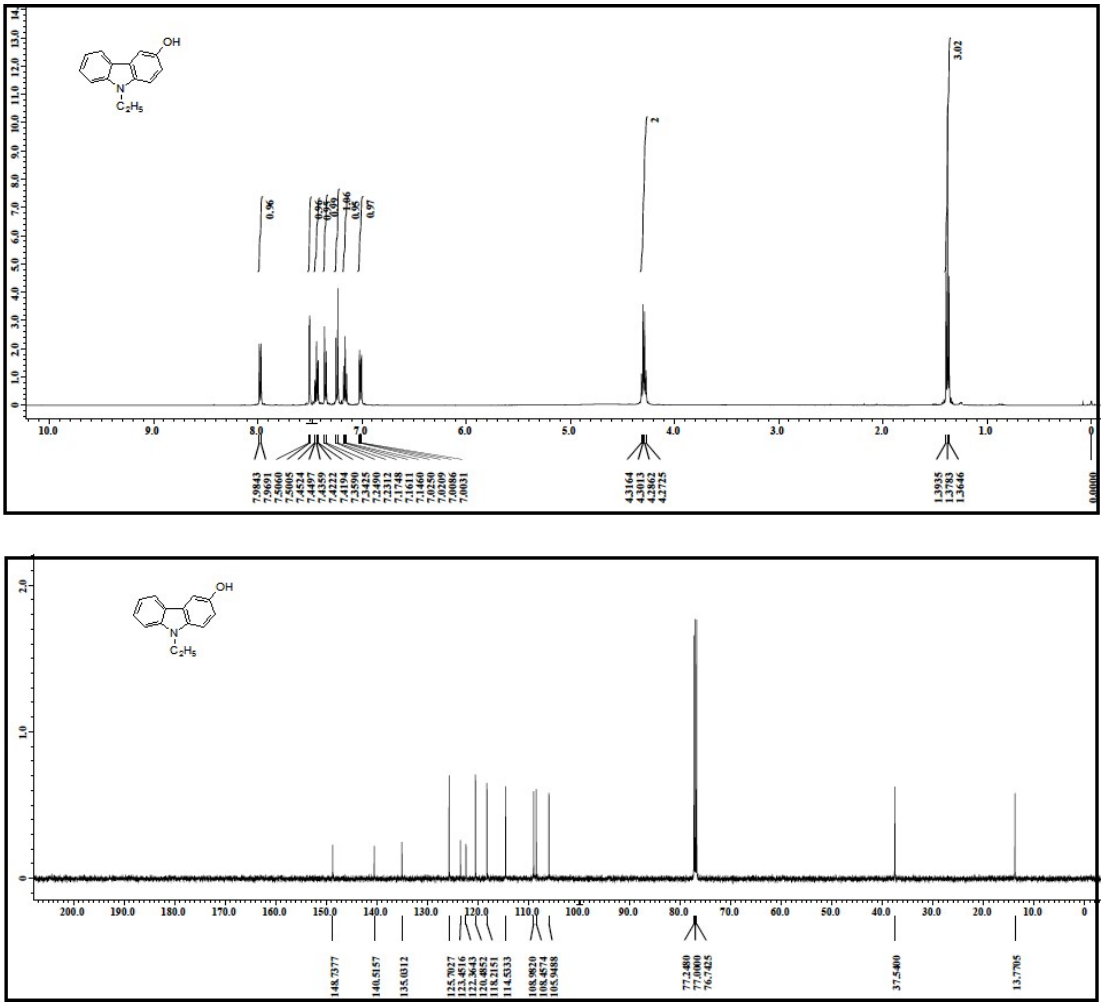

Fig. S41 ^{1}H and ^{13}C spectra of **L12**.

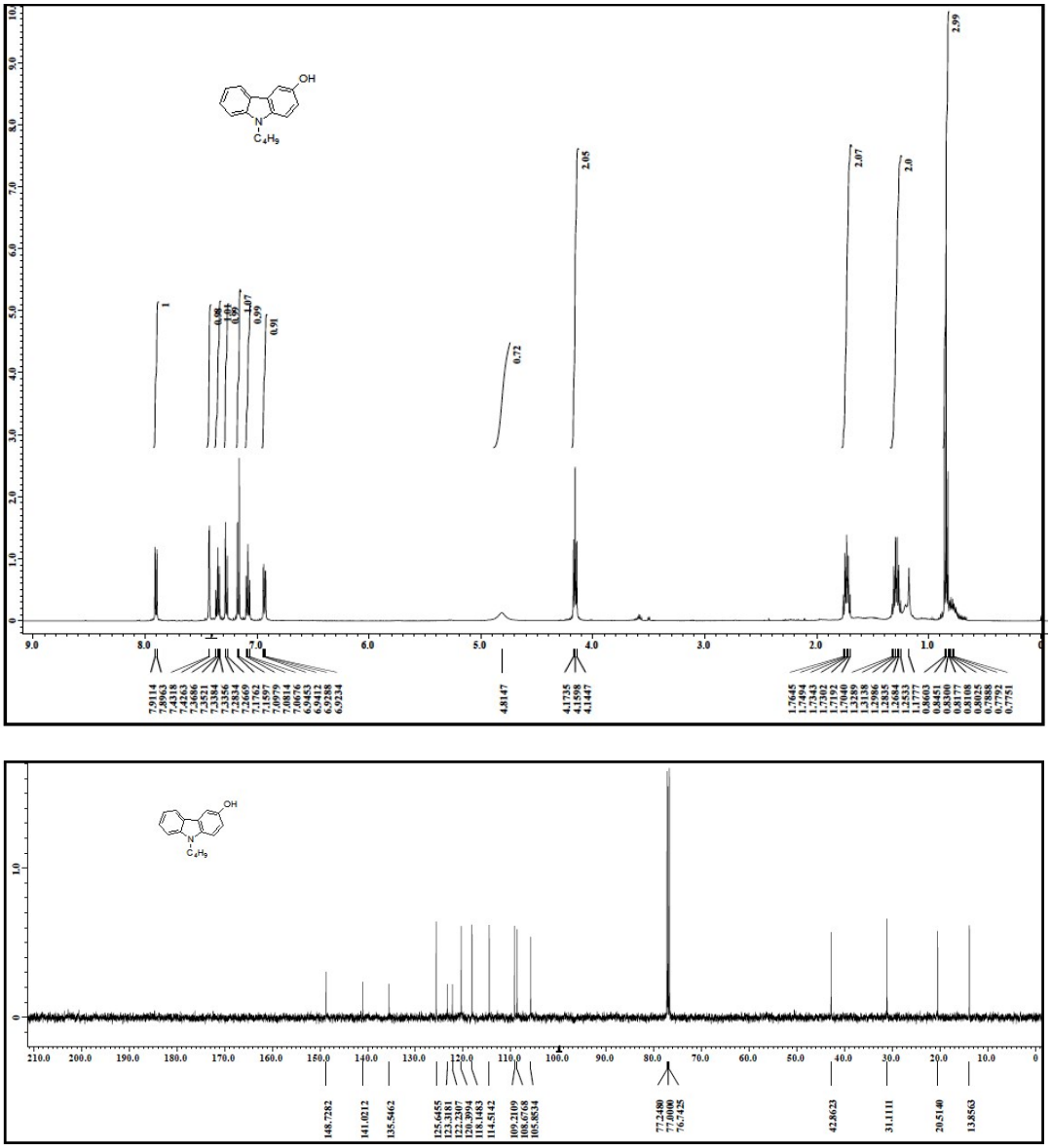

Fig. S42 ^{1}H and ^{13}C spectra of **L13**.

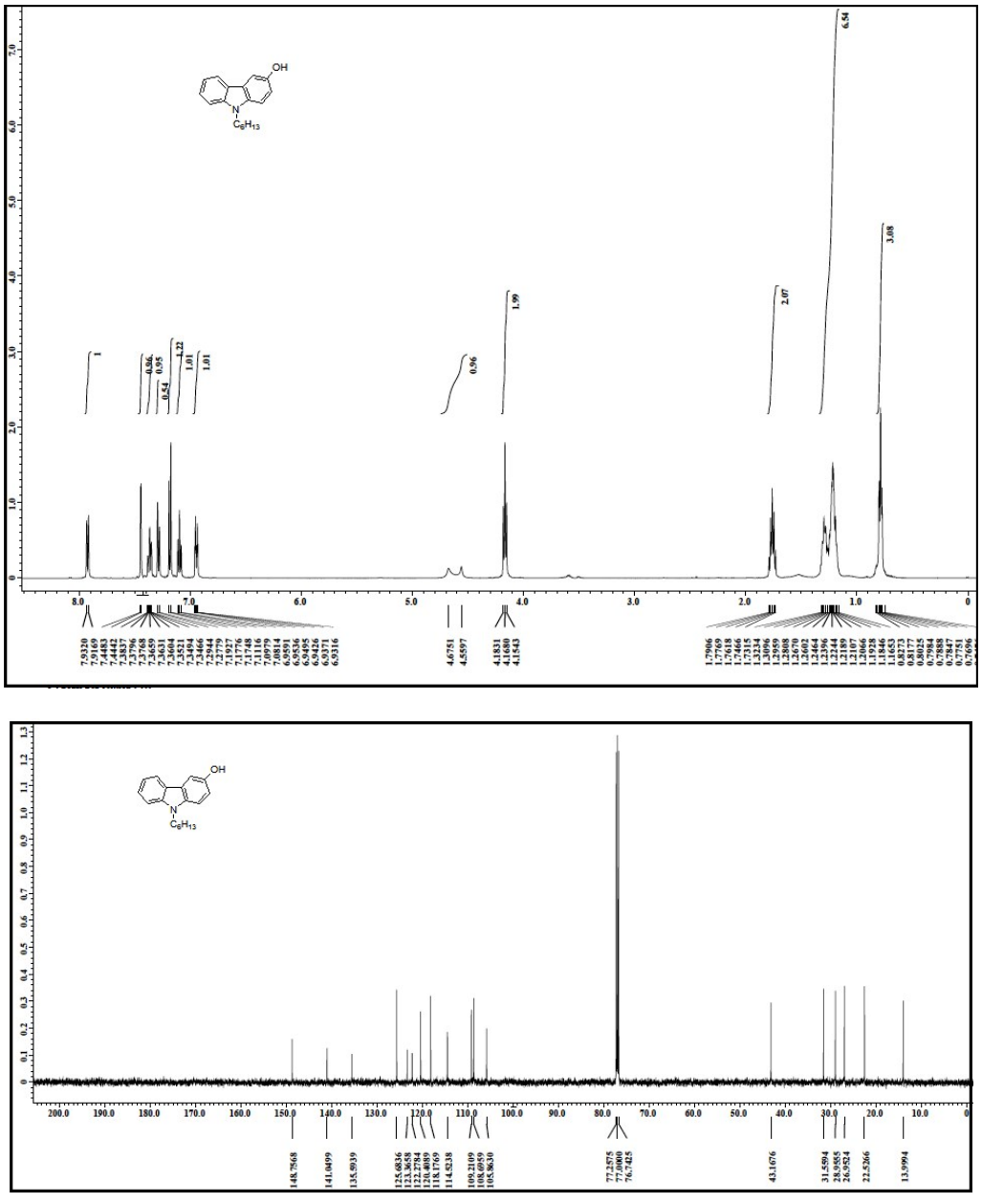

Fig. S43 ^{1}H and ^{13}C spectra of **L14**.

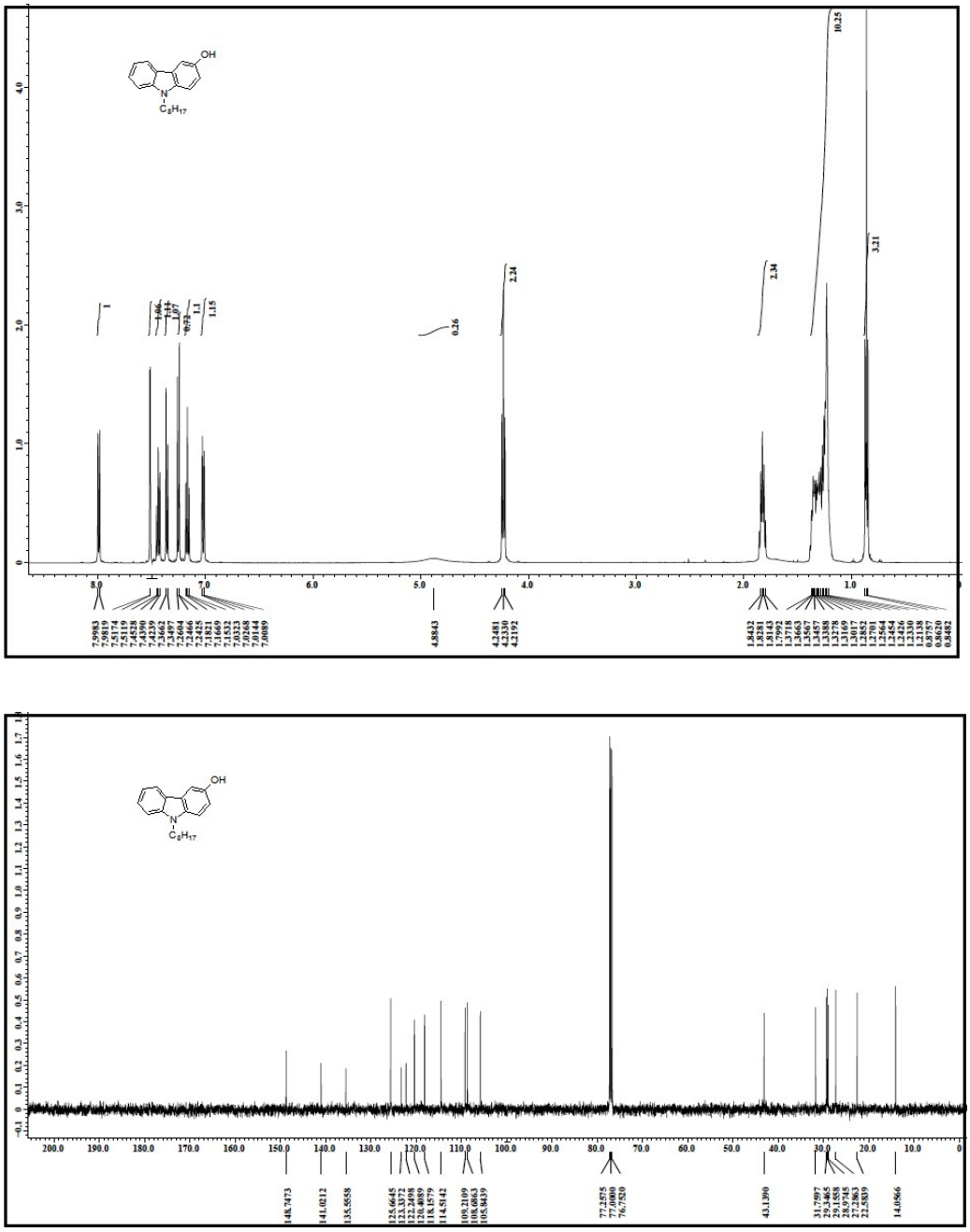

Fig. S44 ^{1}H and ^{13}C spectra of **L15**.

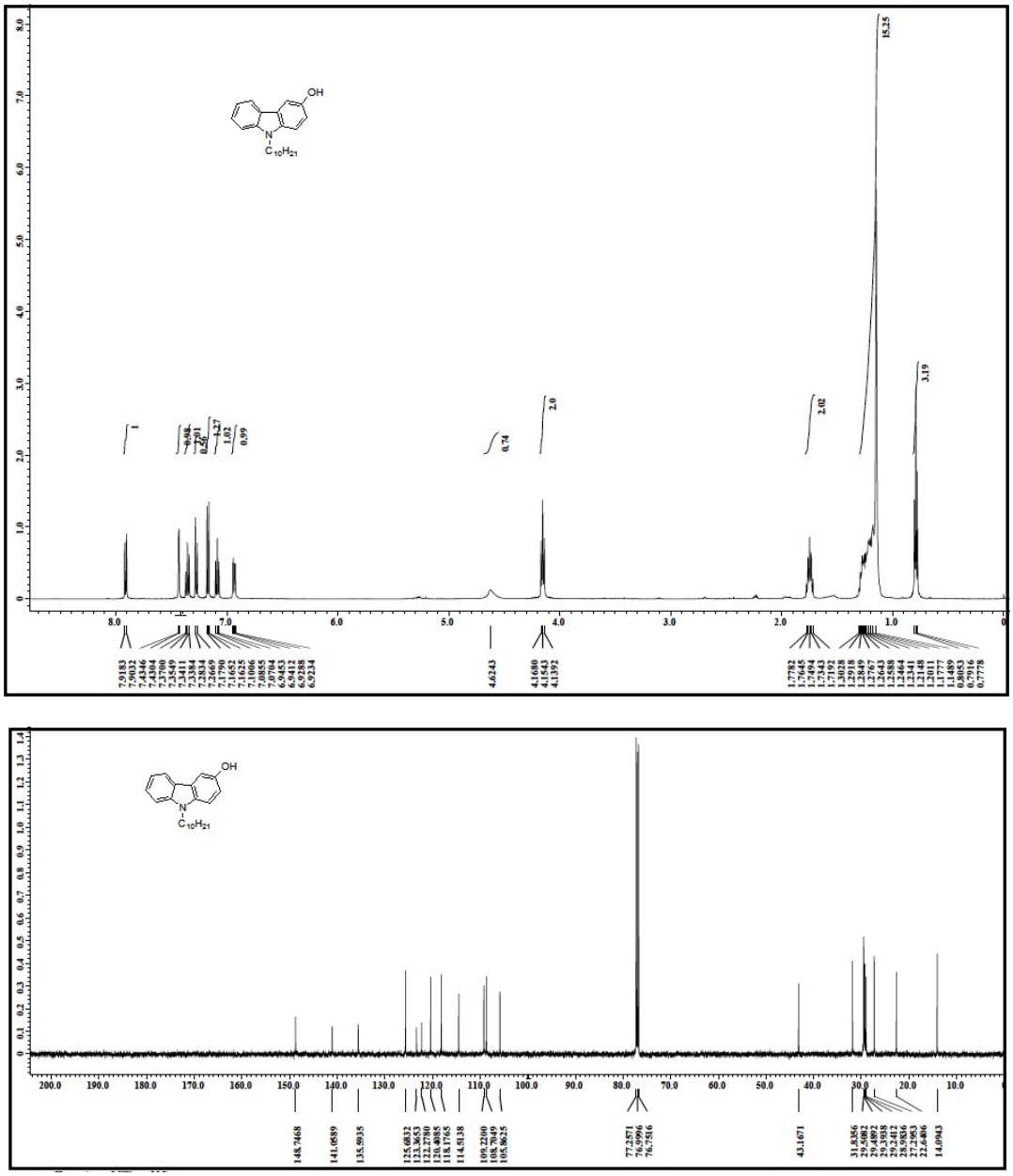

Fig. S45 ^{1}H and ^{13}C spectra of **L16**.

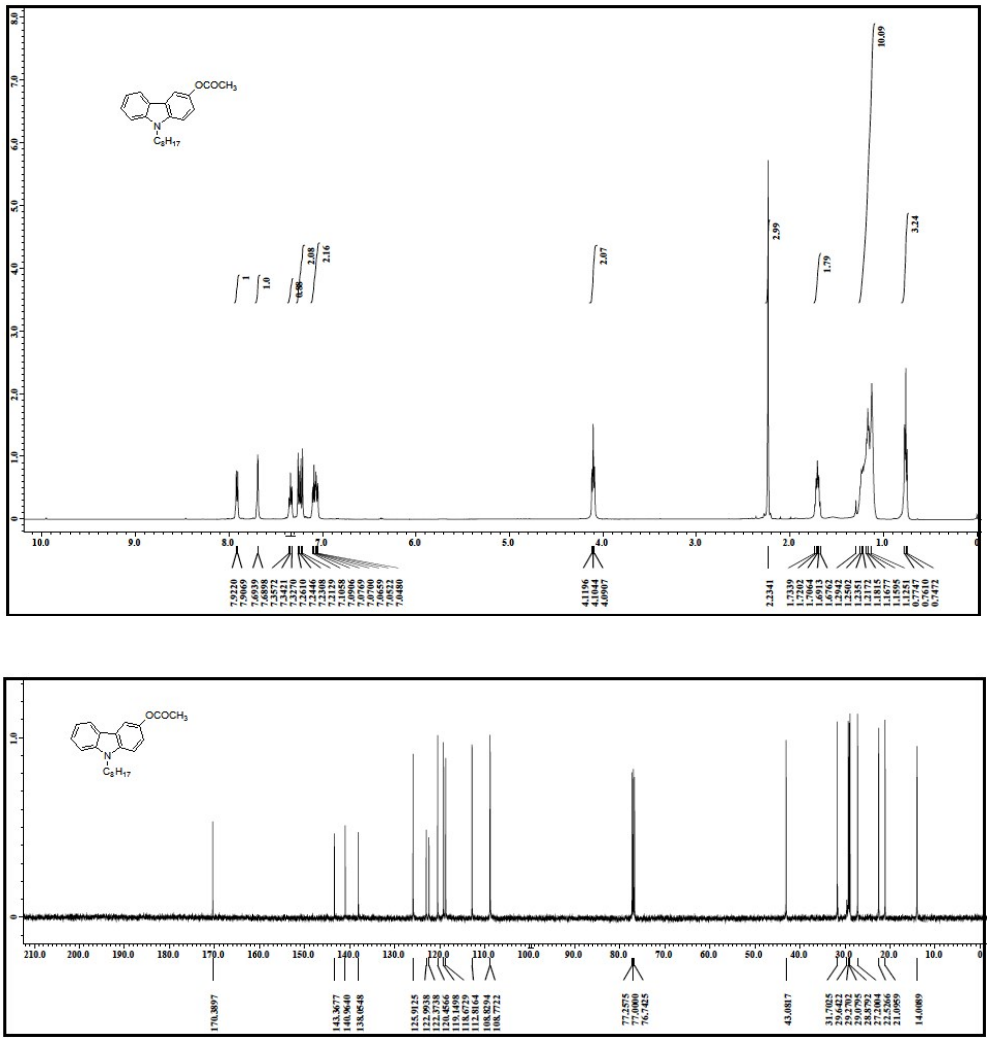

Fig. S46 ^{1}H and ^{13}C spectra of **L17**.

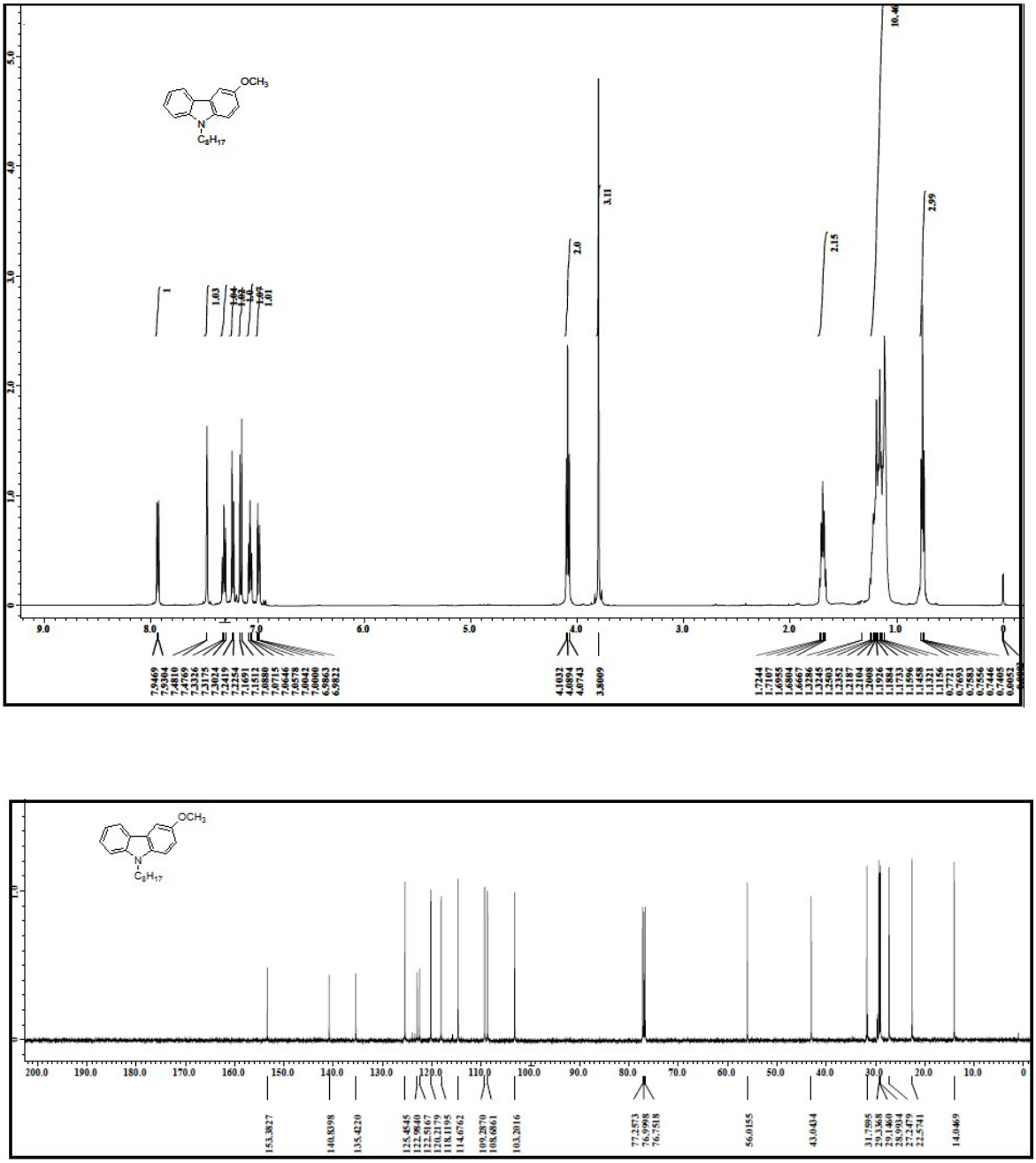

Fig. S47 ^{1}H and ^{13}C spectra of **L18**.

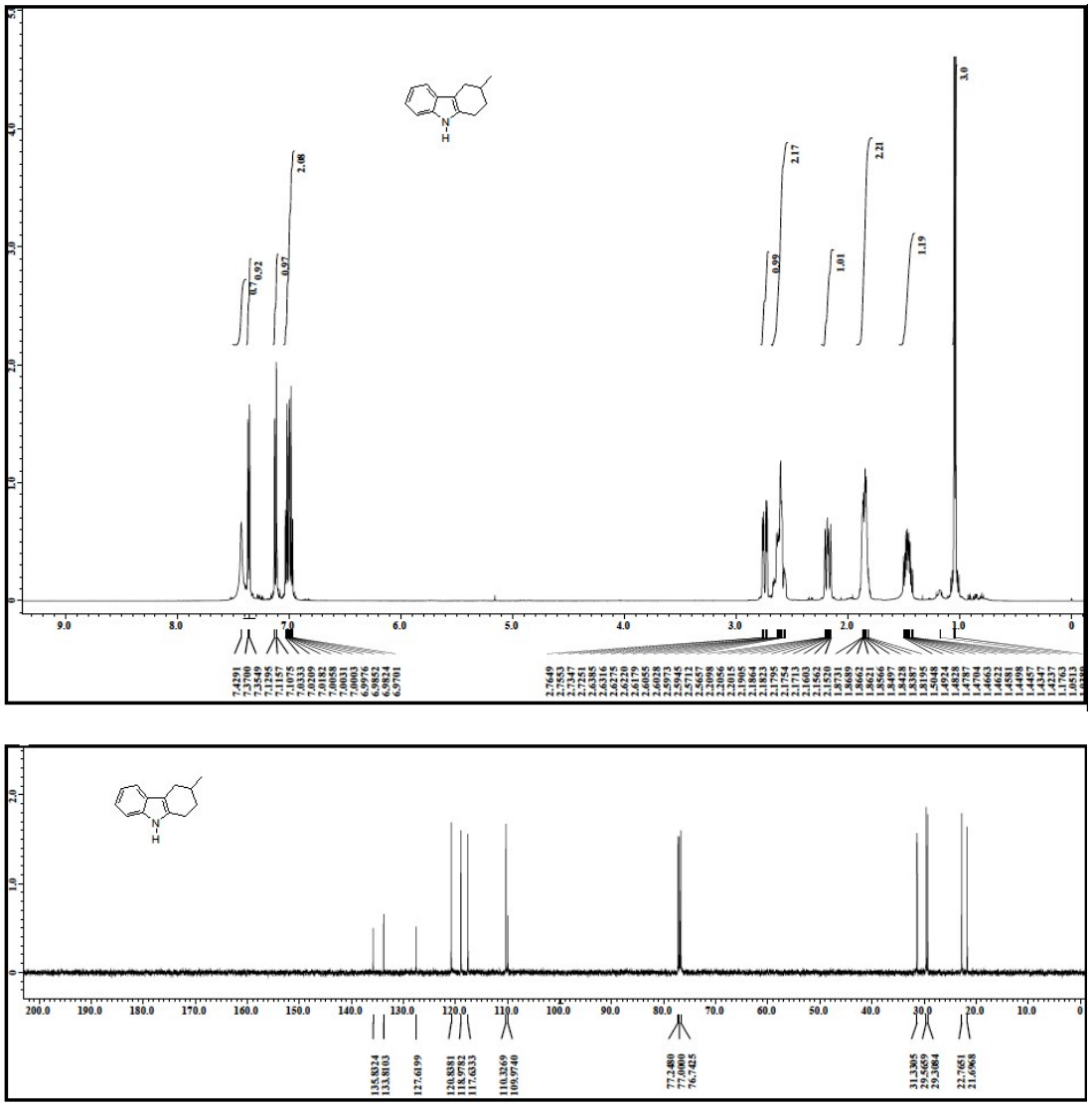

Fig. S48 ^{1}H and ^{13}C spectra of **23**.

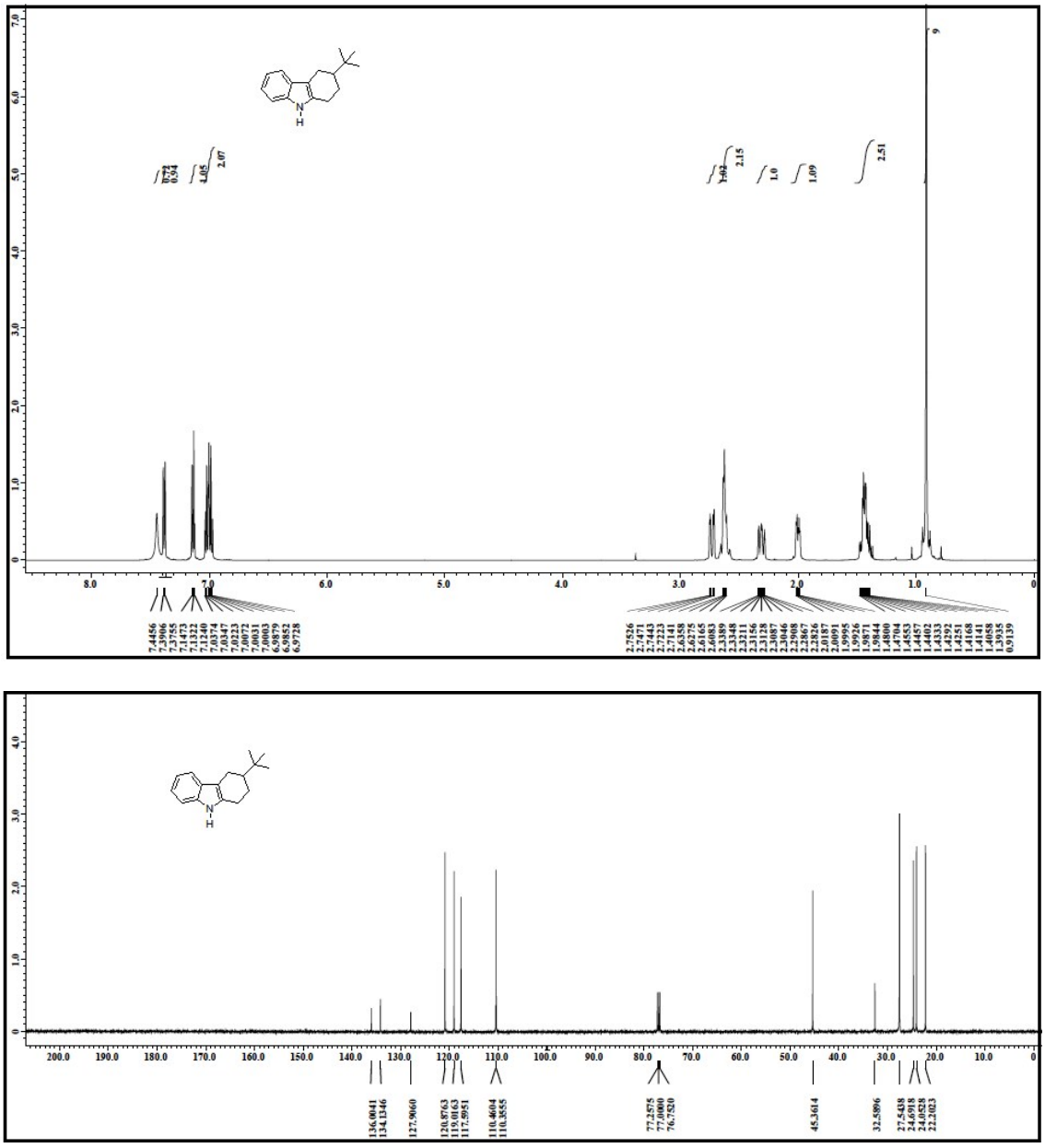

Fig. S49 ^{1}H and ^{13}C spectra of **24**.

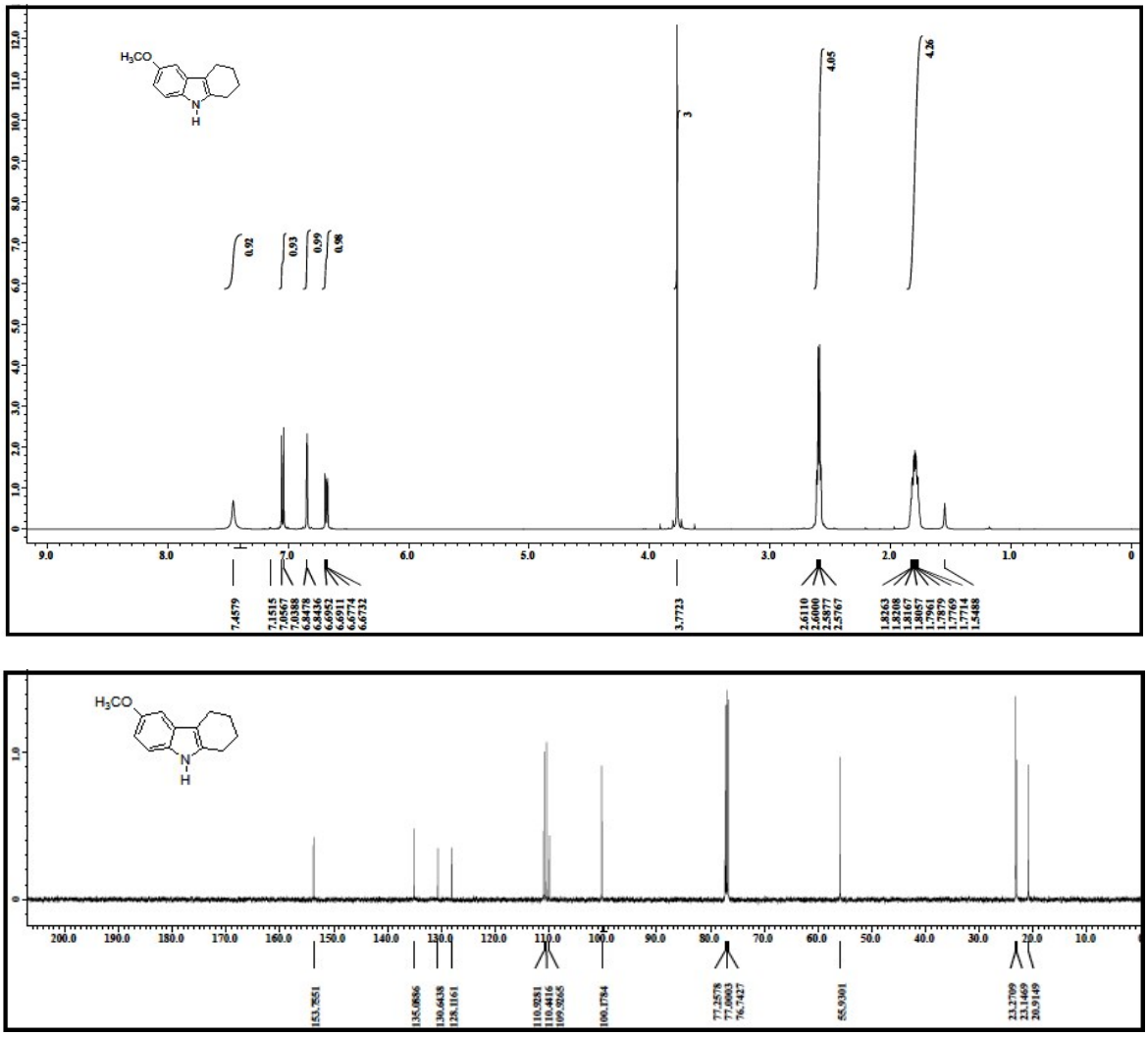

Fig. S50 ^{1}H and ^{13}C spectra of **25**.

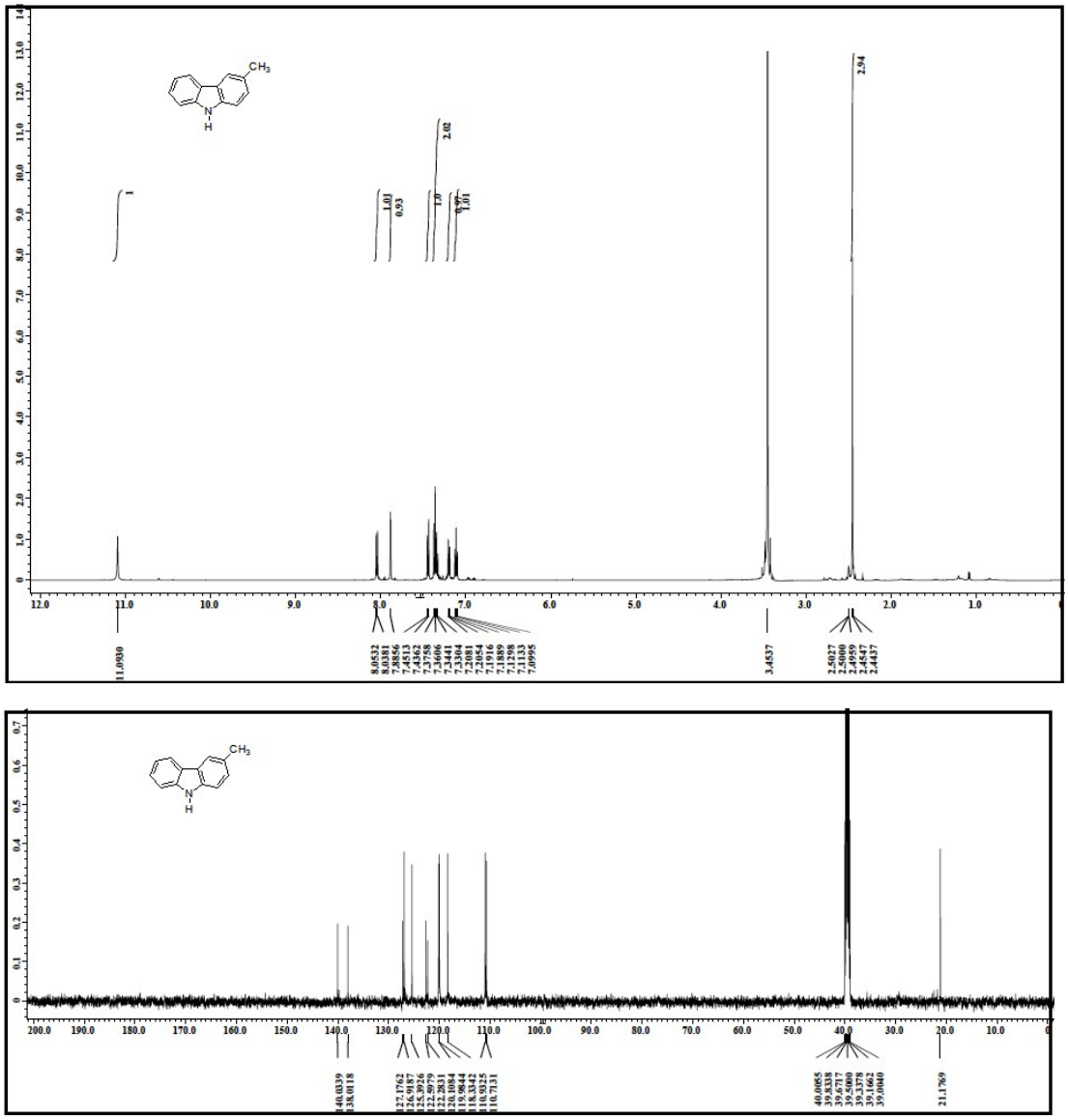

Fig. S51 ^{1}H and ^{13}C spectra of **26**.

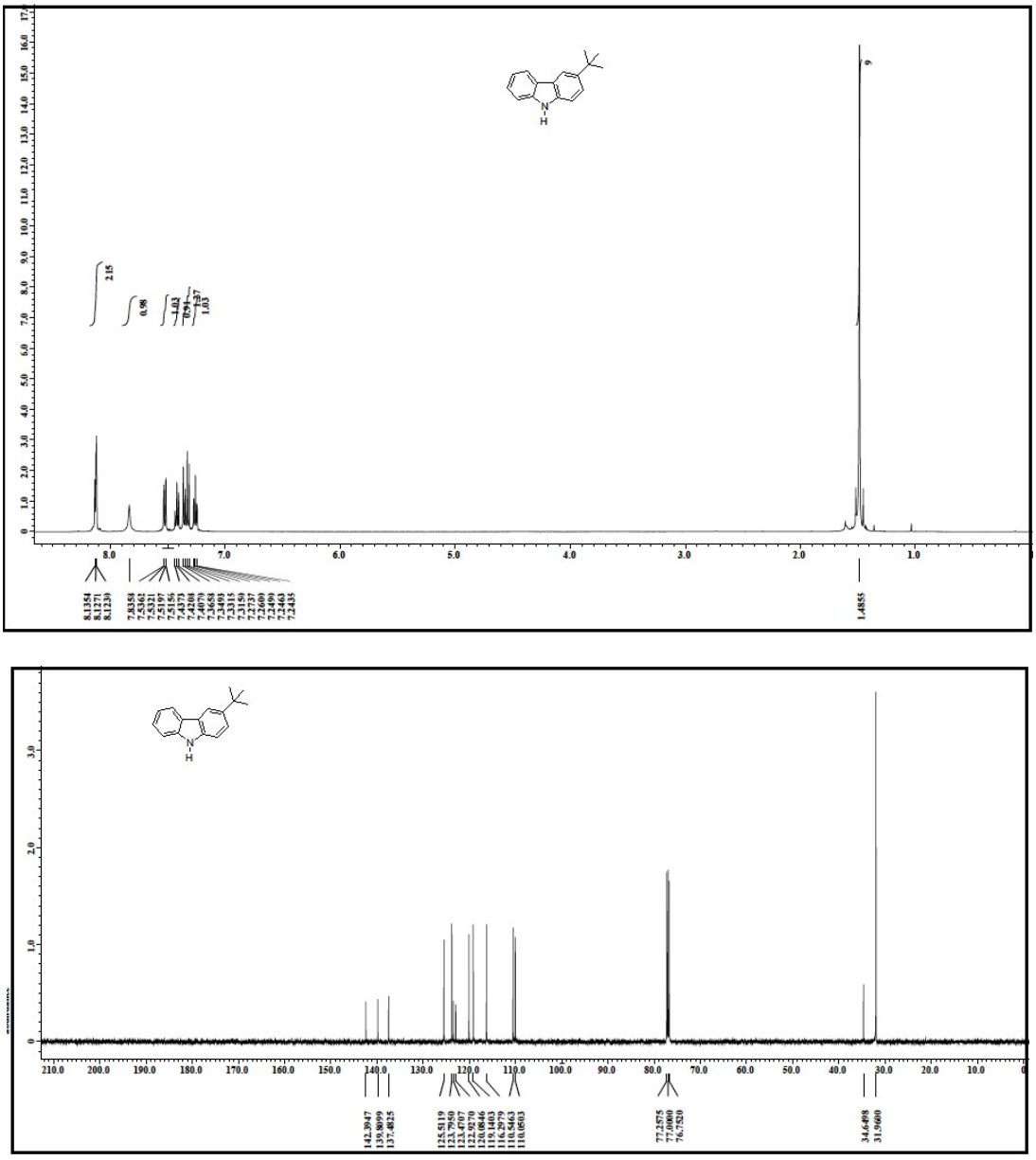

Fig. S52 ^{1}H and ^{13}C spectra of **27**.

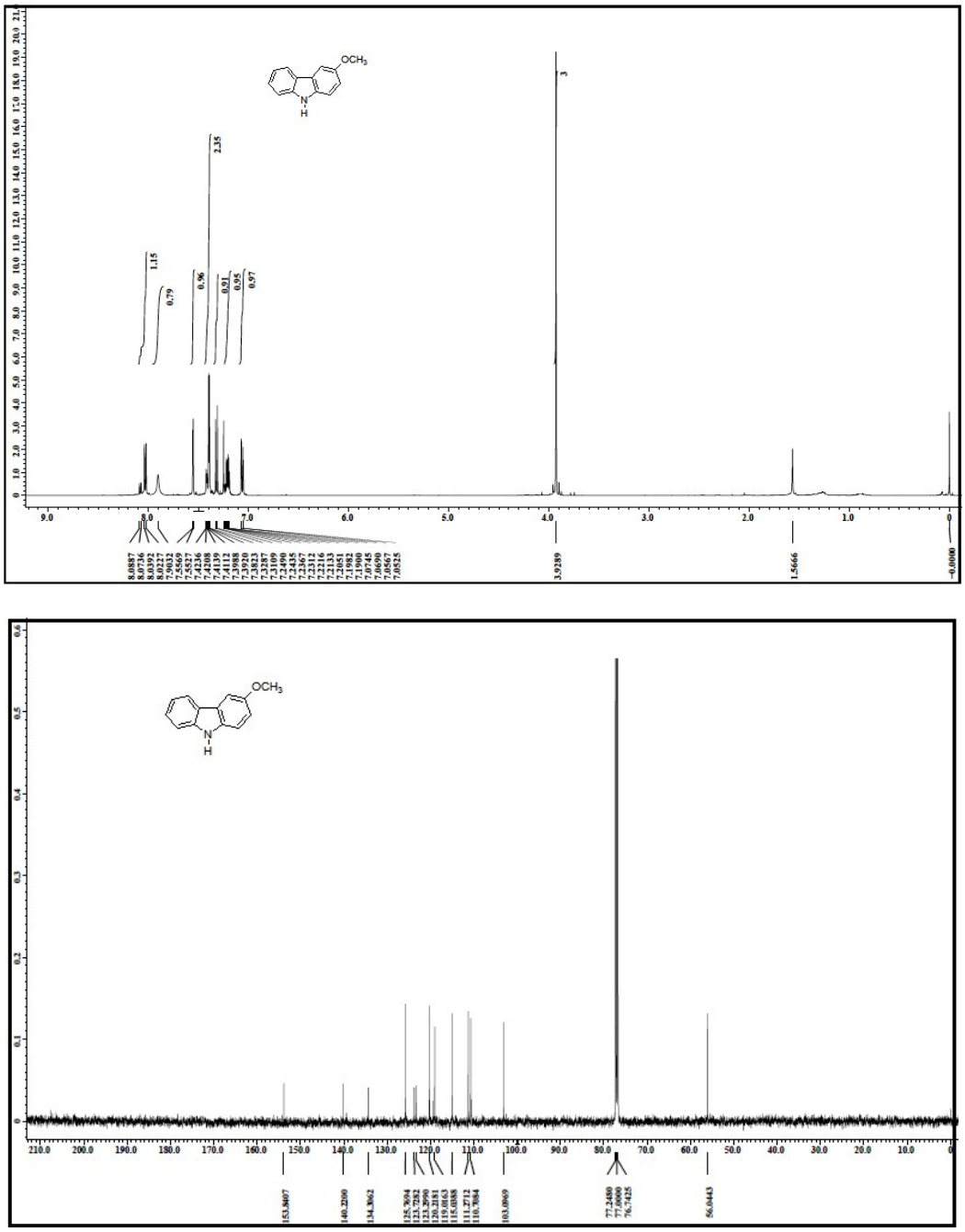

Fig. S53 ^{1}H and ^{13}C spectra of **28**.

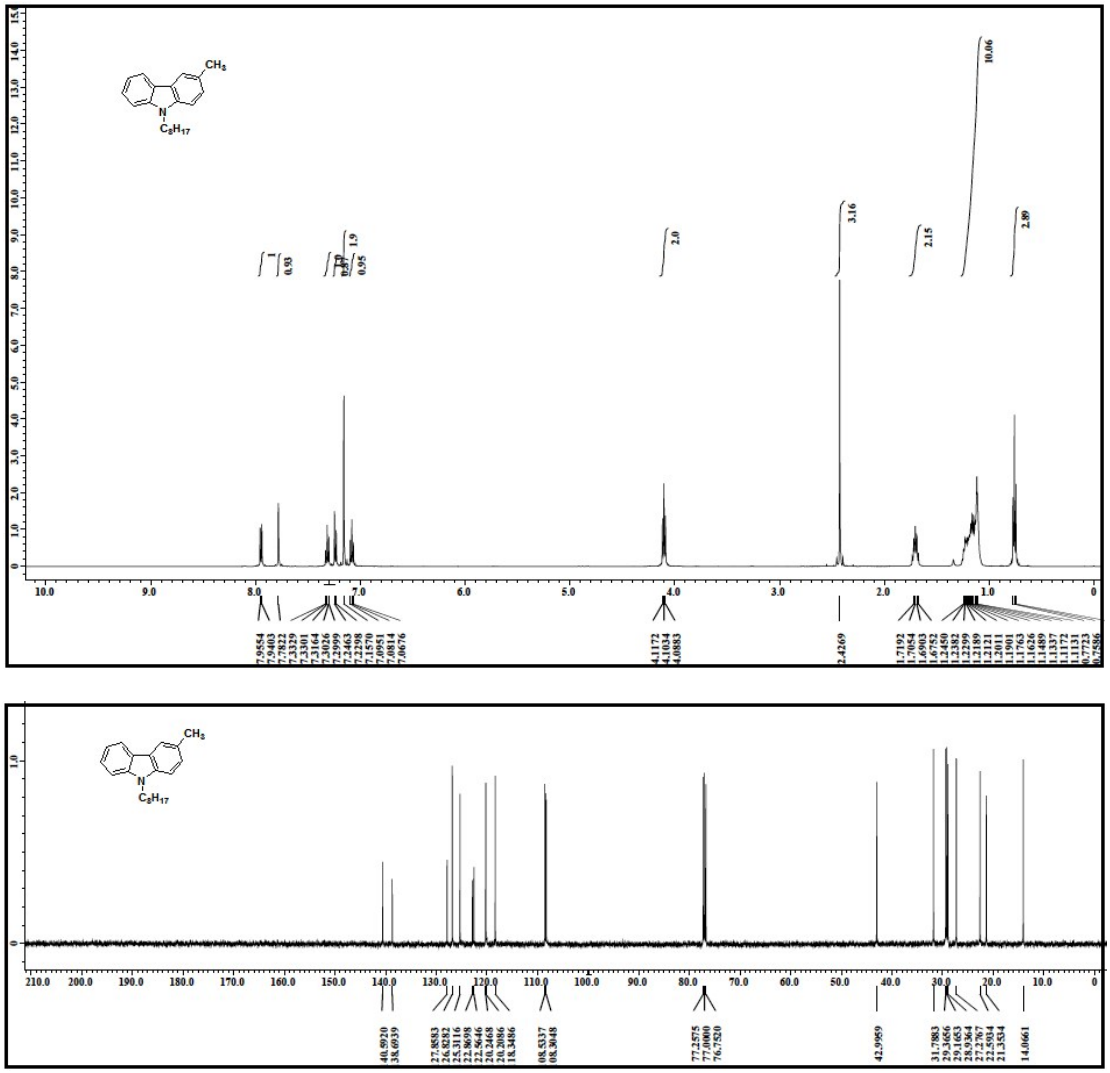

Fig. S54 ^{1}H and ^{13}C spectra of **L30**.

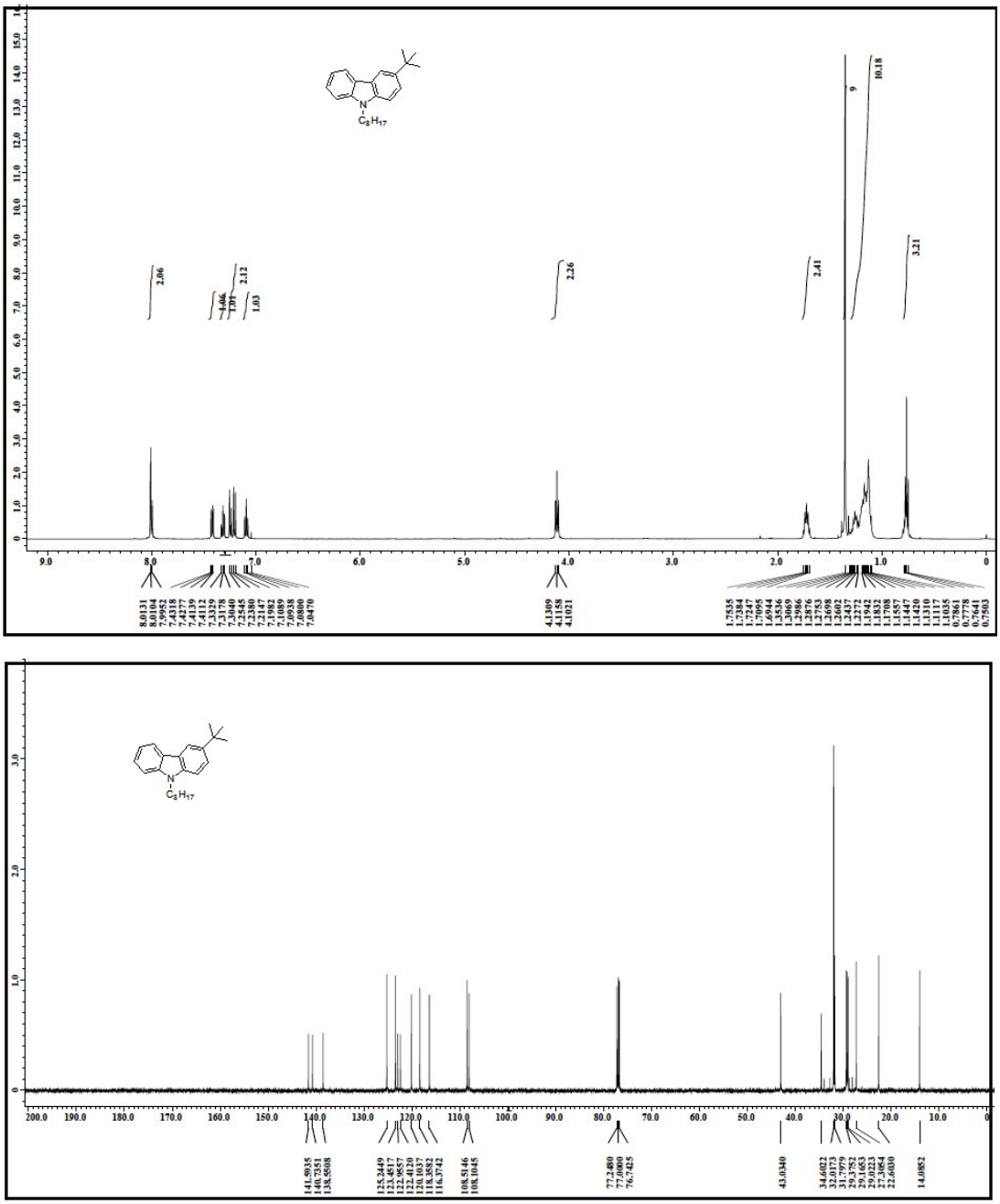

Fig. S55 ^{1}H and ^{13}C spectra of **L31.**

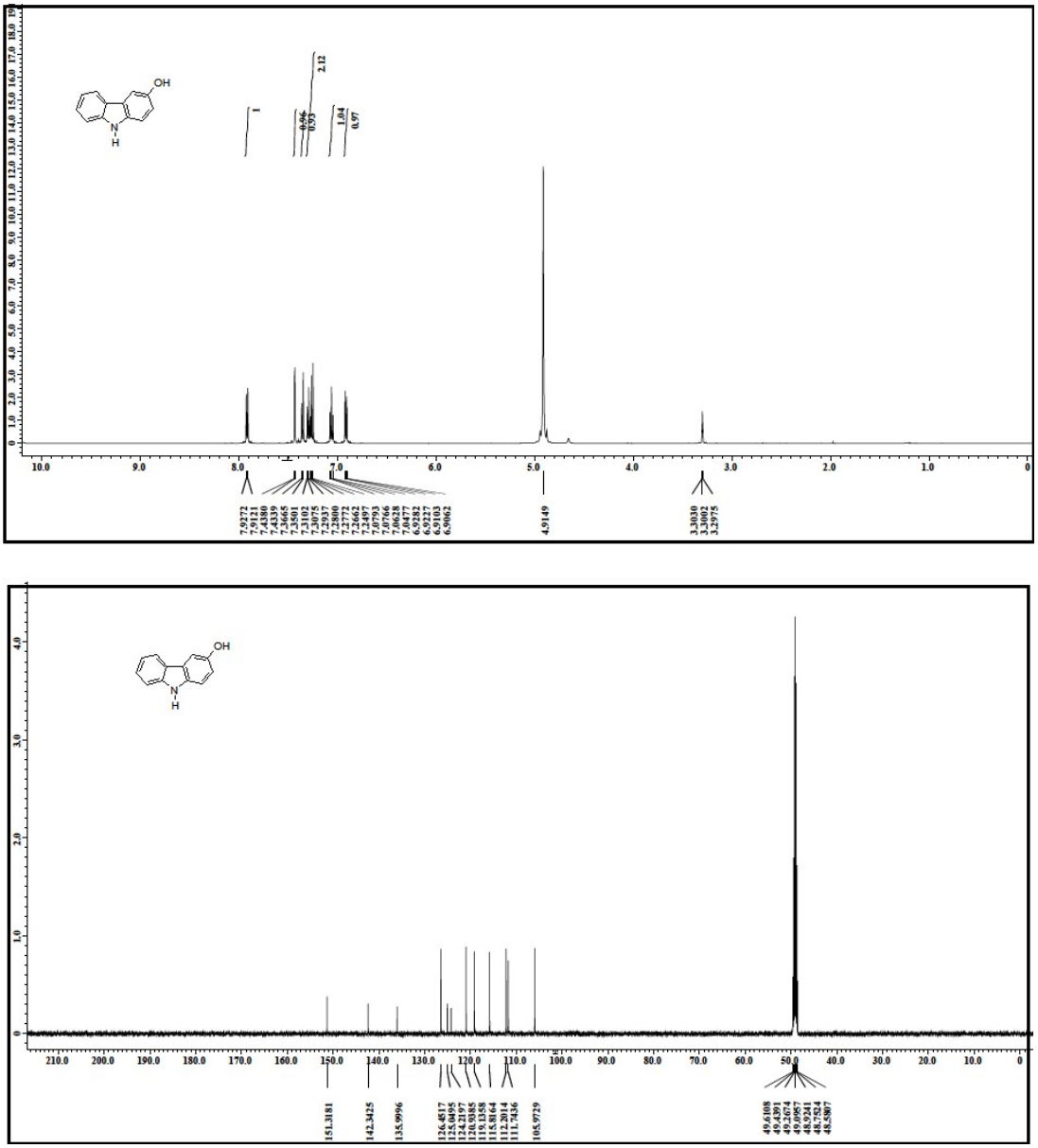

Fig. S56 ^{1}H and ^{13}C spectra of **L29**.

References:

1. B. Ojha and G. Das, *Chem. Commun.*, 2010, **46**, 2079.
2. D. F. Eaton, *Pure &Appl. Chem.,* 1988, **60**, 1107.
3. R. Swaminathan, G. Krishnamoorthy and N. Periasamy, *Biophys J.,* 1994, **67**, 2013.
4. P. V. Kamat, S. Das, K. G. Thomas and M. V. George, *J. Phys. Chem.,* 1992, **96**, 195.
5. A. Wolfe, G. H. Shimer and T. Meehan, *Biochemistry*, 1987, **26**, 6392.
6. S. Neelam, M. Gokara, B. Sudhamalla, D. G. Amooru and R. S ubramanyam, *J. Phys. Chem. B,* 2010, **114***,* 3005.
7. B. Ojha and G. Das, *J. Phys. Chem. B,* 2010, **114***,* 3979.
8. G. Dey, A. Gupta, T. Mukherjee, P. Gaur, A. Chaudhury, S. K. Mukhopadhyay, C. K. Nandi and S.Ghosh, *ACS Appl. Mater. Interfaces* 2014, **6**, 10231.